Morphogenetic Specializations at the Tip of the Branching Epithelium of the Kidney

Lydia Michael

Doctor of Philosophy,

University of Edinburgh, 2003

To my always supporting parents

and

to my wee brothers, Dimitris & Spyros

Την μια μονότονην ημέραν άλλη
μονότονη, απαράλλακτη ακολουθεί. Θα γίνουν
τα ίδια πράγματα, θα ξαναγίνουν πάλι –
η όμοιες στιγμές μας βρίσκουνε και μας αφίνουν.
(...)
Και καταντά το αύριο πια σαν αύριο να μη μοιάζει.

(Κ.Π. Καβάφης, Μονοτονία, 1908)

Τους Λαιστρυγόνας και τους Κύκλωπας,
τον άγριο Ποσειδώνα δεν θα συναντήσεις,
αν δεν τους κουβανείς μες στην ψυχή σου,
αν η ψυχή σου δεν τους στήνει εμπρός σου.

(Κ.Π. Καβάφης, Ιθάκη, 1911)

Κι αν είσαι στο σκαλί το πρώτο, πρέπει
να' σαι υπερήφανος κ' ευτυχισμένος.
Εδώ που έφτασες λίγο δεν είναι
τόσο που έκαμες, μεγάλη δόξα.

(Κ.Π. Καβάφης, Το πρώτο σκαλί, 1899)

Contents

Acknowledgements

I would like to thank my supervisor, Dr. Jamie Davies, for his constant help, support and encouragement over the past few years; without him, this work would never have seen the light of day. Also, my second supervisor, Dr. John West, for his essential comments and suggestions.

I have many important debts to acknowledge. To Dr. Gillian Gray, for the precise scientific orientation of this thesis; to Professor M. H. Kauffman; to Dr. Mark Barnett for teaching me differential display; to Dr. Carolyn Fisher, for her constant support and, more importantly, for becoming a friend; to Dr. Paulette Zaki, for initiating me into the perplexities of the PhD process; to Dr. Peter Bush, for his valuable suggestions on the image analysis. Also, to Ms. Linda Sharp, from the Confocal facility, for training me to the use of the confocal microscope, for trusting me with the "precious", for always being ready to help and for trying to make my life easier which is not always simple... Linda, I am deeply indebted.

I thank all my friends in Edinburgh, for their immense contribution to my general well-being. Especially, Jos Houdijk, Nikos Karoulias and Dimitris Vagenas, for their help in crucial moments of need. Also, I thank Alby who made me laugh during the painful long nights of the writing up, Molly, and Nadia, for providing me with the necessary peace of mind even without really knowing it.

Last, I am deeply grateful to Spyridoula Athanasiadou and Alexis Tattis for their true involvement and invaluable support. Thanks for having a special place in my life.

Declaration

I declare that:

(a) this thesis was composed by myself;

(b) the work presented here is my own, except where stated; and

(c) the work has not been submitted for any other degree or professional qualification

Lydia Michael

List of Abbreviations

α	Alpha
β	Beta
BDM	2,3 Bunetadione monoxime
BMP	Bone morphogenetic protein
BrdU	5-Bromo-2′-deoxy-uridine
BSA	Bovine serum albumin
CAKUT	Congenital anomalies of the kidney and urinary tract
CD28k	Calbindin D28k
CLSM	Confocal laser scanning microscope
Cyto D	Cytochalasin D
DBA	*Dolichos Biflorus* agglutinin
DD-PCR	Differential display PCR
DMSO	Dimethylsulfoxide
dNTP	Deoxyribonucleoside triphosphate
E	Embryonic day (mouse)
E_r	Embryonic day (rat)
ECM	Extracellular matrix
EDTA	Ethylenediaminetetraacetic acid
ERK	Extracellular signal-regulated kinase
F-actin	Filamentous actin
FITC	Fluorescein isothiocyanate
FGF	Fibroblast growth factor
Γ	Gamma
GAG	Glycosaminoglycan
GDNF	Glial cell-derived neurotrophic factor
GFRα	Glial cell-derived neurotrophic factor receptor alpha
GPI anchor	Glycosulphosphatidylinositol anchor
HGF	Hepatocyte growth factor
HGFA	Hepatocyte growth factor activator
Hox genes	Homeobox-encoding genes
Ig	Immunoglobulin
IMCD	Inner medullary collecting duct

ld	Limb deformity
µ	micro
m	milli
mAb	Monoclonal antibody
MAP Kinase	Mitogen-activated protein kinase
MDCK	Madin-Darby canine kidney
MET	Mesenchyme to epithelium transition
MK	Midkine
MM	Metanephric mesenchyme
MMP	Matrix metalloproteinase
MT-MMP	Membrane type-matrix metalloproteinase
NCS	Newborn calf serum
NTN	Neurturin
Pax genes	Paired box genes
PBS	Phosphate buffered saline
PCR	Polymerase chain reaction
PFA	Paraformaldehyde
PI3K	Phosphoionositide 3-kinase
PD98059	2′amino-3′-methoxyflavone
PG	Proteoglycan
PKA	Protein kinase A
PKC	Protein kinase C
PSP	Persephin
RAR	Retinoic acid receptor
Rho GTPase	Rho family of small guanosine triphosphatases
RTK	Receptor tyrosine kinase
RT	Room temperature
RT-reaction	Reverse transcription reaction
SDS	Sodium dodecyl sulfate
SEM	Standard error of the mean
SF	Scatter factor
siRNA	Short interfering RNA
STAT	Signal transducers and activator of transcription
TBE	TRIS-BORATE-EDTA
TEMED	N,N,N′,N′-tetramethylethelenediamine

TGF	Transforming growth factor
TIMP	Tissue inhibitor of metalloproteinases
TRIS	2-amino-2-hydroxymethyl-1,3-propanediol
TRITC	Tetrarhodamine isothiocyanate
UB	Ureteric bud
WD	Wolffian duct
WT	Wilms tumour

Abstract

Branching morphogenesis is a common mechanism of mammalian development. Branched epithelia of kidneys, lungs, mammary glands etc develop from an initially unbranched epithelial bud which develops under the control of reciprocal interactions between the growing epithelium and the mesenchyme that surrounds it. To examine how morphogenetic signals change the shape of the epithelium this thesis examines the urinary collecting duct as a model for branching and tests the hypothesis that the tips of the epithelium are specialized for morphogenesis.

Kidney development begins when the ureteric bud, an outgrowth of the Wolffian duct, invades the metanephric mesenchyme. This then induces the bud to grow and bifurcate repeatedly to form the collecting duct system. To better understand how the ureteric bud tips are specialized to produce branches, this thesis compares their cell biology to that of the rest of the ureteric bud using the murine metanephric organ culture as a model system. Specifically, it describes the pattern of cell proliferation, cytoskeletal organization as assessed by immunofluorescence and confocal laser scanning microscopy, glycoconjugate expression in the tips and in the rest of the bud by means of lectin histochemistry and gene expression by differential display PCR.

Increased cell proliferation, measured by bromodeoxyuridine incorporation, is found at the tips of the branching epithelium. This pattern of increased cell proliferation correlates with branching activity and is lost when branching is arrested in kidney rudiments depleted of sulphated glycosaminoglycans. Known mediators of ureteric bud branching in culture such as GDNF and TGF-β were examined for their effect on cell proliferation at the ureteric bud tips; TGF-β reduced proliferation and GDNF either increased it or had no effect, depending on whether it was applied locally or generally.

Microfilaments, detected by fluorescent-tagged phalloidin, are strongly expressed in the apical parts of the ureteric bud tips during branching. Inhibition of branching (either by depletion of sulphated glycosaminoglycans or by a MAP kinase inhibitor) disrupts this localized expression. Cytochalasin D disruption of filamentous actin inhibits branching, results in cell scattering from the ureteric bud tips and alters the cell junctions as revealed by E-cadherin distribution. Actomyosin interactions also regulate branching of the ureteric epithelium as shown by a general myosin inhibitor.

Expression of lectin binding glycoconjugates at the ureteric bud tips differs from the stalks. *Dolichos Biflorus* Agglutinin (DBA), a known collecting duct marker, is found to selectively binding to stalks. This binding pattern is present during active branching but is lost when branching is blocked. Organ recombination experiments show that the ureteric bud stalk cells are able to generate DBA-negative tip cells upon amputation and regeneration. Finally, genes expressed differentially between ureteric bud tips and stalks provide further evidence to support the hypothesis that the tubule tips are specialized structures.

Chapter 1

An Introduction to Early Kidney Development

1.1 Kidney development on kidney disease

Clinically significant abnormalities of kidney development affect 10 percent of the population (Potter, 1972). Developmental anomalies of the kidney fall into two main groups. There are those related to the complete organ, which include changes in the size, shape, location or number of the organ and those related to individual parts of the organ such as changes in the collecting tubules, nephrons or stroma (Potter, 1972). There are also numerous syndromes with a renal phenotype, such as the Von Hippel-Lindau syndrome and Kallmann's syndrome (Stephens *et al.*, 1996).

Ureteric branching morphogenesis is a key event in the development of the collecting duct system of the permanent kidney. The branching pattern of the collecting duct epithelium largely defines the final histoarchitecture of the kidney. Abnormalities in branching morphogenesis can lead to abnormalities in renal structure and function. Defective branching morphogenesis and growth of the collecting duct are likely to reduce the number of nephrons produced during kidney development, as newly formed nephrons arise at the tips of the branches of the ureteric epithelium. Inherited or acquired reduction in number of nephrons is associated with an increased risk of developing hypertension and chronic renal failure.

Renal dysplasias are morphologically heterogeneous and of variable aetiology. Many congenital cystic kidney disorders are caused by defective morphogenesis of the ureteric bud and abnormal development of the collecting duct system. Infantile (autosomal recessive) polycystic kidney disease is characterized pathologically by enlarged reniform kidneys with very numerous, fine, elongated collecting ducts radiating from pelvis to the cortex (described in Stephens *et al.*, 1996). Multicystic dysplastic kidneys may have either a characteristic grape-like appearance or small microcysts and some minicysts. Only a few generations of collecting ducts are produced. The lumens are increased in diameter and many terminate in cysts. Dysplasia of the nephrons and stroma is present, along with a

reduction in nephron endowment (Potter, 1972; Stephens *et al.*, 1996). Cases of unilateral or bilateral kidney agenesis are associated with total absence of the ureter which is caused by absence of the lower portion of the mesonephric duct or by failure of the duct to give rise to the ureteric epithelium (Potter, 1972).

Research on genes and other molecules that are required for normal development of the collecting duct may help towards an understanding of the causes of the congenital renal abnormalities. The research evidence presented in this thesis focuses on intrinsic mechanisms during the early stages of the collecting duct development.

The paragraphs that follow introduce kidney development focusing on ureteric bud branching morphogenesis that gives rise to the collecting duct system and on key regulators that have been found to play a significant role in the process.

1.2 Organogenesis of the permanent kidney

During embryogenesis, the developing kidney forms in three distinct stages. The mammalian permanent kidney (*metanephros*) follows the appearance and subsequent degeneration of two transient and primitive structures, the *pronephros* and the *mesonephros.* All three structures develop along the nephric duct (or Wolffian duct) as it grows caudally and reaches the cloaca (figure 1.1). In the present thesis the term Wolffian duct will be used to describe the nephric duct from the region of the mesonephros caudally.

The renal system derives from the intermediate mesoderm whereas the bladder and urethra are of endodermal origin. The intermediate mesoderm consists of a longitudinal ridge of cells just lateral to the paraxial mesoderm of the somites that run from the cervical through to the caudal regions of the embryo (for a review, see Sakurai and Nigam, 2000). The first epithelial tubule to differentiate from the mesoderm is the pronephric duct (Saxen, 1987). It is the drainage tube

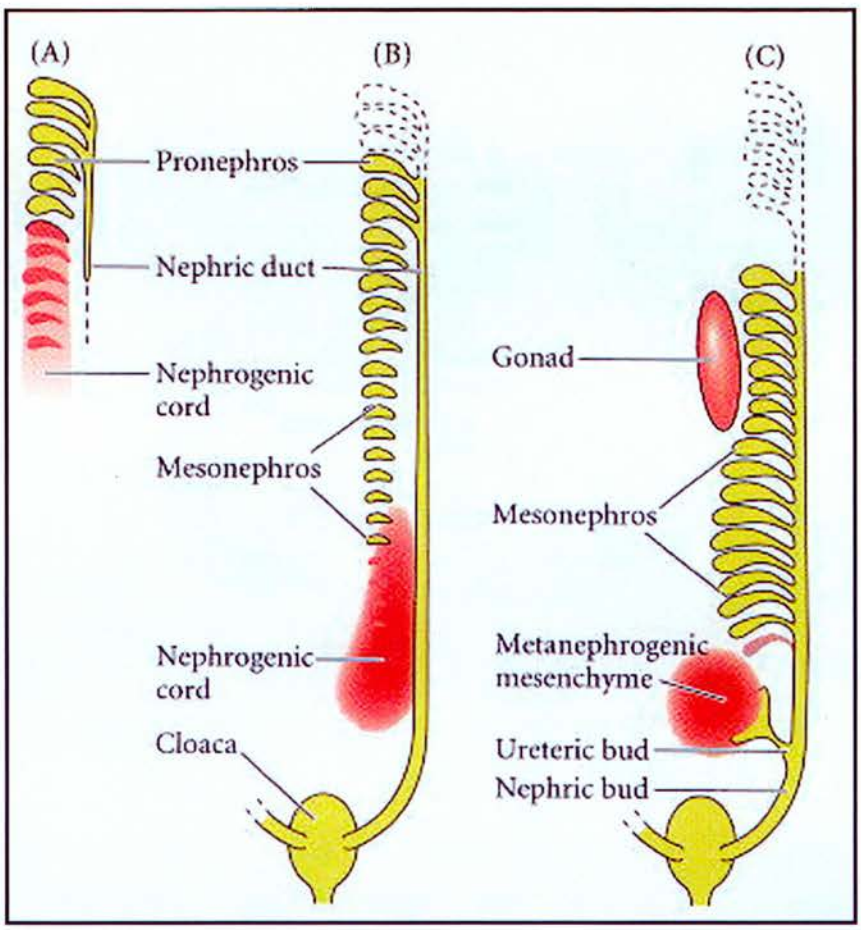

Figure 1.1: The three major stages of mammalian kidney development

(A) The pronephric tubules are induced from the nephrogenic mesenchyme by the pronephric duct as it migrates caudally, **(B)** as the pronephros degenerates the mesonephric tubules are formed, **(C)** the final mammalian kidney, the metanephros, is induced by the ureteric bud. (From Gilbert, 1997).

of the functional pronephros and mesonephros. It also organizes the metanephros and contributes to the male genital system (Saxen, 1987).

In the human embryo the *pronephros* (figure 1.2) is visible in the intermediate mesoderm of the 10-somite embryo between the second and sixth somite (Potter, 1972). It consists of a few epithelial tubular structures variably connected to the pronephric duct (Sakurai and Nigam, 2000). This temporary organ is non-functional and degenerates shortly after its appearance, by the 20 somite stage (Potter, 1972). In mice, the pronephros appears at embryonic day 8 (E8). Glomerulus-like structures are present but do not appear to be physically connected to the tubules (Sakurai and Nigam, 2000). Even though the pronephros has no function in mammals, it is functional and essential for survival in fish and amphibian larvae (Saxen, 1987). The pronephroi of fish and amphibia typically contain 1 to 3 nephrons. The amphibian pronephros is a simple structure composed of three principle parts: the pronephric corpuscle, the pronephric tubules and the pronephric duct. The corpuscle consists of the pronephric capsule and a vascular component, the glomus. The pronephric tubules are composed of three segments; ciliated nephrostomes, connecting tubules and a common tubule (Brandli, 1999). The pronephros undergoes regression and apoptosis and its function is replaced by the mesonephros which in lower vertebrates is the permanent kidney of the adult organism (Brandli, 1999; Vize *et al.*, 1997).

Soon after/during pronephric degeneration, the mesonephric kidney appears along the Wolffian duct. The *mesonephros* (figure 1.2) is a less complex kidney found in embryos of higher vertebrates. In mammals, the mesonephros later degenerates and is followed by the development of metanephros. Its basic structure is similar to that found in metanephros. It consists of glomeruli with a well-developed vasculature, proximal and distal tubules and collecting ducts but no loops of Henle. The glomeruli of the mesonephros are relatively large in comparison to the glomeruli of the metanephros but they are fewer (Moritz and Wintour, 1999). The mesonephros usually contains about 30 nephrons of two

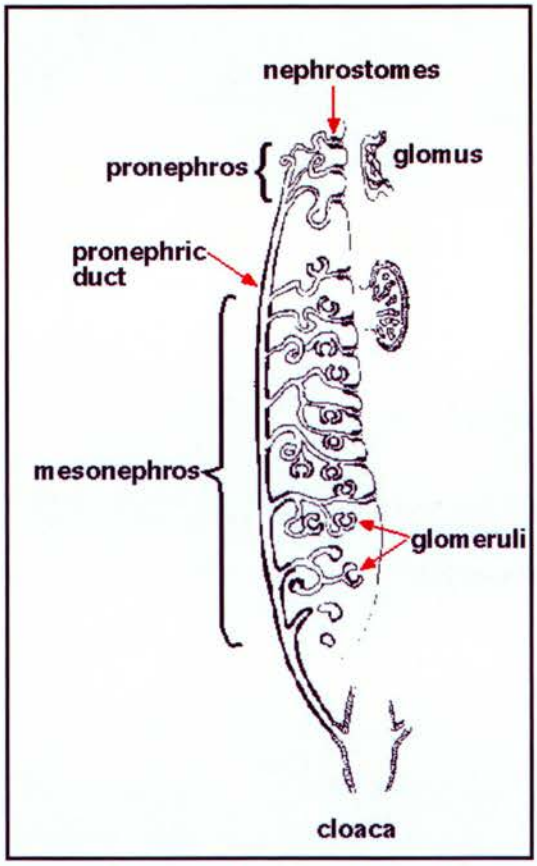

(Picture credit P. Vize, from http://biology.kenyon.edu/courses)

Figure 1.2: Anatomy of pronephros and mesonephros

basic types (Vize *et al.*, 1997). One set is a cranial outgrowth of the Wolffian duct whereas the other is caudal and not fused to the duct. In humans and pigs, the mesonephros is a primitive functional secretory organ whereas in mice is non functional (Sainio *et al.*, 1997a). In human embryos, the mesonephros appears by gestational day 24 and in mice at E9.5. It then regresses (by E15 in mice) in females whereas in males becomes part of the reproductive tract including the vas deferens and the cranial tubules will become the epididymal ducts (Sakurai and Nigam, 2000).

In mammals, just before the Wolffian duct reaches the cloaca, the permanent kidney (*metanephros*) develops (figure 1.3). In human embryos this occurs on day 28 and in mice at E11. The metanephros develops when an epithelial evagination (called the ureteric bud) from the Wolffian duct grows into an area of condensed mesenchyme, the metanephric or nephrogenic mesenchyme. From this point forward the metanephros will develop through epithelial-mesenchymal reciprocal interactions. The metanephric mesenchyme signals to the epithelial bud, which as a result will grow and bifurcate in a process called branching morphogenesis, and will give rise to the collecting duct system of the kidney. The signals and signaling pathways that regulate the branching of the collecting duct tree will be introduced in *section 1.4.3*. The branching ureteric bud in turn signals to the metanephric mesenchyme, which has two fates: it will form the stroma and the nephrons through a mesenchyme-to-epithelial transition (MET) (reviewed in Davies, 1996).

Kidney nephrogenesis and vascularization are simultaneous and coordinated processes. Nephron formation begins with the aggregation of mesenchymal condensates around the tips of the ureteric bud branches, it is followed by the epithelialization of these mesenchymal cells, vesicle formation, comma shape and S-shape bodies formation and subsequent fusion with the ureteric bud (reviewed in Davies, 1993; Davies and Bard, 1998; Horster *et al.*, 1999) (figure 1.4). One cusp of the S-shaped body will develop into Bowman's capsule while

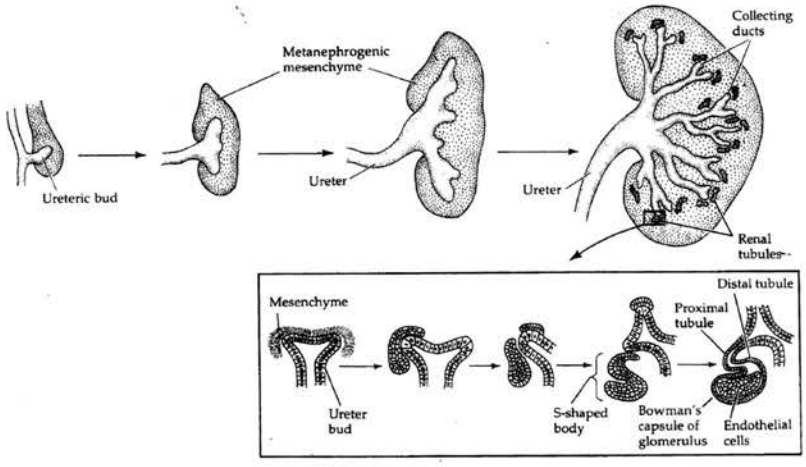

(From Gilbert, 1997)

Figure 1.3: Development of metanephros

Reciprocal induction in the development of the mammalian kidney. The ureteric bud enters the metanephric mesenchyme which then induces the bud to branch. At the tips of the branches, the epithelium induces the mesenchyme to aggregate to form the renal tubules. The formation of the nephron from mesenchyme is shown in the insert.

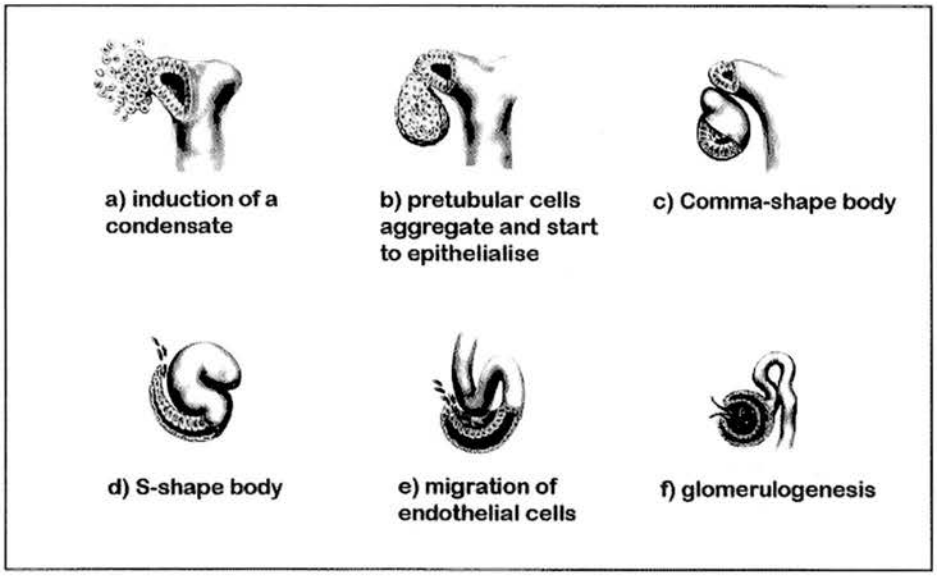

Figure 1.4: Stages of nephrogenesis during kidney development

(a) The metanephric mesenchyme forms a condensate around the ureteric bud tip. **(b)** the ureteric bud secretes signals that induce formation of mesenchymal pretubular cell aggregates, which are precursors of the nephrons. **(c)** induced tubules undergo mesenchymal-to epithelial transition via comma-shaped and **(d)** S-shaped bodies and subsequent fusion to the collecting duct. **(e)** the epithelializing body expresses angiogenic factors that attract ingrowth of endothelial cells into the developing nephron. **(f)** glomerulogenesis follows. (From Kuure *et al.,* 2000, adapted from Saxén, 1987).

the other elongates and differentiates to form the proximal and distal convoluted tubules and loop of Henle (Davies, 1993). Each nephron is composed of a filtering glomerulus and a segmented epithelial tube. The glomerulus is formed by interaction of Bowman's capsule with a capillary. The development of kidney vasculature is still under debate. It is probably formed *in situ* (vasculogenesis) from stem cells of the metanephric mesenchyme migrating into the vascular cleft of the developing glomerulus and from the ingrowth of tube-like angiogenic sprouts derived from external vessels (angiogenesis) (Abrahamson *et al.*, 1998; Saxen, 1987).

Nephron formation in human embryos occurs between gestational week 28 and continues as late as the 36^{th} week (Sakurai and Nigam, 2000). In mice, nephrogenesis starts at E15 and continues in the postnatal period. Nephron number varies between approximately 500,000 to 1,000,000 in humans and reaches approximately 12,000 in mice (Vainio and Lin, 2002). The number of nephrons produced (nephron endowment) depends on the branching of the ureteric bud.

1.3 Models used to study branching morphogenesis

The mature adult kidney is a complex organ but the embryonic kidney is a relatively simple organ. Classical experiments in the 1950s by Grobstein established: (i) that the embryonic metanephros will develop in culture, (ii) that after the mechanical separation of the two cell type components (epithelium and mesenchyme) the epithelium undergoes morphogenesis in the presence of homologous tissue (its own mesenchyme) recombination but not in the presence of heterologous mesenchyme such as submandibular mesenchyme (the terms 'homogeneous combination' and 'heterogeneous combination' were used by Grobstein), (iii) that the metanephric mesenchyme is required for proper ureteric

growth and (iv) the transfilter technique (Grobstein, 1953a; Grobstein, 1953b; Saxen, 1987).

Several kinds of model systems have been established and the evidence available to date on kidney development is a result of their extensive use. The *in vitro* models to study branching morphogenesis include the classical organ culture established by Grobstein and improved by Saxén (Saxen, 1987) and the three-dimensional tubulogenic cell culture models.

1.3.1 Metanephric organ culture

Metanephric organ culture has been extensively used to study the various aspects of metanephric development including branching morphogenesis (described in Saxen, 1987). As this is the model used in this thesis, I am going to introduce it in more detail than the other models. Whole kidney rudiments are isolated from mice or rats at the stage of ureteric bud outgrowth from the Wolffian duct. They are placed on a piece of polycarbonate Millipore filter, which is transferred to a Trowell-type screen of stainless steel. The screen is placed in a simple petri dish and culture medium is added to the level of the surface of the screen. The medium consists of Eagle's basal medium in Earle's balanced salt solution supplemented with 10% foetal calf serum. Due to the surface tension, the tissue is covered with a thin layer of medium and the kidney rudiments become flat. Organ cultures are placed in an incubator with an atmosphere of 5% CO_2 in air. The 11-day metanephric anlagen survive well in culture for up to 12 days and ureteric bud branching and nephrogenesis take place. However, the organ is avascular. The advantage of this technique is that organ culture in conjunction with the use of advanced microscopy (confocal laser scanning microscopy) allows the development of the branching epithelium to be observed in whole mounts. The limitation of the technique however is the presence of both cell type components of the metanephric kidney.

1.3.2 Three-dimensional cell culture

Two kidney derived cell lines are commonly used for the production of three-dimensional tubulogenesis models; the mouse inner medullary collecting duct-3 (mIMCD-3) cell line and the Madin-Darby canine kidney (MDCK) epithelial cells. These cell lines when suspended in an extracellular matrix (ECM) gel (either type I collagen or collagen-Matrigel mixture) form tubules that undergo branching morphogenesis. MDCK cells growing in three-dimensional type I collagen substrate form spherical cysts that extend tubular extensions within the collagen matrix when treated with hepatocyte growth factor (HGF) (Montesano *et al.*, 1991a; Montesano *et al.*, 1991b); reviewed in (Balkovetz, 1998). The presence of the epithelial component alone make these three-dimensional tubulogenesis cell lines good models for identification of possible positive or negative factors responsible for branching. The limitation of these models is that the branching pattern differs from that observed during metanephric development making difficult to assess the effect of the regulatory signals on the branching architecture.

1.3.3 Isolated ureteric bud culture

Another model has recently been established where isolated ureteric bud cells are grown in culture in the absence of mesenchymal contact (Qiao *et al.*, 1999a). In this model the ureteric bud cells are cultured in a mixture of type I collagen and growth depleted-Matrigel. After the addition of a mixture of growth factors and pleiotrophin, dichotomous branching-morphogenesis resembling the structures of the developing kidney is achieved (Qiao *et al.*, 1999a; Sakurai *et al.*, 1997; Sakurai *et al.*, 2001). The advantage of this technique is the presence only of the epithelial component.

1.3.4 Genetically engineered mice

The construction of transgenic mice expressing green fluorescent protein (GFP) throughout the ureteric bud epithelium allows branching morphogenesis to be followed by time-lapse confocal microscopy which overcomes the limitation of examining ureteric bud branching at single time-points (Srinivas *et al.*, 1999).

Introduction of null mutations of the gene of interest in mouse embryonic stem cells is used for the generation of knockout mice. The role of a particular gene important for kidney development can be demonstrated. Many key regulators of kidney development have been identified by gene-knockout technology. The limitations of this technology is that mice may not have an apparent phenotype due to redundancy or the gene of interest may be important for early embryogenesis well before the emergence of the urogenital system or the embryo dies before organogenesis. Recently the transfection of synthetic small interfering RNAs (siRNAs) into human cells has been found to effectively inhibit gene expression and the use of siRNA in mammalian organ culture has been established (Davies *et al.*, unpublished). Therefore, in the case of genes vital to early embryogenesis the siRNA-mediated knockdown may establish their role in kidney development.

1.4 Branching morphogenesis of the developing collecting duct

1.4.1 Branching morphogenesis

Branched tubular epithelial structures are found in most animals and function to transport gases and liquids in the body. Many organs such as the lung, pancreas, prostate and kidney are composed of ramifying networks of epithelial tubes. They develop through branching morphogenesis, which is a commonly used

developmental mechanism where there is a need of maximization of surface area relative to the size of the organ.

The branched epithelial tubes arise from initially unbranched epithelial buds of relatively undifferentiated cells. Subsequent to its initial outgrowth, the bud undergoes growth, elongation and bifurcation in a highly reproducible way that leads to the formation of a characteristic three-dimensional, tree-like structure (Hogan, 1999). The pattern of branching is complex and seldom random. The earliest branch generations show a highly stereotyped branching pattern, which suggests that they are under fixed developmental control (Metzger and Krasnow, 1999). For this kind of stereotyped branching to occur, the pattern information should specify where the branch will bud, the direction it will grow, the size and shape of the branches and when and where the next generation of branches will develop (Metzger and Krasnow, 1999).

The development of the branching organs of most vertebrates involves dynamic and reciprocal interactions between two cell populations, an epithelium and its mesenchyme. The epithelial bud invades its surrounding mesenchyme as a result of inducing signals derived from the mesenchyme. The bifurcation of the epithelial bud is coordinated by positive and negative reciprocal feedback loops between signaling centers in the mesenchyme and epithelium. Branching of the epithelial component can proceed by cellular rearrangement alone or it might require cell proliferation as well.

The pattern of branching morphogenesis can be divided in two types: (i) lateral branching (also termed monopodial) and (ii) bifid branching (or dipodial). The former involves lateral branches emerging from a main stem at equally spaced or random intervals whereas the latter involves the division of the main stem into two daughter branches of similar size (al-Awqati and Goldberg, 1998; Davies, 2002).

The branching of the ureteric bud is highly structured and shows several types of repeating patterns of divisions. It requires both lateral and bifid branches, which

then form three different patterns of branching that unfold one after the other (al-Awqati and Goldberg, 1998). The first bifurcation of the ureteric bud involves two symmetric dichotomous branches at an angle of 180° (Saxen, 1987). The growth and division of ureteric bud branches proceeds in two steps that occur in rapid succession. The first is a lateral branch emerging from the ureteric bud stalk, which then divides dichotomously into two terminal branches. This branching pattern is referred to as a terminal bifid branching system (al-Awqati and Goldberg, 1998). This is the case because each tip of a branch will induce and be connected to a nephron. The connection to a nephron removes the tip from the possibility of further branching (al-Awqati and Goldberg, 1998). The terminal branches that have stopped their branching programme, retain their capacity to induce the formation of nephrons that in humans will form the arcades (Potter, 1972; Saxen, 1987).

1.4.2 Morphogenesis of branched organs

Even though this introduction is mainly about the branching morphogenesis of the collecting duct system, I will briefly introduce some of the organs that develop through branching morphogenesis and which are widely used as model systems for the study of this important developmental mechanism. The following branching epithelia share anatomical similarities suggesting the idea of conserved mechanisms. Branching morphogenesis is probably controlled by a conserved set of molecular mechanisms based on evidence that they share common signaling pathways, they require members of the same growth factor families to activate or inhibit branching and their branching pattern is regulated by the extracellular matrix (Davies, 2002).

The embryonic submandibular salivary glands (figure 1.5) require epithelial-mesenchymal interactions for proper development. The murine salivary gland epithelium develops at gestational day 12 (day 13 in rat). The salivary gland

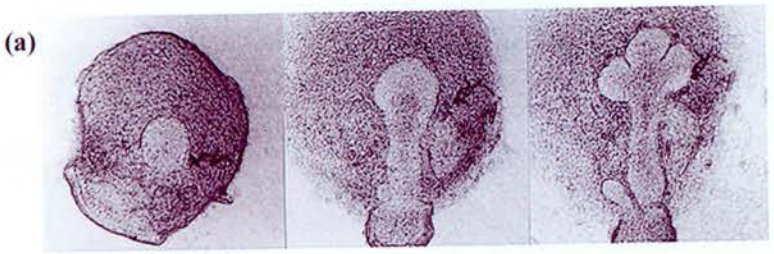

(From Gilbert, 1997)

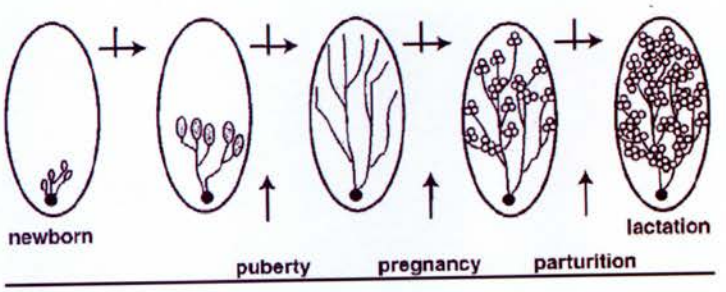

(From Hennighausen and Robinson, 1998)

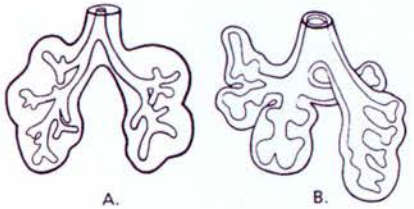

(From Warburton *et al.*, 2000)

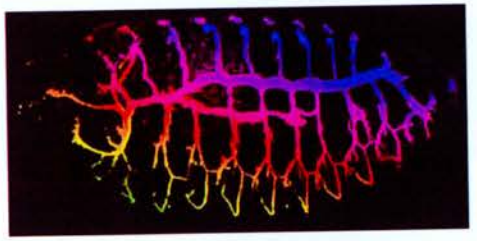

(From Samakovlis @ www.wgi.su.se)

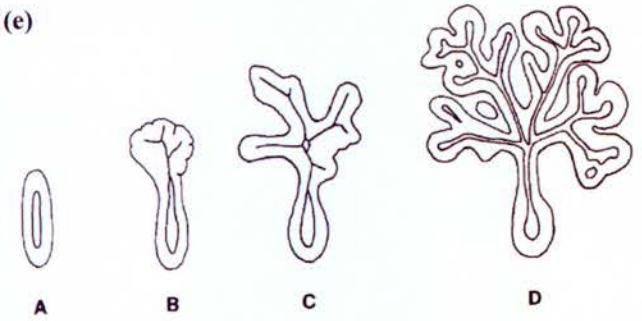

(From Slack, 1995)

Figure 1.5: Branching morphogenesis during embryonic development

(a) Murine salivary gland in culture, **(b)** human 7-8 week embryonic lung (left, A) and E12 murine lung (right, B), **(c)** the developing tracheal system in a *Drosophila* embryo, **(d)** diagram of the distinct stages of murine mammary gland development, **(e)** murine embryonic pancreas (E9.5, E10.5, E12.5, E15.5). Pictures & drawings not to scale.

consists of large and small ducts that terminate in lumen-containing presumptive acini that express embryonic mucin (Jaskoll and Melnick, 1999). Development of the submandibular salivary glands is separated into stages: prebud, initial bud, pseudoglandular, canalicular and terminal bud stages (Jaskoll and Melnick, 1999). The primordium (prebud) arises from the oral epithelium which is of endodermal origin, interacts with the underlying mesenchyme to form a stalk with a bulbous lobule (initial bud) (reviewed in Hardman and Spooner, 1992b). Between embryonic days 12.5 and 13 in mice the primary clefts and lobules are formed (Miyazaki, 1990). At the end of E13 the epithelial stalk is elongated and its end consists of three to four primary lobules separated by prominent clefts (Miyazaki, 1990). During the pseudoglandular stage repeated division at the distal ends of the buds occurs. A bush-like structure of a network of elongated epithelial branches with terminal epithelial buds surrounded by loosely packed mesenchyme is produced (Jaskoll and Melnick, 1999). During canalicular and terminal bud stages the branches and buds become hollow and form the ductal system and presumptive acini (Jaskoll and Melnick, 1999).

The mammalian lung (figure 1.5) develops through branching morphogenesis. The murine lung primordium arises at gestational day 9.5 from the ventral foregut just anterior of the stomach (for reviews see Hilfer, 1996; Hogan, 1999; Hogan *et al.*, 1997). Two bud outgrowths of endodermal origin emerge surrounded by splachnic mesoderm. Lung development progresses in four morphological stages (Hilfer, 1996). In the earliest embryonic or pseudoglandular phase the basic branching pattern is established, in the second or canalicular stage the narrower bronchial passageways are formed by continued branching. During the third or saccular stage the distal branches expand into alveolar sacs, at the fourth or alveolar stage more alveolar sacs are formed, and mature alveoli are formed by outpouching of the alveolar sacs. During the early (pseudoglandular) stage, the lung is composed of three cell layers: an inner endodermal epithelium, a splachnic mesodermal mesenchyme and an outer mesothelium. The two primary buds elongate, and through reciprocal interactions

of the epithelial-mesenchymal components, undergo branching in a highly reproducible pattern giving rise to five lobes, four on the right and one on the left. The mesodermal mesenchyme secretes soluble factors that act on the branching endoderm. In the early, pseudoglandular stage two branching mechanisms are used; lateral and dichotomous branching (Ten Have-Opbroek, 1981). The first mechanism establishes the length and overall shape of the main lobes whereas the dichotomous branching involves the bifurcation of a terminal bud into two branches, which continue to grow along a different axis.

Formation of the *Drosophila* tracheal (respiratory) system (figure1.5) involves branching morphogenesis (Shilo *et al.*, 1997). The tracheal system delivers oxygen directly to the tissues. It consists of a complex network of hollow epithelial tubules of ectodermal origin. The tracheal epithelium is a monolayer without any surrounding support tissue. The tracheal system develops from ten clusters of ectodermal cells (placodes) on each side of the embryo (Samakovlis *et al.*, 1996). The clusters invaginate at mid-embryogenesis and form twenty elongated epithelial sacs of approximately 80 cells. Primary branches emerge from each sac which grow out in different directions, then secondary branches emerge from the primary branches and the terminal branches appear as continuations of the secondary branches at fixed developmental stages (Samakovlis *et al.*, 1996). The pattern of primary and secondary branching is stereotyped whereas the pattern of terminal branching varies (Samakovlis *et al.*, 1996).

Mammary gland development (figure 1.5) proceeds in distinct stages defined by the hormonal status of the animal (reviewed in Hennighausen and Robinson, 1998). During embryonic development the mammary anlage is established. At the time of birth it consists of a few rudimentary ducts in the vicinity of the nipple. Ductal elongation and branching begins after the onset of puberty and the onset of gonadal hormone secretion. The rudimentary ducts invade the mammary fat pad through dichotomous branching. Large club-shaped terminal end buds

emerge. The terminal end buds consist of two histologically distinct cell types: the body cells which give rise to mammary epithelial cells and the cap cells which are the precursors of myoepithelial cells (Humphreys *et al.*, 1996). Branching ceases when the fat pad is laced with the ductal tree. In pregnancy an expanded lobulo-alveolar compartment develops which obtains functional differentiation during parturition and lactation.

Another organ that develops through branching morphogenesis and epithelial-mesenchymal interactions is the pancreas (figure 1.5) (for reviews see Debas, 1997; Scharfmann, 2000; Slack, 1995). It is formed from an evagination of the foregut of the embryo at E9.5 in mice (Debas, 1997). It develops as two buds on the dorsal and the ventral side of the duodenum (Slack, 1995). The ventral bud emerges adjacent to the hepatic diverticulum and the dorsal bud on the opposite side of the gut tube. After the rotation of the stomach and duodenum the two buds come into contact and fuse together. As the buds grow they form new protrusions leading to a branched structure. The epithelial cells of the bud differentiate into endocrine and exocrine cells. The endocrine cells are grouped into the islets of Langerhans and the exocrine cells are grouped into acini. Both the endocrine and exocrine cells of the pancreas develop from the endoderm of the foregut. Differentiation of the pancreatic cells depends on factors secreted from the surrounding mesenchyme.

1.4.3 Molecular regulation of ureteric bud branching morphogenesis

The ramification of an epithelial bud is coordinated by positive and negative reciprocal feedback loops between the mesenchyme and the epithelial component. This section focuses on some of the key molecules currently known to be involved in ureteric bud branching morphogenesis.

Genes involved in ureteric bud outgrowth and branching

The important role of genes in kidney organogenesis comes from evidence either through identification of mutations responsible for heritable renal disease, or through expression studies and from the phenotypes of transgenic knockouts that show renal defects (for reviews see Davies and Fisher, 2002; Dressler, 1997). The development of the collecting duct system begins with the outgrowth of the ureteric bud from the Wolffian duct and subsequent repetitive branching of the epithelium after invasion of the metanephric mesenchyme. Some of the major genes involved in these initial stages (i) UB evagination and (ii) branching morphogenesis are summarized (table 1.1).

Genes required for ureteric bud outgrowth

During early embryogenesis the LIM-homeodomain factor, *Lim-1* is expressed in the Wolffian duct and the ureteric bud (Barnes *et al.*, 1994). Mice lacking *Lim-1* show bilateral renal agenesis and absence of the urogenital tract (Shawlot and Behringer, 1995). *Lim-1* and a paired box transcription factor *Pax-2* are essential for the early steps of nephrogenesis and function cooperatively in intermediate mesoderm (for review Rauchman, 2000). *Pax-2* is expressed in both epithelial and mesenchymal components deriving from the intermediate mesoderm during the development of pronephros, mesonephros and metanephros (for review see Dressler and Woolf, 1999). During ureteric bud outgrowth *Pax-2* mRNA is found in the ureteric bud epithelium and the UB branches and induced mesenchymal condensates (Dressler *et al.*, 1990). *Pax-2* homozygous mutant mice lack kidneys, since the ureteric buds do not form (Torres *et al.*, 1995). Loss of c-ret expression at the time of the UB outgrowth (see below) accounts for the lack of ureteric buds in the *Pax-2* mutants (Torres *et al.*, 1995). Activation of GDNF which is responsible for ureteric bud outgrowth (see below) depends on *Pax-2* (Brophy *et al.*, 2001). In humans, a relatively rare disease called Renal-Coloboma syndrome results from mutations in the *PAX2* gene (Eccles *et al.*, 2003). Patients with *PAX2* mutations show urological abnormalities, which

Table 1.1: Major genes involved during early kidney development

Gene	Phenotype	Reference
Ureteric bud induction		
Lim-1	Bilateral renal agenesis	Shawlot and Behringer, 1995
Pax-2	Agenesis	Torres et al., 1995
WT-1	Agenesis	Kreidberg et al., 1993
Eya-1	Agenesis (-/-), renal hypoplasia & unilateral agenesis (+/-)	Xu et al., 1999
Sall-1	Renal agenesis or severe dysgenesis	Nishinakamura et al., 2001
Foxc1	Hydronephrosis & hydroureter	Kume et al., 2000
Id	Bilateral renal agenesis or renal hypoplasia	Maas et al., 1994
GDNF	Bilateral renal agenesis	Moore et al., 1996
c-ret	Agenesis or severe hypodysplasia	Schuchardt *et al.*, 1996
UB branching morphogenesis		
Emx-2	Lack of urogenital system	Miyamoto et al., 1997
Hoxa11/d11	Rudimentary or absent kidneys	Patterson et al., 2001
Bf-2	Reduced size of collecting duct system, reduction in UB branching, reduced nephron no.	Hatini et al., 1996
RARα/β2	Small kidneys, impaired UB branching, reduced nephron no.	Mendelsohn et al., 1994; Mendelsohn et al., 1999

UB: ureteric bud

involve hypoplastic kidneys with decreased renal function and occasionally unilateral renal agenesis (Eccles *et al.*, 2003).

The Wilms tumour-associated gene, *WT-1*, has been identified as an important gene involved in early kidney development (Kreidberg *et al.*, 1993). During the initial stages of metanephric development it is expressed in the uninduced metanephric mesenchyme and homozygous mutant mice show mid gestation lethality and lack kidneys (Kreidberg *et al.*, 1993). In E11.5 mutant embryos the ureteric buds are absent, the mesenchyme present is apoptotic and does not express *Pax-2* (Kreidberg *et al.*, 1993).

Mice lacking the *Eya-1* gene, a homologue of the *Drosophila* gene eyes absent (*eya*), lack kidneys (Xu *et al.*, 1999). *Eya-1* is expressed initially in the uninduced mesenchyme (E10.5) and thereafter in the induced mesenchyme (Xu *et al.*, 1999). In homozygous mutant mice the ureteric bud fails to invade the mesenchyme which becomes apoptotic (Xu *et al.*, 1999). Another gene expressed in the metanephric mesenchyme but not the ureteric bud epithelium at the time of the epithelial evagination is *Sall-1 (Sal like-1)*, a mammalian homologue of the *Drosophila* region specific homeotic gene *spalt* (sal) (Nishinakamura *et al.*, 2001). It is essential for early metanephric development as loss of *Sall-1* results in renal agenesis or dysgenesis due to lack of ureteric bud invasion of the metanephric mesenchyme and subsequent apoptosis of the uninduced mesenchyme (Nishinakamura *et al.*, 2001). In humans, mutation of the *SALL1* gene results in renal dysplasia and lower urinary tract malformations in Townes-Brockes syndrome (Woolf *et al.*, 2003). The metanephric expression of the transcription factors *Foxc1/Mf1 (Mesoderm/mesenchyme forkhead-1)* and *Foxc2/Mfh1 (Mesenchyme forkhead-1)* is overlapping and concentrated at E10.5 in the uninduced mesenchyme but not in the epithelium (Kume *et al.*, 2000). Their loss is responsible for the formation of duplex kidneys and double ureters with unilateral fluid filled dilation of the kidney and ureter in mice (Kume *et al.*,

2000). This phenotype is a result of more anterior expression of GDNF and Eya-1 transcripts leading to formation of ectopic ureteric buds (Kume *et al.*, 2000).

Formins are nuclear proteins expressed in both the metanephric mesenchyme and ureteric bud at the time of the kidney induction (E11.5) (Maas *et al.*, 1994). The loss of formin in mice homozygous for the *limb deformity (ld)* mutation, results in renal abnormalities ranging from agenesis to renal hypoplasia due to deficient ureteric bud outgrowth (Maas *et al.*, 1994).

Genes required for ureteric bud branching

Hox genes are a family of clustered genes that encode homeodomain-containing transcription factors. Mutant mice of either *Hoxa11* or *Hoxd11* have normal kidneys suggesting functional redundancy whereas double mutants have rudimentary or in extreme cases absent kidneys (Patterson *et al.*, 2001). Their expression in the early developing kidney is similar and is restricted to the caudal end of the intermediate mesoderm (Patterson *et al.*, 2001). At the time of ureteric bud evagination their expression is found in the metanephric mesenchyme surrounding the emerging ureteric bud and the expression continues in the induced mesenchyme surrounding the branching ureteric tips (Patterson *et al.*, 2001). In the double mutant mice, the ureteric bud emerges from the Wolffian duct as in the wild type embryos of the same age. However in the most severe cases the ureteric bud does not grow or branch further; in the less severe cases its branching is impaired in the mid-ventral region of the kidney (Patterson *et al.*, 2001). The mutant mesenchyme shows downregulation of mesenchymal markers such as WT-1 and Pax-2 suggesting a defective response to ureteric bud induction (Patterson *et al.*, 2001). There is also a reduced expression of GDNF from the ventral region at the area of the branching defect (Patterson *et al.*, 2001).

Emx-2 is a homeobox transcription factor expressed in the ureteric epithelium at the time of the ureteric bud induction (E11.5) but not in the mesenchyme or the pretubular aggregates (Miyamoto *et al.*, 1997; Pellegrini *et al.*, 1997). Mice

lacking *emx-2* show lack of urogenital system (Miyamoto *et al.*, 1997). The ureteric bud at E11.5 invades the mesenchyme bud there is no dilation of the bud tip and no further branching (Miyamoto *et al.*, 1997). Loss of *emx-2* affects the epithelial compartment since in the mutant embryos (at E11.5) the mesenchymal markers WT-1 and Pax-2 are expressed normally whereas there is a reduction of c-ret and GDNF expression essential for ureteric bud branching (see below) (Miyamoto *et al.*, 1997).

The Wnt gene family comprises one superfamily of developmentally important signaling molecules which are involved in metanephric development (for review see Cadigan and Nusse, 1997; Carroll and McMahon, 2000; Vainio *et al.*, 1999). In early metanephric development *Wnt-2b* is expressed as early as E11.5 in the perinephric mesenchymal cells as well as in the mesenchymal cells in the region close to the stalk of the ureteric bud and supports ureteric bud growth and branching in culture (Lin *et al.*, 2001a). *Wnt-6*, *Wnt-11* and *Wnt-7b* are expressed in the ureteric epithelium (Lin *et al.*, 2001a; Kispert *et al.*, 1996). *Wnt-11* is expressed specifically at the tip of the branching epithelium, expression which correlates with the sites of epithelio-mesenchymal interactions and its expression is regulated by GDNF and sulphated proteoglycans (see below) whereas *Wnt-7b* expression is excluded from the tip and is suggested to play a role in duct maintenance and growth (Carroll and McMahon, 2000; Kispert *et al.*, 1996).

Stromal genes required for ureteric bud branching

The metanephric mesenchyme will give rise to both the epithelial cells of the nephrons and the stromal cells of the mature kidney. *Foxd1/Bf2 (Brain factor-2)* is expressed specifically in the stromal mesenchymal cells of the kidney (Hatini *et al.*, 1996). At E12.5 it is restricted to a population of cells that surround the condensations of the metanephric mesenchyme, and at later stages its expression is detected in the cortical stroma that surrounds differentiating nephrons (Hatini *et al.*, 1996). Homozygous mutant mice die after the first 24 hours after birth from renal abnormalities (Hatini *et al.*, 1996). In the mutant mice, the ureteric

bud shows an abnormal branching pattern probably due to ectopic *c-ret* expression as well as a 8- to 16- fold reduction in the number of branches, with abnormally large mesenchymal condensates (Hatini *et al.*, 1996).

The retinoic acid receptor (RAR) β2 is expressed in the stromal cells surrounding the ureteric bud and the induced mesenchyme (E12), overlapping with Bf-2 expression (Mendelsohn *et al.*, 1999). RARα is also expressed in the embryonic kidney in the ureteric bud, metanephric mesenchyme and stromal cells where is co-expressed with RARβ2 (Mendelsohn *et al.*, 1999). Generation of RARα/β2 double homozygous mice results in renal defects which demonstrate the essential function of retinoids during metanephric development (Mendelsohn *et al.*, 1994). The double mutants exhibit bilateral renal hypodysplasia (often ectopic) which is also associated with dilation of the renal pelvis (hydronephrosis) (Mendelsohn *et al.*, 1994). The ureteric bud of the double mutant embryonic kidneys display impaired branching morphogenesis with a fourfold reduction in the number of tips compared to wild type embryos of the same age accompanied with a reduction in c-ret expression (Mendelsohn *et al.*, 1999). Restoring c-ret expression in the ureteric bud epithelium has been shown to rescue the ureteric bud branching in RARα/β2 double homozygous mice (Batourina *et al.*, 2001).

The role of secreted peptide growth factors

Research evidence has shown that several secreted peptide growth factors, expressed in the ureteric bud or the metanephric mesenchyme, exert regulatory effects on ureteric bud branching morphogenesis *in vivo* and *in vitro*. Some of them include members of the Transforming growth factor (TGF-) β superfamily, the Fibroblast growth factor (FGF) family, and HGF/SF (figure 1.6; table 1.2).

GDNF and related neurotrophic factors

The glial cell line-derived neurotrophic factor (GDNF) family consists of five members (GDNF, neurturin, persephin, artemin and enovin) which are distant

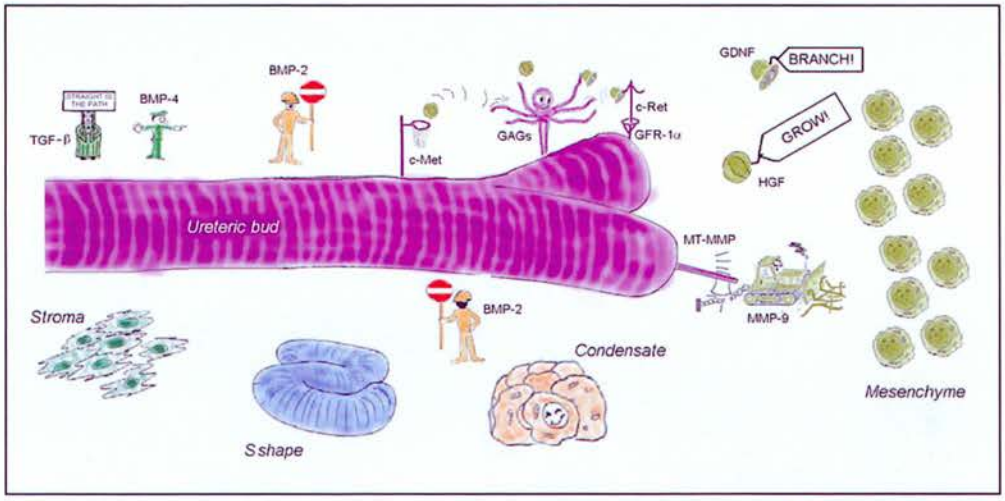

(From Davies and Fisher, 2002)

Figure 1.6: Key regulatory signals during ureteric bud branching morphogenesis

Table 1.2: Major regulators of ureteric bud branching morphogenesis

Growth factors		
Activin	Abnormal UB branching pattern with failure to produce many secondary branches (OC)	Ritvos *et al.*, 1995
BMP-2	Inhibits branching (3DC)	Piscione *et al.*, 1997
BMP-4	Reduction in branching (T)	Miyazaki *et al.*, 2000
	Promotes elongation of UB (OC)	
BMP-7	Low doses stimulate branching (3DC)	Piscione *et al.*, 1997
	High doses inhibit branching (3DC)	
FGF-1	Promotes elongation of UB branches (IUBC)	Qiao *et al.*, 2001
FGF-2	Promotes growth of UB (IUBC)	Qiao *et al.*, 2001
FGF-7	Promotes growth of UB (IUBC)	Qiao *et al.*, 2001
FGF-10	Promotes elongation of UB branches (IUBC)	Qiao *et al.*, 2001
GDNF	Promotes UB outgrowth from WD (OC)	Sainio *et al.*, 1997,
	Promotes branching (OC)	Towers *et al.*, 1998,
		Vega *et al.*, 1996
HGF/SF	Promotes branching, rescues elongation of UB branches (OC)	Woolf *et al.*, 1995,
		Davies *et al.*, 1995
Neurturin	Slight increase in UB branching, rescues UB branching (OC)	Davies *et al.*, 1999
Persephin	Rescues UB branching (OC)	Milbrandt *et al.*, 1998
Pleiotrophin	Promotes branching (IUBC), promotes growth of UB (OC)	Sakurai *et al.*, 2001
TGFβ	Inhibits UB growth, abnormal branching with long UB branches (OC), inhibits branching (3DC)	Clark *et al.*, 2001,
		Ritvos *et al.*, 1995,
		Santos and Nigam, 1993
Matrix components		
Heparan sulphate PGs	Required for UB branching (OC, T)	Davies *et al.*, 1995,
		Bullock *et al.*, 1998
Integrins α8	Impaired UB branching (T)	Muller *et al.*, 1997
Integrins α3 & α6	Required for UB branching (OC)	Zent *et al.*, 2001
MMP-2 & -9	Required for UB branching (OC)	Barasch *et al.*, 1999,
		Lelongt *et al.*, 1997
Signal transduction pathways		
Erk MAP kinase	Required for UB branching (OC)	Fisher *et al.*, 2001
PI3 kinase	Required for UB branching (OC)	Tang *et al.*, 2002
Protein kinase A	Inhibition of branching (3DC)	Gupta *et al.*, 1999

3DC: data from three-dimensional tubulogenesis model culture experiments, IUBC: data from isolated ureteric bud culture model experiments, OC: data from organ culture experiments, T: data from transgenic mice, UB: ureteric bud, WD: Wolffian duct

members of the TGF-β superfamily (reviewed in Masure *et al.*, 1999; Saarma, 2000). The neurotrophic factor GDNF is the first member of the GDNF family and was identified by its ability to promote the survival of midbrain dopaminergic neurons in culture. GDNF does not signal through receptor serine/threonine kinases but activates the transmembrane receptor tyrosine kinase (RTK) Ret (Worby *et al.*, 1996). GDNF induced activation of the Ret protein kinase requires the specific binding of the ligand to a glycosyl-phosphatidyl inositol- (GPI-) linked cell surface protein called GDNF family receptor α1 (GFRα1) (Jing *et al.*, 1996). The amino acid homology between the members of the GDNF family is between 40 and 50%. They all signal through the activation of the receptor tyrosine/kinase Ret and one of four GPI-anchored proteins GFRα1-4 (reviewed in (Rosenthal, 1999; Saarma, 2000). Neurturin binds to GFRα2, artemin binds to GFRα3 and persephin activates Ret by binding to GFRα4 (Saarma, 2000). GDNF, NTN and artemin cross-talk weakly with other GFRα receptors (reviewed in Rosenthal, 1999; Saarma, 2000). GDNF can also activate Ret by binding to GFRα2 (Sanicola *et al.*, 1997).

In the murine developing kidney GDNF, Ret and GFRα1 level of mRNA expression is high from E12 through to E18 (Golden *et al.*, 1999). The receptors are primarily expressed in the branching tubular epithelial components whereas GDNF is expressed in the areas of the surrounding mesenchyme (Golden *et al.*, 1999; Moore *et al.*, 1996). At earlier stages (E9-E10.5), Ret is expressed in the nephric duct of the pronephros and mesonephros (Pachnis *et al.*, 1993). At more advanced stages (E13.5- E17.5) Ret expression is confined to the tips of the branching ureteric bud and not to the mesenchymal-derived epithelial components (Pachnis *et al.*, 1993). GFRα1 mRNA is detected in the terminal buds and at low levels in the mesenchyme closely associated with the terminal buds (Towers *et al.*, 1998). GFRα1 protein is found localized to the ureteric bud as well as the condensed mesenchymal cells of the comma- and S- shaped bodies (Ehrenfels *et al.*, 1999).

Mice lacking GDNF show complete bilateral renal and ureteral agenesis (Moore *et al.*, 1996). Heterozygous embryos show an increased incidence of unilateral renal agenesis or hypoplasia with approximately 30% fewer nephrons (Cullen-McEwen *et al.*, 2001; Moore *et al.*, 1996). Newborn mice, homozygous for a mutation in c-ret, display renal agenesis or severe hypodysplasia (Schuchardt *et al.*, 1996). In the mutant kidneys, at the embryonic days 11 and 12.5, the ureteric buds either never contact the mesenchyme or their entering is delayed. When the mutant ureteric buds have entered the mesenchyme the branching pattern appears abnormal (Schuchardt *et al.*, 1996). Mice lacking the GFRα1 co-receptor demonstrate renal agenesis or unilateral or bilateral dysgenesis, phenotypes similar to those of GDNF and Ret-deficient mice whereas the heterozygotes show no kidney defects (Cacalano *et al.*, 1998; Enomoto *et al.*, 1998). The metanephric mutant kidneys (E11.5), show lack of formation of the ureteric bud or inability of the UB to penetrate the metanephric mesenchyme. This leads to failure of the latter to form condensates hence the small nephron numbers observed after the histological analysis of the dysplastic kidneys (Enomoto *et al.*, 1998).

At early developmental stages (E10.5), local application of a GDNF source promotes the initiation of ureteric bud in culture (Brophy *et al.*, 2001; Sainio *et al.*, 1997b). Since GDNF is expressed at the mesenchyme around the tips of the ureteric bud it is has been reported that it binds directly to the tips (Sainio *et al.*, 1997b; Towers *et al.*, 1998). In culture, addition of exogenous GDNF results in an increase in number of branching ureteric bud tips whereas blocking GDNF function results in a reduction in branching morphogenesis (Towers *et al.*, 1998; Vega *et al.*, 1996). In kidneys cultured in chlorate, addition of exogenous GDNF results in the rescue of ureteric bud branching (Sainio *et al.*, 1997b). Local application of GDNF attracts the ureteric bud branches towards the growth factor source suggesting a chemoattractant effect (Sainio *et al.*, 1997b; Tang *et al.*, 1998). Recently the Erk1/2 mitogen-activated protein kinase (MAP kinase) and the phosphoinositide 3-OH kinase (PI-3 kinase) have been identified to act

downstream of GDNF signaling regulating ureteric bud branching (Fisher *et al.*, 2001; Tang *et al.*, 2002).

Neurturin (NTN) is expressed at the ureteric bud as early as E10.5 in mice (Davies *et al.*, 1999). At later embryonic stages (E16, E18) its expression is increased but is detected to a moderate level in relation to the expression of Ret and GDNF (Golden *et al.*, 1999). Both neurturin and its receptor GFRα2 are primarily expressed in the branching tubular epithelial components of the developing metanephros suggesting an autocrine role (Davies *et al.*, 1999; Golden *et al.*, 1999). In organ culture, addition of NTN results only in a slight increase of ureteric bud branching probably due to the presence of endogenous GDNF (Davies *et al.*, 1999). Addition of neurturin in organ cultures in the presence of function blocking anti-GDNF results in an increase of ureteric bud branching (Davies *et al.*, 1999).

Persephin (PSP) mRNA is expressed at low levels in the developing rat metanephric kidney (E_r18) (Milbrandt *et al.*, 1998). In murine kidney organ cultures when branching morphogenesis is blocked (treatment with sodium chlorate that deprives them of sulphated proteoglycans (Davies *et al.*, 1995)(see below) the addition of PSP rescues the branching (Milbrandt *et al.*, 1998).

Transforming Growth Factors-β and Activin

Transforming growth factors-β (TGF-β) are expressed throughout embryogenesis and their receptors are ubiquitously expressed (reviewed in Massague, 1990). Three isoforms of TGF-β have been identified in mammals: TGF-β1, 2, and 3. The biological activities of the TGF-β are diverse: they control cell proliferation either in a stimulatory or inhibitory fashion, they control cell adhesion by enhancing synthesis and deposition of extracellular matrix components and they also promote cell differentiation (reviewed in Massague, 1990; Moses *et al.*, 1990).

Expression of TGF-β is high in sites undergoing intense development and morphogenesis including the epithelial/mesenchyme interface (Lehnert and Akhurst, 1988). TGF-β1 mRNA is expressed by the mesenchymal cells that will develop into stroma, at E15.5 in mice (Lehnert and Akhurst, 1988). At earlier stages (E12.5) only TGF-β2 is present in the embryonic kidney at a very restricted pattern in the basement membrane of the cuboidal epithelium (Pelton *et al.*, 1991).

In culture, TGF-β exerts an inhibitory effect on kidney growth and branching morphogenesis. In mouse organ culture, addition of TGF-β results in an abnormal branching pattern where the ureteric bud appears to grow rapidly in length and does not branch until it reaches the periphery of the metanephric mesenchyme (Ritvos *et al.*, 1995). In rat metanephric organ cultures, addition of TGF-β1 inhibits the overall organ growth accompanied with reduced nephron number (Clark *et al.*, 2001; Rogers *et al.*, 1993). A similar effect is seen with the addition of TGF-β2 in rat organ cultures, which significantly impairs ureteric growth and results in smaller kidneys (Martinez *et al.*, 2001). In the MDCK tubulogenesis model, addition of TGF-β results in inhibition of tubulogenesis and formation of branching processes (Santos and Nigam, 1993). Even though TGF-β seems important for ureteric bud branching in culture, TGF-β1 homozygous null mutant mice do not display kidney defects (Kulkarni and Karlsson, 1993).

Inhibins and activins are members of the TGF-β family. Activins are hetero/homodimers of two closely related subunits ($\beta_A\beta_A$, $\beta_B\beta_B$ and $\beta_A\beta_B$) (reviewed in Massague, 1990). In the developing kidney the β_B subunit is detected in the kidney capsule, the β_A subunit transcripts are detected in the smooth muscle cells surrounding the ureter (E17) and none is detected on the ureteric epithelium (Ritvos *et al.*, 1995). However, the addition of activin in E11 kidney organ culture disrupts normal branching morphogenesis. Branching is

delayed, characterized by abnormally short intercalating distances between branches and by failure to produce as many secondary branches as the control metanephroi (Ritvos *et al.*, 1995).

Bone morphogenetic proteins

Members of the bone morphogenetic protein (BMP) family, a subgroup of the TGF-β superfamily, have been shown to be important signaling molecules throughout mouse development, and many BMPs display dynamic expression patterns during murine kidney organogenesis (for review see Godin *et al.*, 1999). Bone morphogenetic protein 2 (BMP-2) is expressed in the induced mesenchymal pretubular aggregates and in culture is found to be inhibitory, resulting in short ureteric buds (Godin *et al.*, 1999; Piscione *et al.*, 1997). In the mIMCD-3 cell model of tubulogenesis, the BMP-2 inhibitory effect is more potent than any other member of the TGF-β superfamily (Piscione *et al.*, 1997). In this tubulogenic model system BMP-2 regulates branching morphogenesis via Smad1/4 signaling pathway and by activation of protein kinase A (PKA) (Gupta *et al.*, 2000; Gupta *et al.*, 1999).

Heterozygous Bmp4 null mutant mice show renal defects that mimic human congenital anomalies of the kidney and urinary tract (CAKUT), and the kidney hypo/dysplasia results from reduced branching of the ureter (Miyazaki *et al.*, 2000). Bone morphogenetic protein 4 (BMP-4) is expressed in the mesenchymal cells that surround the Wolffian duct (at E10.5), then is expressed at the stromal mesenchymal cells surrounding the main trunk and the stalk of the branching ureteric bud (at E12.5) but not around the tip (Miyazaki *et al.*, 2000). Results from culture experiments showed that BMP-4 does not increase the number of branches, however it is important for bud growth and elongation (Miyazaki *et al.*, 2000). BMP-4 specifically inhibits GDNF signaling to or within the ureteric epithelium without directly modulating the expression pattern of GDNF itself (Miyazaki *et al.*, 2000). In the mutant mice the ureteric bud evaginates cranially from the WD (Miyazaki *et al.*, 2000) suggesting that BMP-4 probably regulates

the initial ureteral budding by antagonizing GDNF signaling on the WD (Brophy *et al.*, 2001).

Embryos lacking BMP-7 show abnormalities in renal and ocular systems (Dudley *et al.*, 1995; Luo *et al.*, 1995). Most of the mutant embryos display severe bilateral renal dysplasia and die within the first 24 hours postpartum from renal failure (Dudley *et al.*, 1995). BMP-7 is expressed at the Wolffian duct before ureteric bud outgrowth and at the epithelium during its evagination (Godin *et al.*, 1998). At E11.5 BMP-7 is expressed in the ureteric bud and surrounding mesenchyme, at E13.5 it is expressed at the epithelium and condensed mesenchyme associated with the ureteric bud tips (Godin *et al.*, 1998). At later stages of development, BMP-7 is detected at the mesenchymal stem cells, condensing aggregates, and the epithelia of the comma and S-shaped pretubular structures, with weaker expression found in the ureteric ducts (Dudley *et al.*, 1995). In three dimensional culture models, low doses of BPM-7 were found to stimulate the branching of the ureteric bud whereas higher doses were inhibitory (Piscione *et al.*, 1997).

Fibroblast growth factors

Members of the fibroblast growth factor (FGF) family are known regulators of epithelial growth and branching morphogenesis in other organs such as the mammalian embryonic lung and the *Drosophila* trachea (Bellusci *et al.*, 1997; Metzger and Krasnow, 1999; Morita and Nogawa, 1999; Weaver *et al.*, 2000). FGF members and their receptors are expressed at the embryonic kidney. Nine FGFs (FGF-1 through FGF-5 and FGF-7 through FGF-10) are expressed early (from at least E_r14) in rat metanephric development and continue to be expressed throughout metanephrogenesis (Cancilla *et al.*, 1999). However knockout mice for FGF-2, 3 and 5 do not have any obvious kidney defects (Cancilla *et al.*, 1999). Only the FGF-7 mutant mice show kidney defects, with smaller ureteric buds, mature renal collecting system and 30% fewer nephrons than the wild type kidneys (Qiao *et al.*, 1999b). In rat organ cultures blocking FGF-7 results in

reduction in branching morphogenesis of the ureteric bud (Qiao *et al.*, 2001). FGF-7 is expressed at the stroma surrounding the growing ureteric bud and is suggested to influence ureteric bud growth (Qiao *et al.*, 1999b). However it is first detected in mice at E14.5, suggesting that the ureteric bud growth between embryonic days 11.5 to 13.5 is regulated by other than FGF-7 factors (Qiao *et al.*, 1999b). The effect of FGFs on ureteric bud branching morphogenesis comes from evidence on the isolated ureteric bud culture system (Qiao *et al.*, 2001; Qiao *et al.*, 1999a; Sakurai *et al.*, 1997; Sakurai *et al.*, 2001). FGF-1, -2, -7 and -10 facilitate UB branching although their ability to induce branching morphogenesis is different (Qiao *et al.*, 2001). FGF-1 and FGF-10 produce elongated branching tubular structures with clear distinction between stalk and ampullae regions whereas FGF-2 and FGF-7 result in the formation of less ordered structures which are more globular with less distinct areas between ampullae and stalks (Qiao *et al.*, 2001).

Pleiotrophin and Midkine

Recently, pleiotrophin, an 18 kDa heparin-binding protein was identified as a paracrine mesenchymal factor involved in ureteric bud branching morphogenesis (Sakurai *et al.*, 2001). Addition of pleiotrophin and GDNF was found to be capable of inducing branching morphogenesis in isolated ureteric buds cultured within an extracellular matrix gel [1:1 mixture of growth factor reduced Matrigel and Type I collagen] (Sakurai *et al.*, 2001). In rats, pleiotrophin mRNA is expressed at the metanephric mesenchyme during developmental stages E_r15 and E_r17 (Vanderwinden *et al.*, 1992). In the mouse, the protein is found to be present in the mesenchyme and the ureteric bud at early development (E12.5-E13.5), whereas at later stages (E14.5- E16.5) it is absent from the mesenchyme and is localized on the surfaces of the epithelial cells (Mitsiadis *et al.*, 1995). Sakurai and others have also found the protein present at the basement membrane of the developing ureteric bud at an even earlier stage (E13) (Sakurai *et al.*, 2001). In organ culture, exogenous pleiotrophin stimulates ureteric bud

growth and results in an enlargement of the whole rudiment (Sakurai *et al.*, 2001).

Midkine (MK) is a heparin-binding molecule sharing a 50% sequence identity with pleiotrophin, that can be induced in some cell types by treatment with retinoic acid (Mitsiadis *et al.*, 1995). In embryonic murine metanephros MK, like pleiotrophin, is found in both metanephric mesenchyme and ureteric epithelium at developmental stages E12.5-E13.5 (Mitsiadis *et al.*, 1995). Unlike pleiotrophin, MK is present at both basement membranes of collecting ducts and condensing mesenchyme (E14.5) (Mitsiadis *et al.*, 1995) suggesting that MK may exert effects on either mesenchymal or epithelial cells. However, knockout mice lacking the MK gene develop normally, showing no kidney defects (Nakamura *et al.*, 1998).

Hepatocyte growth factor

The hepatocyte growth factor/ scatter factor (HGF/SF) was identified as a mesenchymal cell-derived cytokine with diverse effects on different target cells during normal development, regeneration and carcinogenesis (reviewed in Birchmeier and Gherardi, 1998; Montesano *et al.*, 1991a; Rosen *et al.*, 1994). The biological activity of HGF expands in a wide range as it dissociates epithelial sheets into individual cells, it stimulates cell motility and invasion, is mitogenic and a potent morphogen of epithelial cells (reviewed in Balkovetz, 1998; Birchmeier and Gherardi, 1998; Rosen *et al.*, 1994).

HGF is a heparin-binding glycoprotein, which belongs to the plasminogen-related growth factor family and signals through receptor tyrosine kinase which is encoded by the *c-met* proto-oncogene (Birchmeier and Gherardi, 1998; Rosen *et al.*, 1994). In the embryonic kidney, both HGF and c-met are expressed from E11.5 onwards corresponding to the onset of tubulogenesis and branching morphogenesis (Santos *et al.*, 1994). At that time HGF mRNA is detected in the metanephric mesenchyme, and met transcripts are detected both in the

mesenchyme and the ureteric bud (Woolf *et al.*, 1995). By E14 the highest expression of the receptor is detected in the branching tips of the ureteric bud (Woolf *et al.*, 1995). Blocking of HGF in culture, inhibits growth of the kidney rudiments, reduces the ureteric bud branching, limits nephron formation and is associated with an increase in apoptosis in mesenchymal cells (Santos *et al.*, 1994; Woolf *et al.*, 1995). Furthermore, the tips of the ureteric bud branches appear dilated or cystic (Woolf *et al.*, 1995). HGF also promotes ureteric branch elongation in sulphated glycosaminoglycans-deprived kidneys in culture (Davies *et al.*, 1995). Mice lacking HGF do not show any kidney defects (Uehara *et al.*, 1995).

HGF is secreted as an inactive zymogen and must be cleaved by a serine protease to initiate Met signaling (for review Rosen *et al.*, 1994). A serine protease specific for HGF, HGF activator (HGFA) is expressed and activated by the ureteric bud (van Adelsberg *et al.*, 2001). HGFA is found localized around the ampullae of the ureteric buds (van Adelsberg *et al.*, 2001). Blocking the activation of HGF with protease inhibitors *in vitro*, results in smaller, dysmorphic kidneys with reduced branching morphogenesis as well as reduced nephrogenesis and glomerulogenesis (van Adelsberg *et al.*, 2001).

The three biological responses induced by HGF (scattering, growth and branching morphogenesis/tubulogenesis) are mediated by a variety of signaling pathways (reviewed in Balkovetz, 1998). Research evidence from the MDCK and mIMCD-3 two-dimensional and three-dimensional (tubulogenesis) models has shown that HGF signaling is dependent on protein kinase C, protein kinase A (Santos *et al.*, 1993), PI 3-kinase (Khwaja *et al.*, 1998) as well as the Ras-Rac/Rho pathway, p42/44 MAP kinase (Karihaloo *et al.*, 2001b; Ridley *et al.*, 1995) and the signal transducers and activator of transcription (STAT) pathway (Boccaccio *et al.*, 1998).

The role of the extracellular matrix

Mammalian organogenesis and especially branching morphogenesis is characterized by extensive tissue growth and remodeling. The ureteric bud cells are surrounded by extracellular matrix proteins which function as to provide mechanical support as well as to mediate biological processes such as cell adhesion and motility. The dynamic remodeling of the extracellular matrix during ureteric bud growth and ramification in coordination with gene expression and the auto/paracrine regulatory molecules result in the formation of the collecting duct tree (reviewed in Wallner *et al.*, 1998).

Extracellular matrix proteins and Integrins

Proteoglycans (PG) are macromolecules composed of glycosaminoglycan (GAG) chains covalently bound to a protein core (reviewed in Kjellen and Lindahl, 1991). Proteoglycans may occur intracellularly, at the cell surface or in the extracellular matrix and their role ranges from mechanical support to functions in adhesion, motility, proliferation, differentiation and morphogenesis (Kjellen and Lindahl, 1991). Hyaluronan (HA), the largest of the glycosaminoglycans, and its receptor CD44 are found localized near the basal cell surface of the developing ureteric bud and at the basolateral surfaces of UB-derived structures respectively (Pohl *et al.*, 2000). In a three-dimensional tubulogenesis model blocking the HA-CD44 axis prevents the branching morphogenesis (Pohl *et al.*, 2000). In the same tubulogenesis model (isolated UB-cells) the receptor is localized at the tips of the branching tubules indicating a function in tip elongation (Pohl *et al.*, 2000).

Heparan sulphate PGs are expressed at the surface of most animal cells, and have been implicated in the presentation of a number of signaling molecules to their receptors during signal transduction (reviewed in Bernfield *et al.*, 1999). They are important during early kidney development (reviewed in Davies *et al.*, 2001). Syndecan-1 is strongly expressed at the tips of the ureteric bud and at the condensing mesenchyme around them (Davies *et al.*, 1995; Vainio *et al.*, 1989). Heparan and chondroitin sulphates are expressed in the basement membranes of the ureteric bud epithelium and the mesenchymal matrix (Davies *et al.*, 1995).

The necessity for GAGs in ureteric bud branching morphogenesis *in vivo* has been demonstrated by a heparan-sulphate-2-O-sulphotransferase-knockout mouse which exhibits bilateral renal agenesis (Bullock *et al.*, 1998). Mutant mice at E11.5 and E12.5 contain unbranched ureteric buds with no signs of mesenchymal condensation (Bullock *et al.*, 1998). In organ cultures, treatment of embryonic kidneys with enzymes that destroy existing glycosaminoglycans impaired ureteric bud branching morphogenesis (Davies *et al.*, 1995). Treatment of kidneys with sodium chlorate, a specific sulphation inhibitor, which competes with sulphate for sulphotransferase enzymes and blocks the formation of new glycosaminoglycan chains results in failure of ureteric bud development (Davies *et al.*, 1995). Sulphated proteoglycans are important for the maintenance of *Wnt-11* expression in the tips of the ureteric bud (Kispert *et al.*, 1996). Ret expression is also lost from the tips of the epithelium in chlorate treated kidneys (Kispert *et al.*, 1996). GDNF requires sulphated GAGs for GDNF-receptor binding (Barnett *et al.*, 2002).

Glypicans are a family of GPI-linked cell surface heparan sulfate proteoglycans which control cellular responses to growth factors and cell proliferation and apoptosis (Cano-Gauci *et al.*, 1999). Mice lacking glypican-3 (GPC3) exhibit several of the clinical features observed in patients with the Simpson-Golabi-Behmel syndrome (SGBS), including developmental overgrowth, lung abnormalities and display cystic and dysplastic kidneys (Cano-Gauci *et al.*, 1999). The ureteric bud of the E12 mutant kidneys shows a larger number of ureteric bud branches (Cano-Gauci *et al.*, 1999).

Basement membrane components and their receptors have been implicated in the regulation of epithelial morphogenesis of developing branching organs such as the salivary gland (Hardman and Spooner, 1992a; Kadoya and Yamashina, 1989). Laminins are a large family of extracellular glycoproteins found in basement membranes. Laminins interact with integrin type of receptors on the cell surface, but binding to other proteins such as dystroglycan as a high affinity

receptor for laminin-1, and nidogen as a high-affinity laminin-binding protein important for basement-membrane assembly has also been demonstrated (Durbeej and Ekblom, 1997; Ekblom *et al.*, 1998). Nidogen is produced by the metanephric mesenchyme of the developing kidney (Ekblom *et al.*, 1994). Antibodies blocking laminin-nidogen interaction *in vitro* result in altered morphogenesis of E12 kidneys with fewer ureteric bud branches and less newly formed epithelium around the tips (Ekblom *et al.*, 1994). Laminin-5 is also expressed on the basement membrane of both the Wolffian duct and ureteric bud (E11) (Airenne *et al.*, 2000). Addition of a function blocking antibody against Laminin-5 results in smaller kidney rudiments with less ureteric bud branching (Zent *et al.*, 2001).

Many of the interactions between cells and the extracellular matrix are mediated by the integrin family of cell surface receptors (reviewed in Juliano and Haskill, 1993; Katz and Yamada, 1997; Tarone *et al.*, 2000). Integrins are heterodimeric transmembrane glycoproteins, composed of a single α and β peptide subunit that can associate in various combinations (Hynes, 1992). A single β subunit is able to form heterodimers with several α subunits, while the α subunit largely determines the substrate specificity with ECM proteins (Tarone *et al.*, 2000). Integrins play a crucial role in tissue and organ morphogenesis as they bind to cytoskeletal proteins of the actin contractile system thus directly mediating cell attachment, spreading and migration and also mediate and co-participate in the activation and regulation of signal transduction pathways (Katz and Yamada, 1997; Tarone *et al.*, 2000).

Mutations in the α3 and α8 integrin genes have resulted in renal defects suggesting a role in collecting duct development (Kreidberg *et al.*, 1996; Muller *et al.*, 1997). Ligands for the α3β1 integrin include laminin (Laminin-1 and –5), certain type of collagen, fibronectin and entactin (nidogen) (Kreidberg *et al.*, 1996). Ligands for the α8β1 include fibronectin, vitronectin and tenascin-C (Muller *et al.*, 1997).

During kidney development (at E14), α3β1 integrin is expressed by podocytes in the glomeruli and on collecting ducts suggesting that it is a receptor for the basement membrane of these cells (Kreidberg *et al.*, 1996). The α3 mutant mice die within the first 24 hours after birth with severe renal abnormalities, which include small sized kidneys and presence of stromal component between the collecting ducts in the renal medulla (Kreidberg *et al.*, 1996). In the developing kidney, α8β1 is expressed at the mesenchymal component as early as E11 corresponding to the ureteric bud outgrowth from the WD (Muller *et al.*, 1997). Upon branching of the ureteric bud, expression of the α8 integrin subunit is present at the mesenchymal condensates surrounding the tips of the branching epithelium and at the pretubular aggregates but not on comma- or S- shaped bodies (Muller *et al.*, 1997). The α8 homozygous mutant mice show a variety of renal defects ranging from kidney agenesis (where the ureteric bud has not invaded the mesenchyme) to dysgenesis (where the ureteric bud shows defective branching morphogenesis and the epithelialization of the metanephric mesenchyme is impaired) (Muller *et al.*, 1997).

Evidence from *in vitro* models, have suggested roles for the α3, α6, β1 and β4 subunits on ureteric bud branching morphogenesis (Zent *et al.*, 2001). In rat organ cultures, blocking the function of the α3 subunit with function blocking antibody disrupts both the branching and elongation of the ureteric bud (Zent *et al.*, 2001). In the same culture system, blocking the β1 subunit also results in impaired branching morphogenesis (Zent *et al.*, 2001). The integrin α6 subunit is known to associate with either the β1 or β4 subunits to form the laminin integrins α6β1 and α6β4 (Durbeej and Ekblom, 1997). The α6 integrin subunit is present in the ureteric bud predominantly as integrin α6β4 and blocking of either subunits with function blocking antibodies in organ cultures results in reduction in branching morphogenesis of the ureteric epithelium (Zent *et al.*, 2001). The addition of a combination of function blocking antibodies to subunits α3 and α6 results in a dramatic effect on UB branching in culture, whereas in the

double mutant embryos $\alpha3^{-/-}/\alpha6^{-/-}$ the ureteric buds show no defects (De Archangelis *et al.*, 1999; Zent *et al.*, 2001).

Extracellular matrix degrading proteins

A constant remodeling of the extracellular matrix is needed at the growing tips of the ureteric bud as it invades the metanephric mesenchyme during branching. The major enzymes that degrade ECM and cell surface proteins are the matrix metalloproteinase (MMP) family of secreted and membrane proteinases (Werb, 1997). MMPs are a large family of zinc requiring matrix-degrading enzymes involved in physiologic and pathologic processes including invasive cell behaviour in cancer and tissue morphogenesis in embryonic development (reviewed in Sternlicht and Werb, 2001).

In the developing kidney (E11), the metanephric mesenchyme is responsible for the production of MMP-2 and MMP-9 (Lelongt *et al.*, 1997). In organ culture, addition of either a function blocking antibody to MMP-9 or exogenous tissue inhibitor of metalloproteinase 1 (TIMP-1), the natural inhibitor of MMP-9, resulted in impaired branching morphogenesis of the ureteric bud (Lelongt *et al.*, 1997).

MMP-2 is activated at the cell surface through an interaction with membrane-type matrix metalloproteinase 1 (MT-1-MMP):TIMP-2 complex (Kanwar *et al.*, 1999; Sternlicht and Werb, 2001). In the developing mouse kidney, MT-1-MMP is expressed at the ureteric bud epithelium (Ota *et al.*, 1998). Inhibition of MMP-2 and MT-1-MMP with antisense oligodeoxynucleotides (ODN) resulted in dysmorphogenesis of the ureteric bud with rudimentary branching and blunted tips (Kanwar *et al.*, 1999). Even though the MMP-2 inhibitor TIMP-2, is synthesized by both the mesenchyme and epithelium in E_r13 metanephroi, the active TIMP-2 is found in the ureteric compartment (Barasch *et al.*, 1999). Immunohistochemical studies showed that TIMP-2 is localized in the condensed mesenchyme surrounding the tips of the ureteric bud and in the ureteric bud stalks and clefts (Barasch *et al.*, 1999). Addition of exogenous TIMP-2 in rat

metanephric cultures resulted in impaired branching morphogenesis and enhanced deposition of collagen IV at areas that are usually devoid of collagen IV, such as the tips of the branching epithelium (Barasch *et al.*, 1999).

Intrinsic mechanisms of the branching epithelium

During branching morphogenesis the newly formed branches arise as outpouchings of the epithelium, either by migration of a local region of epithelium or by local, oriented cell divisions in some cases accompanied by formation of a cleft in an existing branch (reviewed in Metzger and Krasnow, 1999).

The intrinsic mechanisms that are involved in the branching process during the early kidney development have received little attention. Most of the research during the early stages of kidney organogenesis has focused on the signals that the ureteric bud receives from the metanephric mesenchyme and the signaling pathways downstream of these signals (reviewed in Davies, 2001; Davies and Davey, 1999).

The importance of efficient ureteric bud branching morphogenesis is a requirement for correct nephron endowment and hence a fully functional kidney. The work in my thesis focuses on the intrinsic mechanisms of ureteric bud branching morphogenesis such as cell multiplication, cytoskeletal rearrangement and differential gene expression that are important during embryonic development and branching morphogenesis of other organs such as the lung, salivary gland and *Drosophila* trachea (Goldin *et al.*, 1984; Metzger and Krasnow, 1999; Spooner, 1973).

1.5 Aim of the thesis

With reference to the intrinsic mechanisms of epithelial development and using the kidney organ culture as an experimental system, my aim was to investigate whether cells in the active branching "tips" have specializations compared to the rest of the ureteric bud epithelium.

The questions that my work aims to answer are the following:

1. Whether localized cell proliferation is a feature of the ureteric bud branching morphogenesis and if this is the case, how it is regulated by known branching promoting or inhibiting factors.
2. Whether the cytoskeleton has a special arrangement which correlates with the branching activity and whether it is lost when branching morphogenesis is arrested.
3. Whether there is a differential gene expression at the ureteric bud "tips" when compared with gene expression at the stalks and whether this difference is correlated with branching activity.

My findings underline the importance of the epithelium itself: it does not just react from the influence of the mesenchyme but from its earliest stages it shows specialization between of newly formed tips. These define the architecture of the developing collecting duct and eventually the efficient nephron formation.

Chapter 2

Materials and Methods

2.1 Culture of whole organs and Wolffian Ducts

2.1.1 Whole organs

Metanephric kidney rudiments were isolated from embryos of MF1 mice at E11.5 (morning of discovery of vaginal plug was taken to be E0.5). The microdissections were performed with 0.5x16 mm needles (Terumo) in 35 mm Petri dishes (CellStar) in Eagle's minimum essential medium with Earle's salts (MEM; Sigma) which will be referred to as "dissecting medium". After isolation, the kidneys were cultured for a set period of time according to the experiment on 5 μm isopore membrane filters (Millipore; Sigma) placed on Trowell screens in culture medium (Davies, 1994) (figure 2.1). The culture medium used was Eagle's MEM with Earle's salts from Sigma with non essential amino acids, supplemented with 10% newborn calf serum (NCS; Labtech) and 5% antibiotics (Penicillin/Streptomycin; Sigma) which will be referred to as "complete medium". Experimental groups were cultured in the complete medium supplemented with various reagents according to the experiment. Organs were collected from either a single or two litters at the day of dissection and were assigned randomly to control or treatment groups. All cultures were incubated in a humidified atmosphere at 5% CO_2 at temperature of 37°C. While the development shown by controls was reasonably constant for a given run of an experiment, there was sometimes variation between experiments done at different times of year and with different batches of mice and media. Controls and experimental samples were therefore compared within a run of an experiment. They could only be compared between experiments when the development shown by the two sets of controls could be shown to be not significantly different.

2.1.2 Wolffian Ducts

Nephric ducts with their surrounding mesenchyme were isolated by microdissection (as above) from E10.5 embryos which are too young to have

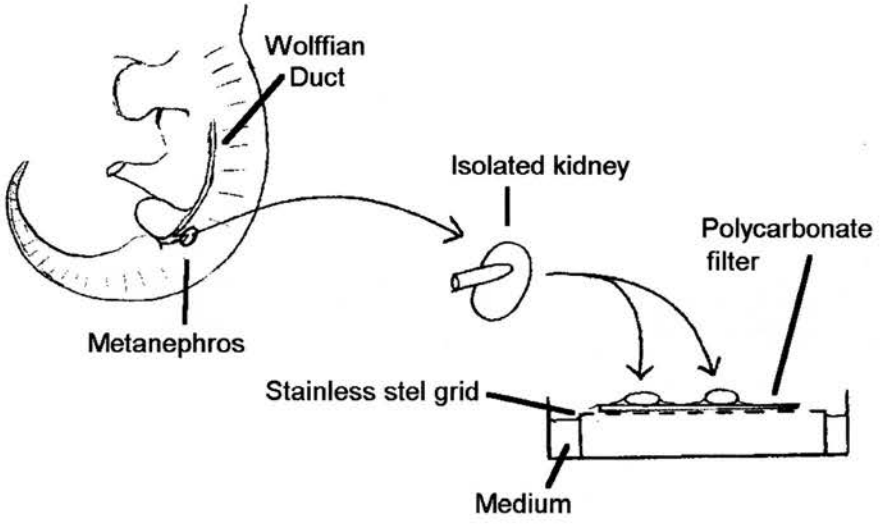

Figure 2.1: Kidney organ culture

Kidneys isolated by microdissection from embryos (E11.5), are placed on polycarbonate filters on Trowell screens of stainless steel in culture medium. Kidneys not to scale. (Courtesy of J.A. Davies.)

formed a ureteric bud. They were cultured for a time period according to the experiment in complete medium (as described above).

2.2 Cell proliferation assay (chapter 3)

2.2.1 BrdU incorporation and experimental treatments

Cell proliferation was measured using 5-bromo-2′–deoxy-uridine (BrdU; Sigma) which was added to the media at a final concentration of 100 μM for either a time course of: 0-16, 16-32, 32-48 and 48-64 hours or for 24 hours prior to fixation. In the case of the Wolffian ducts, BrdU was present for the total culture period.

The experimental treatments were as follows: Whole kidney rudiments were cultured for 48 hours in the presence of 30 mM sodium chlorate (AnaLaR, BDH), an inhibitor of sulphated glycosaminoglycan synthesis, which blocks ureteric bud branching in culture (Davies *et al.*, 1995). Exogenous GDNF (Sigma) was added to the cultures at the final concentration of 100 ng/ml for 24 hours and 48 hours. For local application of growth factor, Biorad Affigel Blue beads were washed in dissecting medium for 30 minutes at 37°C, they were then soaked in 1% bovine serum albumin (BSA) in PBS for the control and 50 μg/ml GDNF (experimental) for further 30 minutes in 37°C. The beads were then placed on one side of the T-stage E11.5 kidney rudiments (as shown in figure 2.2) for 48 hours. Kidney rudiments were also cultured in 10 μg/ml anti-GDNF (function blocking antibody from R&D systems) (Davies *et al.*, 1999) for 48 hours. TGF-β1 (Sigma) was added to the complete medium at final concentrations of 1 nM for 24 or 72 hours.

Wolffian ducts were cultured for a time course of 4, 6, 8, 12 and 24 hours in order to establish the approximate time that the ureteric bud evaginates from the

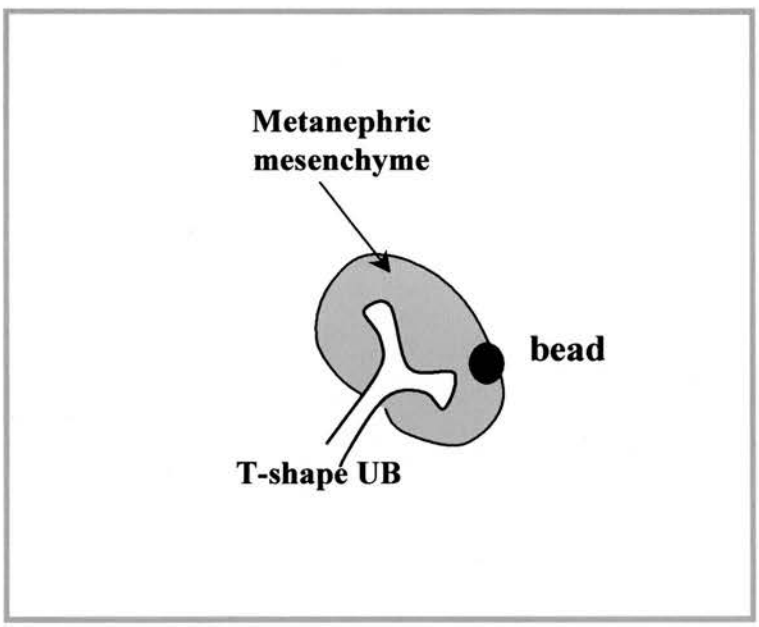

Figure 2.2: Local application of growth factor

Illustration showing the position of the control (1% BSA) or GDNF-soaked beads, placed in close proximity to one of the epithelial tips at the T-shape stage of an E11.5 metanephric kidney at the time of the dissection.

duct in culture. Then Wolffian ducts were cultured for 6 and 8 hours in the presence of 100 μM BrdU.

2.2.2 BrdU detection by whole mount immunofluorescence

The procedure followed was according to Davies et al. (Davies *et al.*, 1995) with some modifications. Cultured rudiments (whole kidneys and Wolffian ducts) were fixed in methanol initially at -20°C and allowed to warm up towards room temperature (RT) during the 10 minute period of fixation. Some were stored in -20°C methanol until required. After fixation, kidneys (or Wolffian ducts) were washed in PBS for 30 minutes then incubated in 4% paraformaldehyde (PFA; BDH) for 30 minutes at RT. They were then washed in PBS, incubated in 0.5 mg/ml trypsin (Sigma) for 7 minutes at 37°C, refixed in 4% PFA for 1.5 hours at room temperature and washed in PBS. To denature the DNA for BrdU detection, rudiments were incubated in 95% formamide, 5% 0.15 M trisodium citrate (BDH) for 1 hour at 70°C. They were washed in PBS for 30 minutes (RT) and incubated at 4°C overnight in the presence of 1/200 anti-calbindin D28k (Chemicon) or 1/100 anti-laminin (Sigma) and 1/50 anti-BrdU (mAb BU-33, Sigma) in PBS. Samples were then washed for 30 minutes in PBS and incubated in secondary antibodies overnight at 4°C. The secondary antibodies used were: 1/100 FITC or TRITC-conjugated anti-rabbit IgG (Sigma) and 1/100 TRITC or FITC-conjugated anti-mouse IgG (Sigma) in PBS. After a last PBS wash samples were mounted on slides and viewed on a Confocal Laser Scanning Microscope (CLSM; LEICA TCS NT). For counterstaining of the nuclei, monomeric cyanine nucleic acid stain TO-PRO-3 (Molecular Probes) was used according to manufacturer's instructions (1 μM TO-PRO-3 in dimethylsulfoxide (DMSO) for 5 minutes followed by another PBS wash) and then kidneys were mounted on slides before scanning on the CLSM.

2.3 Cytoskeleton experiments (chapter 4)

2.3.1 Experimental treatments

Whole kidney rudiments were cultured under control conditions in complete medium for a time course of 24, 48 and 72 hours. Kidneys were also cultured for 48 hours in the presence of 30 mM sodium chlorate to block ureteric bud branching as described before (Davies *et al.*, 1995). Kidneys were cultured in the presence of 10 μM 2′amino-3′-methoxyflavone (PD98059; Calbiochem) in DMSO for 72 hours as described in Fisher *et al.* (Fisher *et al.*, 2001).

Cytochalasin D (Cyto D; Sigma), a specific inhibitor of filamentous actin formation (Sampath and Pollard, 1991), was added in the culture medium at the beginning of the incubation period at concentrations 0.5, 0.3 and 0.1 μg/ml from a stock of 1 mg/ml in DMSO. In controls, DMSO was added at 0.05%, 0.03% and 0.001%. All organs were cultured for 72 hours in the above concentrations. The lowest concentration (0.1 μg/ml) was also used in cultures incubated for a time course of 24, 48 and 72 hours. To verify that the effect of the lowest concentration of cytochalasin D used was reversible the kidneys were cultured in the presence of 0.1 μg/ml cytochalasin D and 0.001% DMSO (control) for 24 hours and then transferred to complete medium alone for 24 hours. Kidneys were also cultured in four different conditions; (i) in the presence of 0.001% DMSO (control), (ii) Cyto D alone (0.1 μg/ml), (iii) 30 mM sodium chlorate alone and (iv) 0.1 μg/ml Cyto D with 30 mM sodium chlorate for 72 hours.

For the adherens junction experiments, kidney rudiments were cultured in the presence of 0.1 μg/ml cytochalasin D and were immunostained (as described below) for anti-E-cadherin.

A potent inhibitor of myosin 2,3 bunetadione monoxime (BDM; Calbiochem) (Cramer and Mitchison, 1995; Herrmann *et al.*, 1992) was used at the concentrations of 5 mM, 10 mM, 20 mM for 72 hours. For reversibility

experiments, 5 mM BDM was included in the cultures for 24 hours and then the medium was changed to complete MEM for further 24 and 48 hours

E10.5 Wolffian ducts were cultured in complete medium for 12 hours.

2.3.2 Immunofluorescence

For F-actin localization experiments, the organs were fixed in 4% PFA for 2 hours at room temperature and washed in PBS supplemented with 1% Triton-X 100 (Sigma) for 30 minutes. They were then stained for actin by incubating them overnight at 4°C using 1/100 TRITC-conjugated phalloidin (Sigma) in PBS (20 μg/ml stock concentration) (Cooper, 1987). There was a final rinse in PBS for an hour and the organs were mounted on slides to be examined on the CLSM.

For the double staining experiments, organs were incubated following the wash step in PBS/ 1% Triton-X 100, in primary antibody (1/100 anti-laminin or 1/200 anti-calbindin D28k in PBS) overnight at 4°C. They were then washed in PBS for 30 minutes and further incubated in the presence of 1/100 FITC-conjugated anti-rabbit IgG and 1/100 TRITC-Phalloidin in PBS.

For adherens junctions immunolocalization, kidneys were fixed in –20°C methanol, washed for 30 minutes in PBS (RT) and incubated overnight (at 4°C) in 1/100 anti-laminin and 1/100 anti-E-cadherin (DECMA; Sigma) antibodies. They were then washed in PBS and further incubated (at 4°C) in 1/100 TRITC-anti rabbit IgG and 1/100 FITC-anti rat IgG.

For BDM experiments, the kidneys were fixed in –20°C methanol and immunostained for FITC-anti-calbindin D28k

All samples were washed in PBS (30 minutes at RT) before mounting on slides and examining on the CLSM.

2.4 Lectin binding assay (chapter 5)

2.4.1 Experimental treatments

Isolated whole kidneys were cultured for 24, 48 and 72 hours at 37°C. GDNF (100 ng/ml) was added to the medium and kidneys were cultured for 48 hours. Function blocking anti-GDNF (10 μg/ml) was added to the culture for 48 hours.

2.4.2 Organ recombination experiments

E11.5 whole kidney rudiments were microdissected as described in *section 2.1*. Kidneys at the time of dissection were at the T-shape stage (a stalk and two tips 180° apart). One ureteric bud tip was removed by dissection from each whole kidney (figure 2.3A). The remaining Γ-shaped ureteric bud epithelium was transferred into a new culture petri dish and isolated metanephric mesenchyme from other whole kidneys was placed in contact with the missing end of the epithelium (figure 2.3B). The technique described is shown in figure 2.3. The control kidneys were cultured for 24 hours and the Γ-shaped ureteric buds were cultured for 48 hours.

2.4.3 Lectin Histochemistry

Kidney rudiments were fixed in ice cold methanol (–20°C) for 10 minutes or kept at –20°C until required. They were washed in PBS for 30 minutes and incubated at 4°C overnight in primary antibody (for the experiments using whole organs: 1/100 anti-laminin, for the experiments of Γ-shaped ureteric buds: 1/200 anti-calbindin D28k in PBS). After 30 minutes wash in PBS, they were then incubated in secondary antibody (1/100 TRITC-anti rabbit IgG in PBS) and 1/100 FITC-conjugated *Dolichos Biflorus* Agglutinin (FITC-DBA; Sigma) overnight at 4°C. After a last 30 minutes wash in PBS they were mounted on slides and examined under the CLSM.

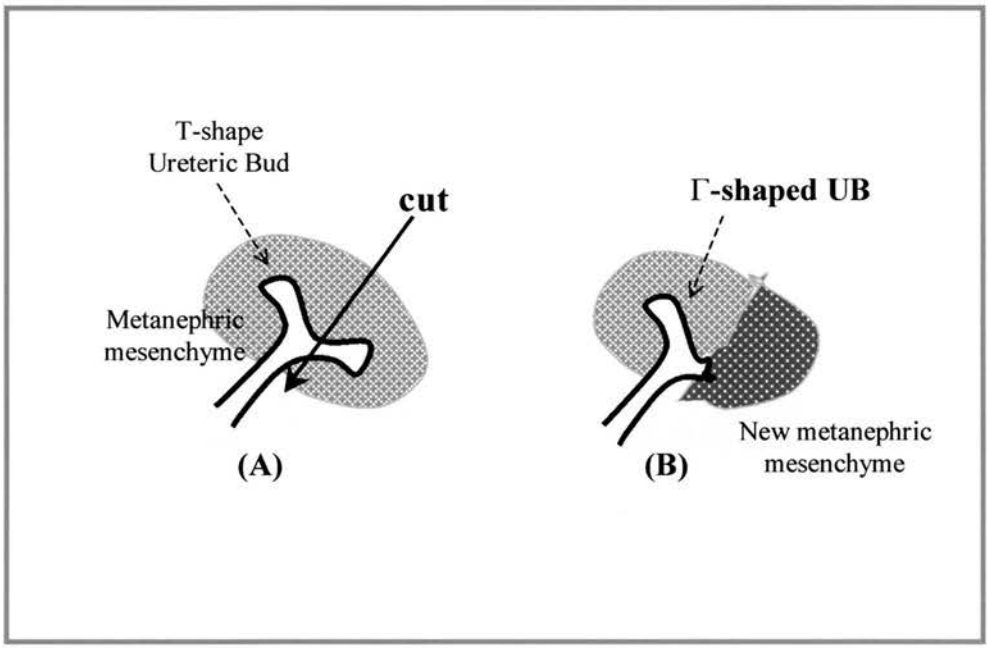

Figure 2.3: Schematic representation of organ recombinations

(A) shows an E11.5 kidney (ureteric bud at T-shape stage) after microdissection. The arrow shows where the ureteric bud (UB) tip is separated from the rest of the kidney **(B)** shows the remaining of the Γ-shaped ureteric bud surrounded by new metanephric mesenchyme (MM) obtained from other E11.5 metanephroi.

2.5 Differential display (chapter 5)

Kidney rudiments were isolated by microdissection from embryos of MF1 mice at E11.5 as described in *section 2.1.1.* After isolation, the stalks and tips were further microdissected as shown in figure 2.4. Stalks and tips were frozen at –70°C until RNA preparation. A total of 20 stalks and 20 tips were isolated.

Total RNA was extracted from the isolated tips and stalks using the RNeasy Mini Kit from Qiagen (cat. No. 74104) according to the manufacturer's instructions; the isolated tips and stalks were lysed in the presence of a highly denaturing guanidinium isothiocyanate containing buffer which inactivates RNases and ensures isolation of intact RNA. The samples were homogenized using a syringe and needle, each lysate was centrifuged and 70% ethanol was added to the supernatant to provide appropriate binding conditions and the samples were applied to RNeasy mini spin columns where the total RNA binds to a silica-gel-based membrane. To eliminate possible DNA contamination an RNase-free DNase Set from Qiagen was used (cat. No. 79254) following manufacturer's instructions. Total RNA was eluted in RNase-free water.

The quality of RNA was evaluated by 1% agarose (Sigma) gel electrophoresis. Agarose gel (1%) was made using 0.5 g agarose in 50 ml 1x TRIS-BORATE-EDTA (TBE; Sigma) buffer. Samples were run for 30 minutes at 80 V.

For cDNA synthesis approximately 2 μg total RNA of each sample were used. Reactions contained 3.33 μM of each anchored primers 5′- TTT TTT TTT TTT VG-3′, 5′- TTT TTT TTT TTT VA-3′, 5′- TTT TTT TTT TTT VC-3′ (V: A, G, C; MWG-Biotech), PCR buffer (x10)(Invitrogen), 3 mM $MgCl_2$ (Invitrogen), 0.5 mM dNTPs (Invitrogen) and 12 Units/μl RNAse inhibitor (Invitrogen) in 15 μl RT-reaction mixture for first-strand cDNA synthesis with Moloney murine leukemia virus (MMLV)-reverse transcriptase (Invitrogen) at 200 Units/μl.

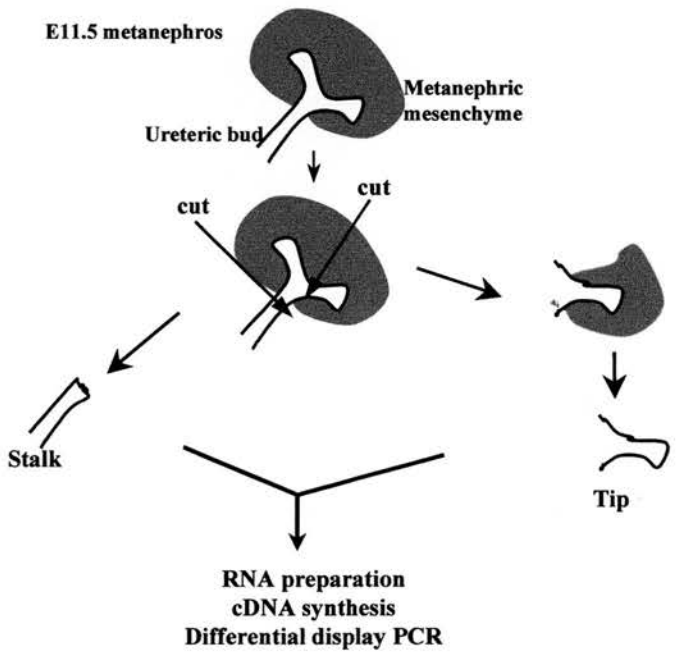

Figure 2.4: Tip vs. stalk microdissection

Illustration of the dissection steps for the isolation of differentially expressed genes at the branching epithelium. The tips and stalks were mechanically removed by microdissection from E11.5 metanephroi at the T-shape stage of the ureteric bud.

Reactions were incubated at 42°C for 1 hour and heated to 95°C for 5 minutes to inactivate reverse transcriptase.

Each differential display PCR reaction contained 1x PCR buffer, 2 μM dNTPs, 2.5 μM of one of three anchor primers, 1000 Ci/mmol ^{35}S dATP (Amersham), 0.075 units/μl Taq polymerase (Promega), 1 μl cDNA from previous step and 0.5 μM of one of arbitrary primers in a total volume of 20 μl. PCR reactions were performed with a Hybaid Omnigene cycler. The cycling parameters were as follows: 94°C for 2 minutes (1 cycle; denaturation), 94°C for 30 seconds 40°C for 2 minutes 72°C for 30 seconds (40 cycles) and 72°C for 5 minutes (1 cycle; extension). Sequences of the 5′ arbitrary primers were as follows: P1: 5′- GGA ACC ATT C-3′, P2: 5′-ACA GAG CAC A-3′, P3: 5′- ACG TAT CCA G-3′, P4: 5′- CTT TCT ACC C-3′ (MWG 527835-1).

Samples were separated in a 6% polyacrylamide/ 7 M urea DNA sequencing gel. [For 1x gel was made as follows: 23 g urea (Sigma), 10 ml 5x TBE buffer, 7.5 ml 40% Acrylamide/Bis 19:1 solution (Biorad), 6 μl 10% sodium dodecyl sulfate (SDS; Biorad) up to 50 ml of distilled water. Last 400 μl 10% ammonium persulfate (APS; Sigma) and 70 μl N,N,N′,N′- tetramethylethelenediamine (TEMED; Biorad) were added.]

Loading dye (3.3 μl of 80% formamide, 0.01% bromophenol blue (Sigma), 0.01% xylene cyanol (Sigma), 1 mM EDTA (Sigma), 10 mM sodium hydroxide) was added to each tube which were heated for 30 minutes at 100°C and 6 μl of each sample were loaded on the 6% polyacrylamide gel. The gel was pre-warmed for 1 hour at 1.5 kV before samples were run for 3.5 hours at 1.5 kV. The gel was fixed (in 10% methanol and 10% acetic acid), transferred to blotting paper (3 MM; Whatmann), dried overnight and exposed overnight to 35x43 cm Kodak scientific imaging film (Sigma).

2.6 Confocal microscopy and image analysis

The samples were examined on the TCS NT Leica confocal laser scanning microscope (Leica Microsystems Heidelburg, GmbH, Germany). For dual-labeled samples, both FITC and TRITC emissions were acquired simultaneously, once appropriate checks had been carried out for any cross-talk between the channels. For all experiments, the pinhole was adjusted to 1.00 before scanning and other critical settings were maintained the same for both experimental and control groups. Serial optical sections of each kidney were acquired with the x10 objective for whole kidney morphology and branching quantification, the x20 objective for tip morphology and nuclei counting, and the x40 (or digitally zoomed by a factor of 2) for specific tip morphology. For the Wolffian ducts, an initial x5 magnification was used to capture the whole nephric duct and then serial, optical sections of the metanephric area were obtained at a higher magnification (x20).

In *chapter 3*, the x20 lens was used (unless otherwise stated), in order to have a clearer view of the BrdU positive nuclei along the ureteric bud tips and stalks. For serial optical sections, the top and bottom scanning points were selected. The thickness of each section was user defined at 3 μm. The Leica software automatically calculated and adjusted the step size (thickness) in a range of ± 0.300 μm in order to best fit in the selected region.

In *chapter 4*, optical sections of the tips were obtained at the x20 and x40 objective.

The software packages used for the analysis (*chapter* 3) were Adobe Photoshop (version 5.0) and Scion Image (version beta 4.0.2) downloaded as a freeware from the world wide web (http://www.scioncorp.com).

P values were calculated using the Student's two sample *t*-test assuming independent measurements and allowing, when necessary, for different values of n in control and experimental groups (Owen and Jones, 1994). Calculations were

performed using Microsoft Excel. Differences were assumed to be significant at $p<0.05$. For quantification of BrdU incorporation, n values represent the number of tips for each independent measurement, while for quantification of branching n values represent the number of kidneys in each sample.

The experiments presented in *chapter 3* were not all performed the same number of times due to technical difficulties.

Chapter 3

Involvement of Localized Cell Proliferation in Ureteric Bud Branching Morphogenesis

3.1 Introduction

3.1.1 Localized cell proliferation during embryonic development

Embryonic morphogenesis and organogenesis are the result of a coordination between the driving forces of morphogenesis and the processes of cell growth, proliferation, differentiation and death (Hogan, 1999). During development, the epithelia of the embryo change shape as they fold into tubes, spheres or pockets as well as during bud evaginations. It has been argued that cell proliferation contributes to these shape changes (for review see Huang and Ingber, 1999).

There is evidence from a number of systems that differential cell proliferation correlates with morphogenesis. For example in the case of thyroid gland organogenesis (figure 3.1), there is an increase in cell number during the period when morphogenetic shape changes. While the gland evaginates from the floor of the pharynx, high cell proliferation is found in the adjacent pharyngeal cells. Differential growth combined with the mechanical forces resulting from the pressure of the increased cell numbers, leads to the evagination of the gland (Smuts *et al.*, 1978).

Morphogenesis of the tooth (figure 3.1) involves epithelial-mesenchymal interactions (reviewed in Jernvall and Thesleff, 2000). Thickening of the oral epithelium to form the tooth bud is the initial sign of tooth development surrounded by condensed mesenchymal cells. In mammals, tooth development progresses as the epithelium undergoes folding morphogenesis (Thesleff and Jernvall, 1997). Members of the fibroblast growth factor family (FGF-4, -9, -10), expressed by the enamel knot cells in the dental epithelium and the mesenchyme, are considered key signals that regulate the growth and folding of the epithelium. Rapid proliferation of epithelial cells around the enamel knot is thought to account for the folding of the epithelium at the sites of the tips of future tooth cusps (Jernvall and Thesleff, 2000).

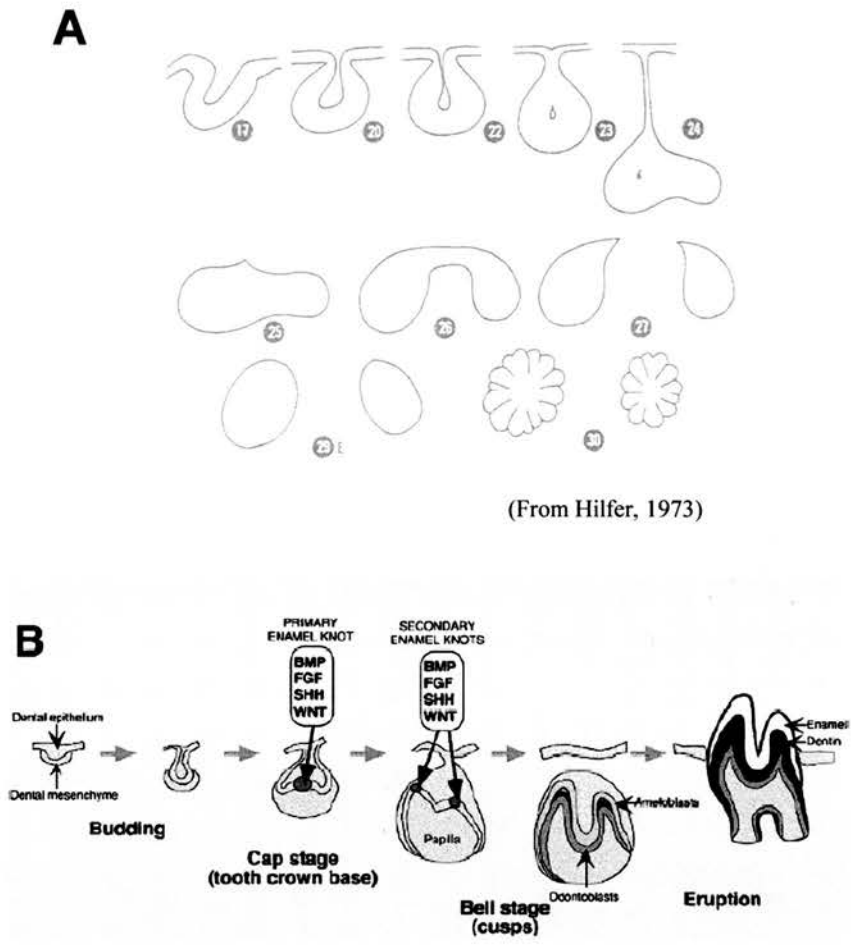

(From Hilfer, 1973)

(From Thesleff and Jernvall, 1997)

Figure 3.1: Folding morphogenesis

(A) Development of chick thyroid gland (stages 17 to 30) and **(B)** stages in development of the tooth

3.1.2 Localized cell proliferation during branching morphogenesis

During branching morphogenesis, where an epithelium evaginates as a bud, elongates and undergoes subdivisions of the terminal branches, localized cell proliferation is one of the factors contributing to the formation of the tree-like structure. This is the case in mammary gland, where the end buds are bulbous and highly mitotic (Daniel *et al.*, 1984). The terminal end buds of the pubertal and postpubertal mammary glands in culture show increased DNA synthesis, in contrast to the duct epithelium (Bresciani, 1968). Also in the developing lung, there is evidence that implicate localized intense cell proliferation in bud formation (Goldin *et al.*, 1984). In the inactive epithelial regions between lung buds the level of cell proliferation is lower than in the growing tips of the actively branching buds (Goldin and Opperman, 1980).

In contrast, the *Drosophila* tracheal system is a branching network that forms without cell proliferation. As described in *chapter 1,* the tracheal system is formed as ten placodes on each side of the embryo. Each placode is composed of approximately twenty cells with the number of cells reaching approximately 80 after two rounds of division. The dramatic growth of the respiratory network takes place from this finite number. The last tracheal cell division occurs just before primary branching begins. Therefore, the total number of tracheal cells does not increase as the primary branches grow (Samakovlis *et al.*, 1996). The new branches are formed by migration and rearrangement of tracheal cells and by cell elongation. Each secondary branch is formed by a single tracheal cell (Samakovlis *et al.*, 1996).

Aim

The aim of this chapter is to develop a technique to measure proliferation in cultured kidney rudiments and, using this technique, to establish whether (i) differential cell proliferation is present during ureteric bud branching in culture;

(ii) differential cell proliferation is present during ureteric bud outgrowth, and (iii) whether two known regulators of UB branching affect cell proliferation in the epithelium.

3.2 Development of a quantification method for measuring cell proliferation

In order to establish a technique to evaluate as objectively as possible the proliferating cells at the tips of the ureteric buds, the analysis was categorised into three distinct groups (*sections 3.2.1, 3.2.2, 3.2.3* respectively) according to the effect that the experimental treatments have on the branching of the epithelium.

3.2.1 Quantification of proliferating nuclei along the branching ureteric bud epithelium and the Wolffian duct

Stacks of three middle optical sections (each of 3 μm thickness) were selected from the original confocal files, where the tips marked out for analysis were at their widest planes. All the stacks were the overlay of green and red channels.

We have described the quantification method used in Fisher *et al.*, (Fisher *et al.*, 2001). Using Adobe Photoshop, three successive lines of 100 μm were drawn across the ureteric bud tubules starting from the terminal tip edge towards the stalk. These lines divided the tubule into 100 μm long segments. In the case of Wolffian ducts, the lines started from the caudal tip of the duct and continued towards the mesonephros (see section *3.3.3*). The BrdU positive nuclei, in each segment, were then counted (manually).

3.2.2 Quantification of proliferating nuclei at ureteric bud tips where experimental treatments affected the tip morphology

Some experimental treatments used affected the morphology of the branching epithelium. For the purposes of the analysis, there was a need to define what is a "tip". Since an antibody specific for "tip" was not available and in situ

hybridization is not compatible with BrdU staining the area considered as the "tip" was based on the morphology of the branching epithelium and was separated in two groups:

- The first definition of the "tip" was chosen on the basis of the branching pattern of the control ureteric buds. In control kidneys the swelling of the ureteric bud stalk tube to form the ampulla was considered the beginning of a tip. In the experimental groups, the presence of a swelling of the branch tube towards the end of the branch was considered to be the beginning of a tip.
- For the second definition, a line was drawn (as described in *section 3.2.1*) across a well-defined control ampullary tip from the outer edge towards the stalk. The length of this line was measured by the software and was used to define the terminal part of all the branches (tips) of the groups (control and experimental) of each experiment.

In order to develop the most objective quantification method to use, a number of possible methods was applied on one experimental set. These methods are described below. They are categorized according to the previously mentioned "tip" definitions (methods I-IV and methods V-VIII), measurements performed on single optical sections or stacks and thresholding and their results are compared (see results section).

Method I (single sections)

Single original optical sections (overlay of red and green channels) were imported to the Scion Image program. All the optical sections were calibrated to the appropriate scale (500 μm^2) as all the original optical sections were scanned at x20 objective. Using the free hand tool to draw round the tip, the tip area was measured in μm^2. The single optical section chosen was the one where the tip was at its widest plane. The BrdU positive nuclei inside the selected area were

then counted (manually). The proliferating nuclei measured were subsequently expressed as the number of BrdU positive per 1000 μm^2 of epithelium.

Method II (stacks)

From the gallery of the original optical sections of each metanephros, three middle sections (where each tip was at its widest plane) were selected and were saved as stacks (overlay of green and red channels). The stacks were then imported to Scion Image and the area of each tip was measured as above. The BrdU positive nuclei inside that area were then counted.

Method III (single sections, threshold)

In order to minimize the possible experimenter's bias on the selection of the positive nuclei present, a user defined adjustment of the fluorescence background threshold was applied. The single optical sections used for method I were imported in Scion Image and converted into gray scale images. The threshold value was taken as three times higher than the mean background value plus the standard deviation of the selected area. Anything above this value was considered as a BrdU positive nucleus.

The tip area was measured in μm^2 as described in method I. The BrdU positive nuclei inside the measured tip area were counted.

Method IV (stacks, threshold)

The stack sections were imported to Scion Image and were converted into gray scale images. A random area was selected within each tip and the background intensity was measured. The background threshold was adjusted as previously described and the BrdU positive nuclei were counted inside the tip (the tip area was measured in μm^2) as in method III.

Method V (single sections, Xμm length)

For this method onwards, the second definition of the "tip" was applied. A specific length from the edge of a control tip was selected and was used in all the tips (control and experimental) of each experiment to be analysed. The choice of the applied length was made upon measuring an average sized and well-structured control tip. This selection was made anew for each experiment.

The single optical sections were again employed; the new terminal tip areas were highlighted and measured in μm^2; the BrdU positive nuclei inside this area were counted (manually).

Method VI (stacks, Xμm length)

This method is a combination of methods II and V. Stacks of the optical sections were imported in Scion Image. The terminal tip areas were measured by the software as in method V (in μm^2) and the BrdU positive nuclei in the selected areas were counted (manually).

Method VII (single sections, Xμm length, threshold)

This method is a combination of methods III and V. Essentially, the single optical sections where the tips were at their widest planes were selected and converted into gray scale images. The terminal tip area was measured as in method V, the background threshold was adjusted as previously described and the BrdU positive nuclei were counted as in method III.

Method VIII (stacks, Xμm length, threshold)

This method is a combination of methods IV and VI. In brief, the stacks of optical sections were converted into gray scale images. The terminal tip area was

selected as described in method V. The background threshold was adjusted and the BrdU positive nuclei were counted as described in method III.

3.2.3 Quantification of BrdU positive nuclei where the treatment affects ureteric bud branching resulting in identifiable tip morphology

In the experiments where treatment affected branching morphogenesis, leaving the morphology of the terminal tips still identifiable, counting method IV was used on stacked optical sections.

The stacks were selected from the gallery of the original files, they were imported to Scion Image and they were converted into gray scale images. The tip area was highlighted and measured in μm^2, the background threshold was adjusted as described in method III and the BrdU positive nuclei were counted manually. Then, they were expressed as a number of BrdU positive nuclei per 1000 μm^2 of epithelium.

3.3 Results

The hypothesis that differential cell proliferation is a feature of the ureteric bud tip during branching morphogenesis of the developing epithelium was tested by bromodeoxyuridine incorporation in cultured kidney rudiments.

3.3.1 BrdU incorporation and labeling index

To measure the levels of proliferation, I initially planned to use the nuclear labeling index (percentage of BrdU positive nuclei/100 nuclei) (Nadasdy *et al.*, 1998). The kidneys grown for 24 hours in BrdU were subsequently immunostained with either anti-calbindin D28k, a specific marker for ureteric bud and developing collecting duct (Davies, 1994), or with anti-laminin which stains the basement membranes and is widely used by our laboratory (Davies *et al.*, 1995). For the nuclear labeling index, proliferating and non-proliferating nuclei were counterstained (figure 3.2) using a monoclonal antibody to BrdU (Davies *et al.*, 1995) and a monomeric cyanine nucleic acid stain (TO-PRO3) suited for the Leica confocal microscope (L. Sharp, personal communication). There was an intense nuclear staining of the mesenchymal component, whereas in the deeper layers where the epithelium is present the staining was much weaker and the fluorescence faded rapidly even in the presence of an anti-fading agent. Because of this, the counterstaining of the nuclei on the epithelium was not efficient for quantification using the nuclear labeling index (figure 3.2). It was therefore necessary to develop an alternative method to measure the BrdU incorporation in the whole mount ureteric buds.

The development of the quantification techniques used for the analysis of the experiments was described in the previous paragraph (see *section 3.2*). To measure the proliferation, I could not use the number of BrdU positive nuclei per 100 nuclei, therefore I measured cell proliferation as the BrdU positive nuclei per area of epithelial tip tissue (calculated by the software).

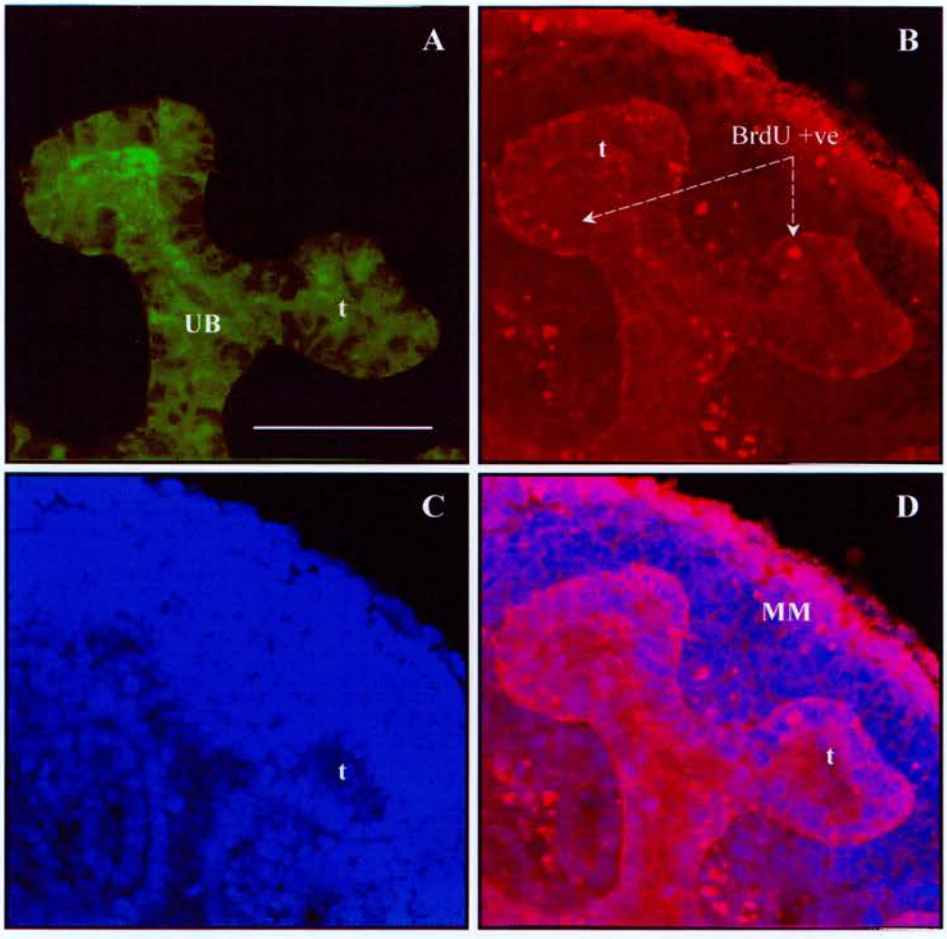

Figure 3.2: Staining of proliferating and non-proliferating nuclei at the tip of the ureteric bud

Ureteric bud terminal tips triple-stained with **(A)** FITC- anti calbindin D28k, **(B)** TRITC- anti BrdU, **(C)** TO-PRO3. Panel **(D)** shows the merged confocal image of anti-BrdU and TO-PRO3. Arrows showing the BrdU positive nuclei on the epithelium. UB: ureteric bud, MM: metanephric mesenchyme, **t**: terminal tip. Scale bars = 100 μm.

Some of the experimental treatments used affected the ureteric bud branching morphology. In these cases, the hypothesis was to investigate the effect that a negative modulator of branching would have on the cell proliferation in the epithelial tip. However, it was not possible to distinguish with certainty the borderline between the stalk and the tip. Therefore, I had to decide what to consider as a "tip" under my experimental conditions. For this reason, I used the two previously mentioned definitions (see *section 3.2*) which are both based on the morphology of the control tips. In the first, a swelling of the stalk tube toward the end of the branch is considered a "tip", whereas the second is based on a specific length (based on a well-defined control tip) drawn from the end of the branch and considers that area as the "tip". In order to establish the proper method to apply I used one experiment as model.

In this model experiment, in order to count the proliferation I used either single sections (3 μm thickness) where the "tip" was at its widest plane or stacks of three optical sections (of 3 μm thickness each). The stacks were composed of the single optical section where the "tip" was at its widest plane, ± an optical section above and below in order to include possible nuclei that might have been missed in the single optical sections. All stack measurements showed a higher average of nuclei present in controls and a variation on the experimentals. This did not affect the difference between control vs. experimental in a single method (compare I-II, III-IV, V-VI, VII-VIII in figure 3.3). For the following experiments, I used the stacks for the analysis.

In order to minimize a possible bias to whether a bright fluorescent "spot" is a positive BrdU nucleus, I adjusted the threshold to 3x higher than background and anything above this value was considered to be a positive nucleus. This resulted in a reduction in difference between control and experimental in the methods using the threshold without affecting the statistical significance (compare methods I-III, II-IV, VII-VIII).

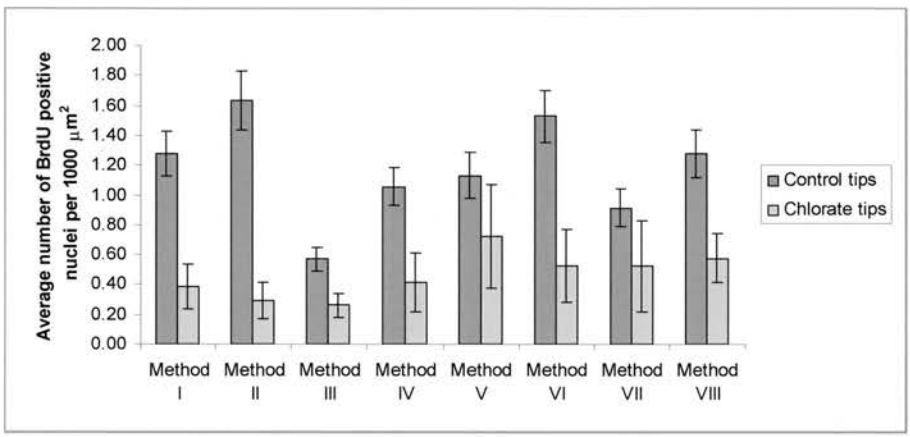

Figure 3.3: Development of the quantification method for measuring cell proliferation

Comparison of counting methods I-VIII. The average number of BrdU positive nuclei per 1000 μm^2 of tissue were measured. Control n= 38, chlorate n= 5 (n values represent the number of tips). Data are shown as mean ± SEM. The values are:

For method I, control: 1.28 ± 0.15, chlorate: 0.39 ± 0.15, p= 0.0008

For method II, control: 1.63 ± 0.19, chlorate: 0.29 ± 0.12, p= 2.22×10^{-6}

For method III, control: 0.57 ± 0.08, chlorate: 0.26 ± 0.08, p= 0.015

For method IV, control: 1.05 ± 0.13, chlorate: 0.41 ± 0.20, p= 0.024

For method V, control: 1.13 ± 0.15, chlorate: 0.72 ± 0.35, p= 0.32

For method VI, control: 1.53 ± 0.17, chlorate: 0.53 ± 0.25, p= 0.009

For method VII, control: 0.91 ± 0.13, chlorate: 0.52 ± 0.31, p= 0.28

For method VIII, control: 1.28 ± 0.16, chlorate: 0.58 ± 0.16, p= 0.008

(the methods are described in *section 3.2.2*)

All methods showed variations among them, but they all showed statistically significant difference between control and experimental treatment. The only exceptions are method V and VII that use the single optical sections using the second "tip" definition, where the experimental group shows a greater standard error. These methods were not used further.

Overall, as the majority of the methods showed statistically significant difference, for the subsequent experiments the stack sections combined with thresholding (method IV) was used as the most objective method of measurement. In the experiments where the tip morphology was ambiguous, the quantification was performed using both "tip" definitions (i.e. methods IV and VIII).

Quantification of the results of all methods is shown in figure 3.3.

3.3.2 Localized cell proliferation is confined at the tips of ureteric bud branching epithelium

To examine whether there is regional variation in levels of BrdU incorporation during branching morphogenesis in culture, E11.5 isolated metanephroi were cultured over a time course of zero to 64 hours (figure 3.4). Cell proliferation (BrdU positive nuclei per unit length) was measured on the ureteric bud branches for the culture period of 16-32 hours, by the method described in *section 3.2.1*. More proliferating nuclei were localized at the first 100 μm (figure 3.5), a distance that for the particular experiment defined the tip, than in the stalk behind it. The mean number of BrdU positive nuclei at the tip (0-100 μm) was 12.1 ± 1.60. The subsequent 100 μm (distance 100-200 μm) defined the stalk immediately away from the tip. The average number of BrdU positive nuclei was 3.47 ± 0.67 and at the subsequent 100 μm of stalk further away from the tip (that is 200-300 μm) the average number of proliferating nuclei was 3.50 ± 1.05. The data are expressed as the mean ± standard error of the mean.

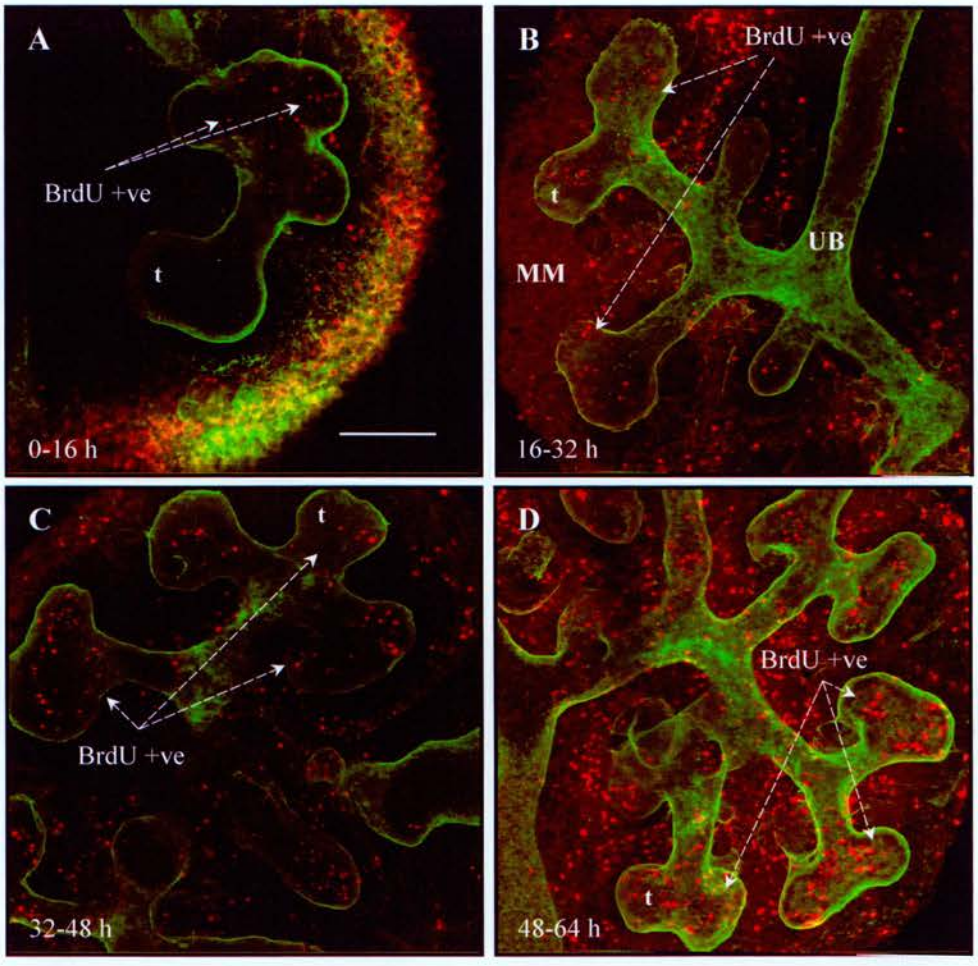

Figure 3.4: Cell proliferation during ureteric bud branching morphogenesis

BrdU incorporation (100 μM) for 16 hours in kidney rudiments cultured at time intervals of 0-16 hours **(A)**, 16-32 hours **(B)**, 32-48 hours **(C)** and 48-64 hours **(D)**. Arrows show the BrdU positive nuclei at the tips of the branching epithelium. Double staining: FITC-anti laminin and TRITC-anti BrdU. UB: ureteric bud, MM: metanephric mesenchyme, t: terminal tip. Scale bar = 100 μm.

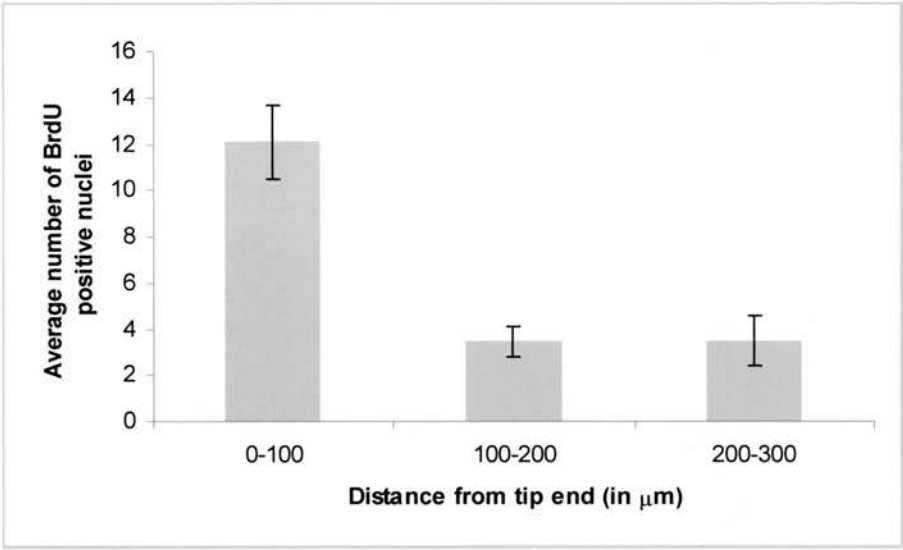

Figure 3.5: Cell proliferation is confined to the ureteric bud tips during branching morphogenesis

BrdU (100 μM) was incorporated for the last 16 hours of 32 hours culture of E11.5 kidney rudiments. BrdU positive nuclei were counted along the ureteric bud at 100μm distance from the tip edge towards the stalk (0-100 μm= tip, 100-200 μm and 200-300 μm= stalk). Data are shown as the mean ± SEM.

These results suggest that there is a local increase in proliferation concentrated at the tips. This difference in local proliferation may be a driving force for the branching pattern of the developing ureteric bud.

3.3.3 Localized cell proliferation is the first sign of ureteric bud outgrowth from the Wolffian duct

Since branching activity is accompanied by localization of cell proliferation at the ureteric bud tips, one could wonder whether localized proliferation precedes the formation of the first tip, the ureteric bud itself. In order to test this hypothesis, BrdU was incorporated in Wolffian ducts at the stage prior to the emergence of the ureteric bud.

The timing of the ureteric bud outgrowth from the nephric duct in culture was established by a time course. E10.5 Wolffian ducts were cultured for 4, 6, 8, 12 and 24 hours (figure 3.6). By 24 hours the ureteric bud had already branched (figure 3.7). The timing of ureteric bud emergence in culture was found to be at around eight hours. BrdU incorporation was quantified along the Wolffian duct (as described in *section 3.2.1*). Consecutive distances of 100 μm were selected at both the metanephric area (seven lines of 100 μm) and further up the duct towards the mesonephros (nine lines of 100 μm). The average number of the BrdU positive nuclei per 1000 μm^2 was measured along these lengths. The results shown in figure 3.8 support the hypothesis that at the presumptive metanephric area there is an area of increased localized cell proliferation where the ureteric bud will evaginate. At a randomly selected area on the nephric duct towards the mesonephros, the cell proliferation at the selected distances measured does not show a specialized pattern (figure 3.8 B).

This result suggests that localized cell proliferation *in vitro,* may be one of the driving forces that lead to the evagination of the ureteric bud.

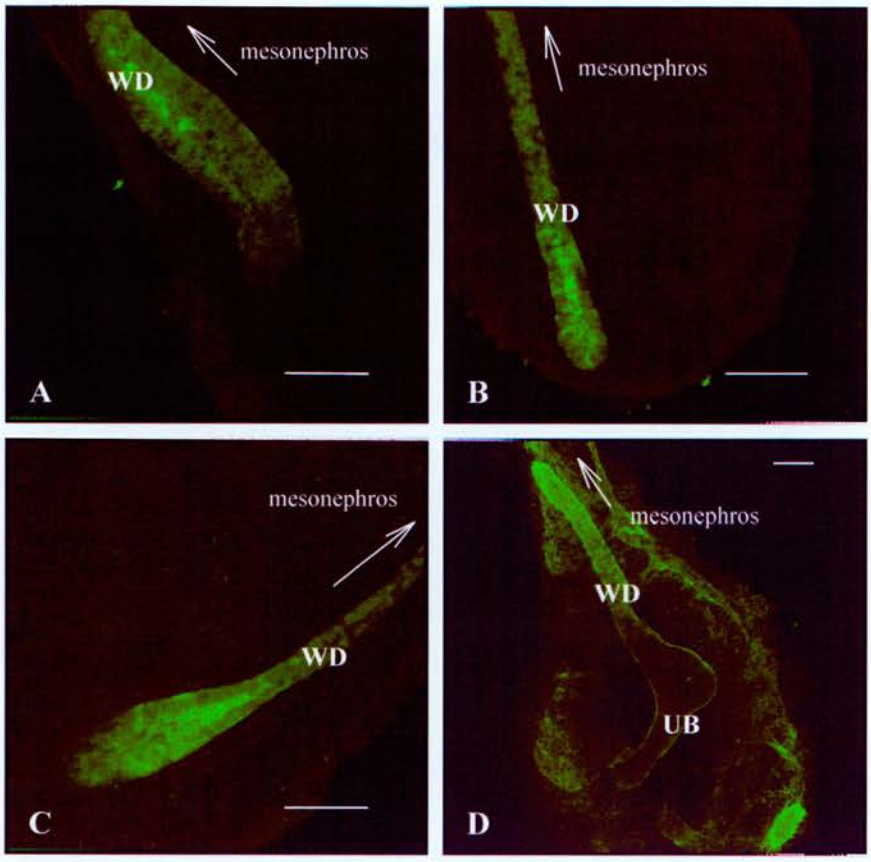

Figure 3.6: Wolffian Ducts in culture

A Wolffian Duct in culture for a time course of **(A)** 4 hours, **(B)** 6 hours, **(C)** 8 hours and **(D)** 12 hours. Open arrows point towards the location of the mesonephros. Staining: FITC-anti calbindin D28k. WD: Wolffian duct, UB: ureteric bud. Scale bar = 100 μm.

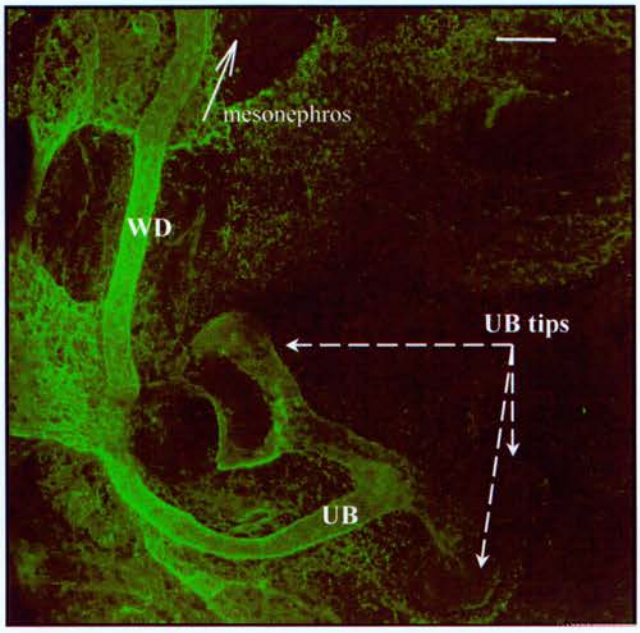

Figure 3.7: Wolffian Duct in culture for 24 hours

A Wolffian Duct in culture for 24 hours. Dashed arrows show the branching ureteric bud, open arrow points towards the location of the mesonephros. Staining: FITC-anti laminin. WD: Wolffian duct, UB: ureteric bud. Scale bar = 100 μm.

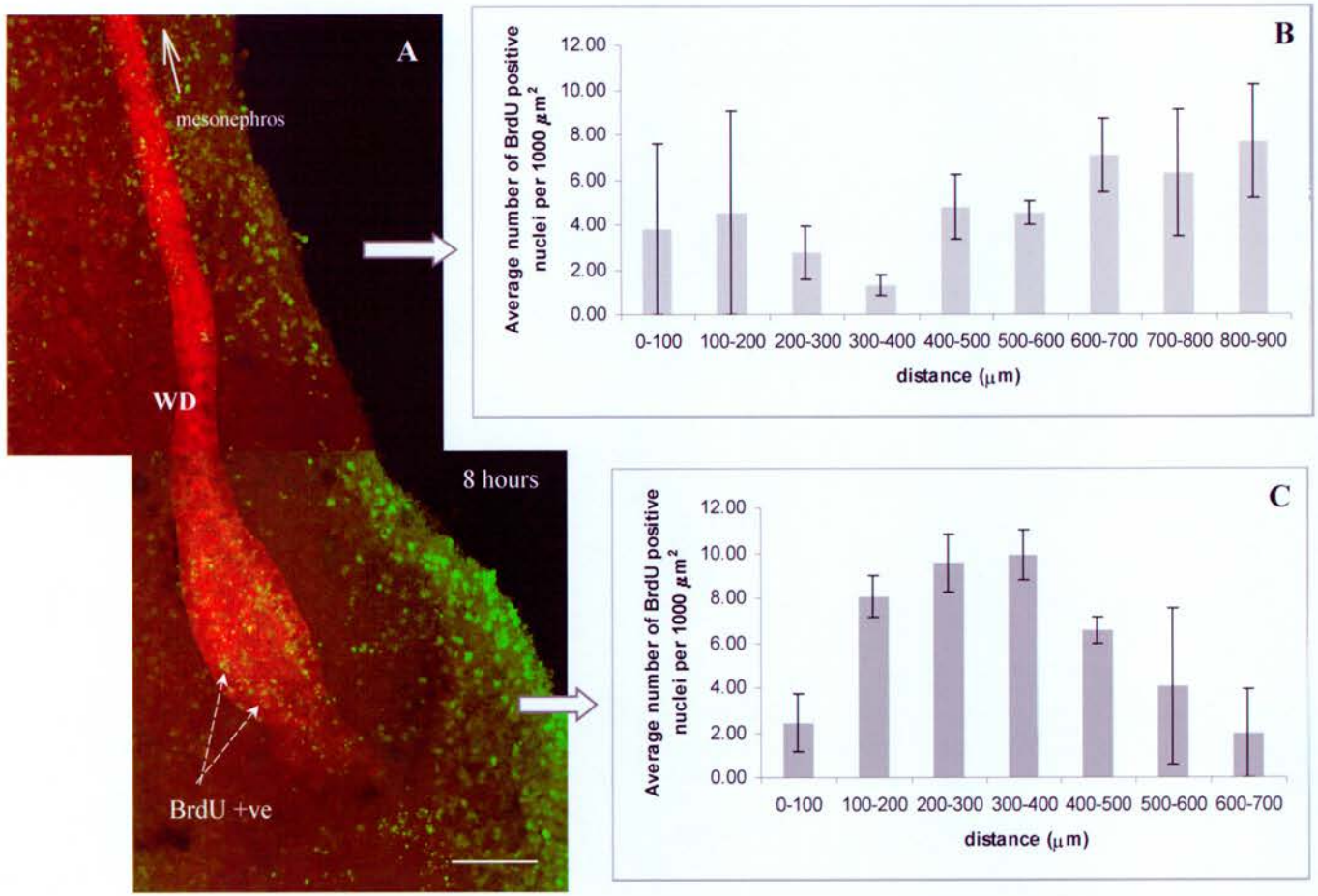

Figure 3.8: BrdU incorporation during ureteric bud ougrowth from Wolffian Duct

(A) A Wolffian Duct in culture for 8 hours, **(B)** is a graphic representation of the average BrdU positive nuclei per 1000 μm^2 for every 100 μm along the nephric duct (randomly selected), (**C**) represents the quantification of the average number of BrdU positive nuclei per 1000 μm^2 along the duct in the area of the presumptive metanephros. Dashed arrows show the BrdU positive nuclei on the epithelium, open arrow points towards the location of the mesonephros. Double staining: TRITC-anti calbindin D28k and FITC-anti BrdU. WD: Wolffian duct. Scale bar = 100 μm.

3.3.4 Localized proliferation is reduced when branching is blocked

In order to test whether the higher proliferation rate observed at the tips is present only during the formation of new branches, branching was arrested and BrdU incorporation was examined.

E11.5 kidney rudiments were cultured in 30 mM of sodium chlorate, a specific sulphation inhibitor which inhibits the synthesis of sulphated glycosaminoglycans, hence blocking ureteric bud development (Davies *et al.*, 1995). The control tree-like branching pattern of the collecting duct is distorted in kidneys growing in chlorate. It has been reported that this reduction of branching is accompanied by inhibition of cell cycling (Davies *et al.*, 1995). However, it is not known whether the fewer cells still proliferating are confined to the tips.

The morphology of the ureteric buds treated with sodium chlorate changes dramatically from the controls. Cell proliferation appears reduced in the kidneys cultured in chlorate (figure 3.9). BrdU incorporation was quantified at the tips of the ureteric buds cultured in chlorate in comparison to control kidneys (figure 3.10). The branching of the chlorate treated kidneys is reduced, but the size of the tips is larger than the size of the control tips. The average size of the control tips was 4570.2 ± 250.3 μm^2 in comparison to the average size of the chlorate tips of 10077.5 ± 1212.9 μm^2. Quantification (by method IV) revealed that the average number of BrdU positive nuclei per 1000 μm^2 of epithelium at the tip was 1.05 ± 0.13 for the control tips and 0.41 ± 0.20 for the chlorate tips. This difference is significant at $p= 0.02$. Measuring cell proliferation by method VIII, the average number of BrdU positive nuclei per 1000 μm^2 of epithelium at the control tips was 1.28 ± 0.16 and 0.46 ± 0.16 for the chlorate tips ($p= 0.008$). Both methods are performed on stack sections, using fluorescent background

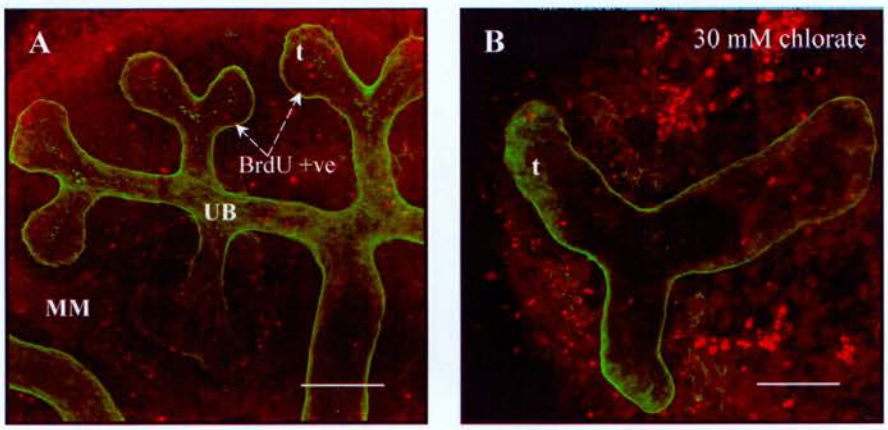

Figure 3.9: Effect of sodium chlorate on cell proliferation at the ureteric bud tips

(A) Control E11.5 kidney in culture for 48 hours, **(B)** E11.5 kidney in culture supplemented with 30 mM sodium chlorate. Arrows showing BrdU positive nuclei at the tips of the ureteric bud. Double staining: FITC-anti laminin and TRITC-anti BrdU. UB: ureteric bud, MM: metanephric mesenchyme, t: terminal tip. Scale bars = 100 μm.

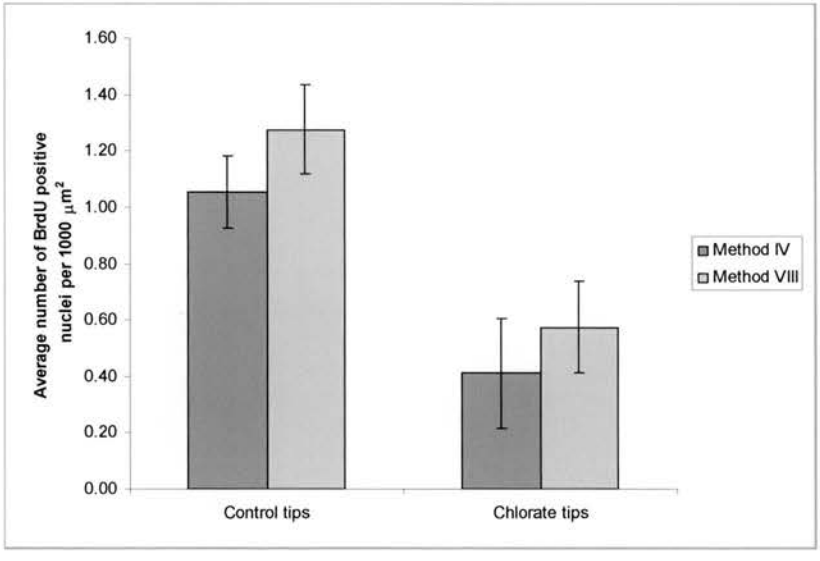

Figure 3.10: Blocking branching results in a reduction of cell proliferation at the tips of the ureteric bud

Quantification methods IV and VIII show a significant difference in cell proliferating at the ureteric bud tips between control and 30 mM sodium chlorate treated kidneys. Data are shown as the mean of BrdU positive nuclei per 1000 μm^2 of epithelial tip (control (IV): 1.05 ± 0.13, chlorate (IV): 0.41 ± 0.20, control (VIII): 1.28 ± 0.16, chlorate (VIII): 0.58 ± 0.16). Control n= 38, chlorate n= 5 (n values represent the number of tips). Error bars are the SEM, p= 0.02 (IV), p= 0.008 (VIII).

thresholding and differ only in the definition of the tip. Method IV uses the first definition of the tip, whereas method VIII uses the second definition.

These results support the hypothesis that when the ureteric epithelium is not actively branching, the cell proliferation at the bud tips is significantly reduced, that is local proliferation is a feature of active tips.

3.3.5 GDNF effect on cell proliferation at the ureteric bud tips

GDNF is a major paracrine factor involved in metanephric development that binds to the ureteric bud tips (Sainio *et al.*, 1997b). Here, the aim is to test the hypothesis that GDNF branch-promoting effect might be due to increased cell proliferation at the ureteric bud tips. In order to test this, GDNF was (i) added to the kidney cultures generally and (ii) applied locally on a bead, and BrdU incorporation was quantified at the tips of the branching epithelium.

When applied to culture medium, GDNF (100 ng/ml) did not result in an increase of the number of tips, but rather in an abnormal morphology of the epithelium with distorted branching pattern. The average number of the tips in control kidneys was 7.83 ± 1.35, whereas in GDNF treated kidneys it was 5.00 ± 0.24 ($p= 0.09$). There was an enlargement of the tips and ectopic tips emerged from the stalks (figure 3.11). The average size of the GDNF treated tips (referred to as "major" tips) was larger (2.6×10^4 μm^2) than the average size of control tips (4.8×10^3 μm^2). The ectopic tips (5.4×10^3 μm^2) were also larger than the control tips. The question is whether this "swollen" morphology of the tips and the presence of the ectopic tips occurs as a result of an increase in the cell proliferation. Quantification of the BrdU incorporation was performed as described in *section 3.2.3*. The average number of BrdU positive nuclei per 1000 μm^2 in control tips was found to be: 4.91 ± 0.58, in GDNF "major" tips: 3.89 ± 0.55 and in GDNF ectopic tips: 3.13 ± 0.43. There was no significant difference in the cell proliferation between control and GDNF "major" tips ($p= 0.38$) whereas the cell proliferation at the ectopic tips was significantly lower than the

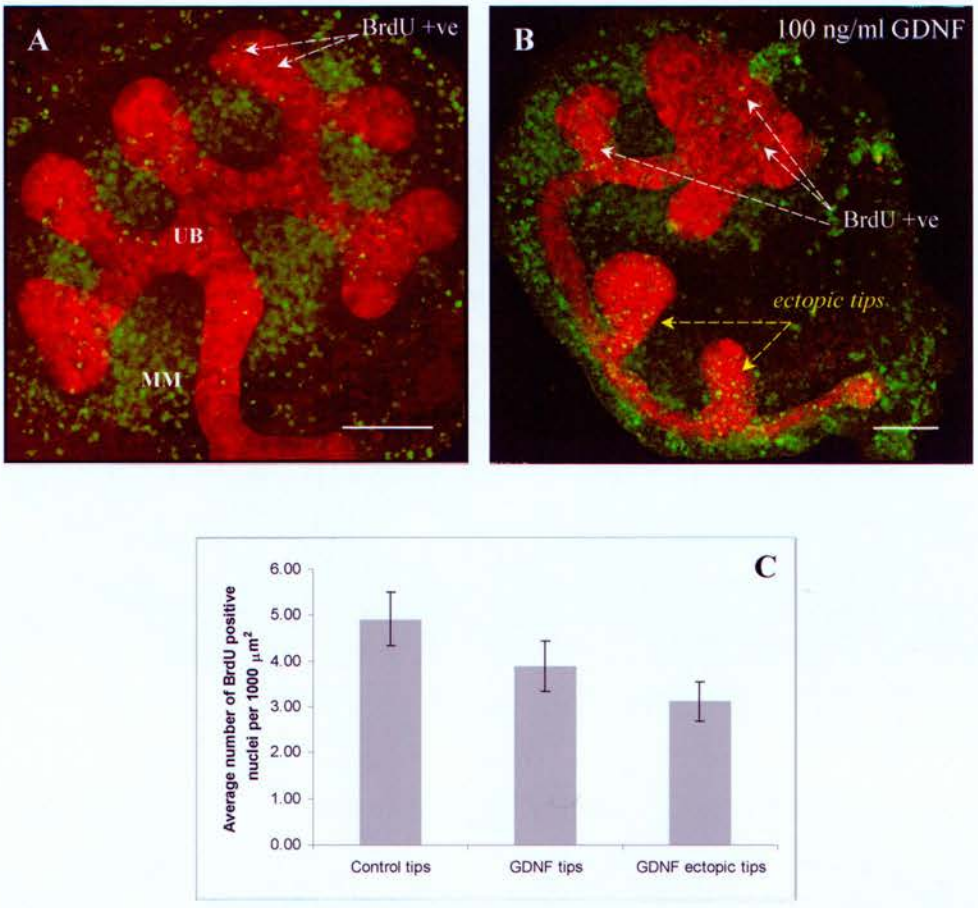

Figure 3.11: GDNF effect on cell proliferation

(A) control kidney in culture for 48 hours, **(B)** kidney culture supplemented with 100 ng/ml GDNF for 48 hours. Arrows showing the BrdU positive nuclei on the epithelium, yellow arrows show the ectopic tips. Double staining: TRITC-anti calbindin D28k and FITC-anti BrdU. **(C)** Average number of BrdU positive nuclei per 1000 μm^2 at the tips of the epithelium (control : 4.91 ± 0.58, GDNF: 3.89 ± 0.55, GDNF ectopic: 3.13 ± 0.43). Control n= 35, GDNF n= 29, GDNF ectopic n= 20 (n values represent the number of tips). Data are shown as mean ± SEM. UB: ureteric bud, MM: metanephric mesenchyme. Scale bars = 100 μm.

control tips ($p= 0.02 < 0.05$). These results suggest that exogenous GDNF does not exert a mitogenic effect on ureteric bud epithelial tips in culture.

A GDNF soaked bead was locally applied adjacent to the tips of T-shape stage E11.5 ureteric buds. The effect of the local application of GDNF on the tip morphology was similar to the exogenous application of the growth factor. The tips were enlarged (average size of 2.6×10^4 μm^2) compared to control tips (5.5×10^3 μm^2) and ectopic buds (6.9×10^3 μm^2) emerged from the stalks (figure 3.12B). However, the effect of the local GDNF application on the cell proliferation at the tips differs from that of the exogenous application of GDNF in culture. Quantification of BrdU incorporation revealed that GDNF causes an increase in the number of proliferating cells at the ureteric bud tips (figure 3.12C). The average number of BrdU labeled nuclei per 1000 μm^2 of epithelium for the control beads was 2.76 ± 0.44 and for the GDNF beads 5.69 ± 1.43 with a p value of 0.05. This increase might be due to the gradient of GDNF as the exact concentration of GDNF that is released from the bead is not known.

The use of a function blocking antibody to GDNF causes reduction in ureteric bud branching (Davies *et al.*, 1999; Towers *et al.*, 1998). Addition of 10 $\mu g/ml$ anti-GDNF in culture for 48 hours resulted in less branching (figure 3.13) [(average control tip number: 7.67 ± 0.88; anti-GDNF: 1.33 ± 0.33) $p= 0.01$]. In addition to the reduced number of tips, their morphology was changed in the experimental group. Since the tip could not be defined clearly by morphological observation, the quantification of BrdU incorporation was performed on stacked optical sections with the adjusted background threshold values, using both tip definitions (methods IV and VIII) (figure 3.14). Both methods revealed a significant reduction in cell proliferation at the tips when GDNF is blocked (figure 3.15). For method IV, the average number of BrdU labeled nuclei per 1000 μm^2 of epithelium for the tips of the control groups was 2.43 ± 0.34 and for anti-GDNF was 1.41 ± 0.31 ($p= 0.048$). For method VIII, the values were 2.83 ± 0.41 and 1.59 ± 0.29 respectively ($p= 0.03$).

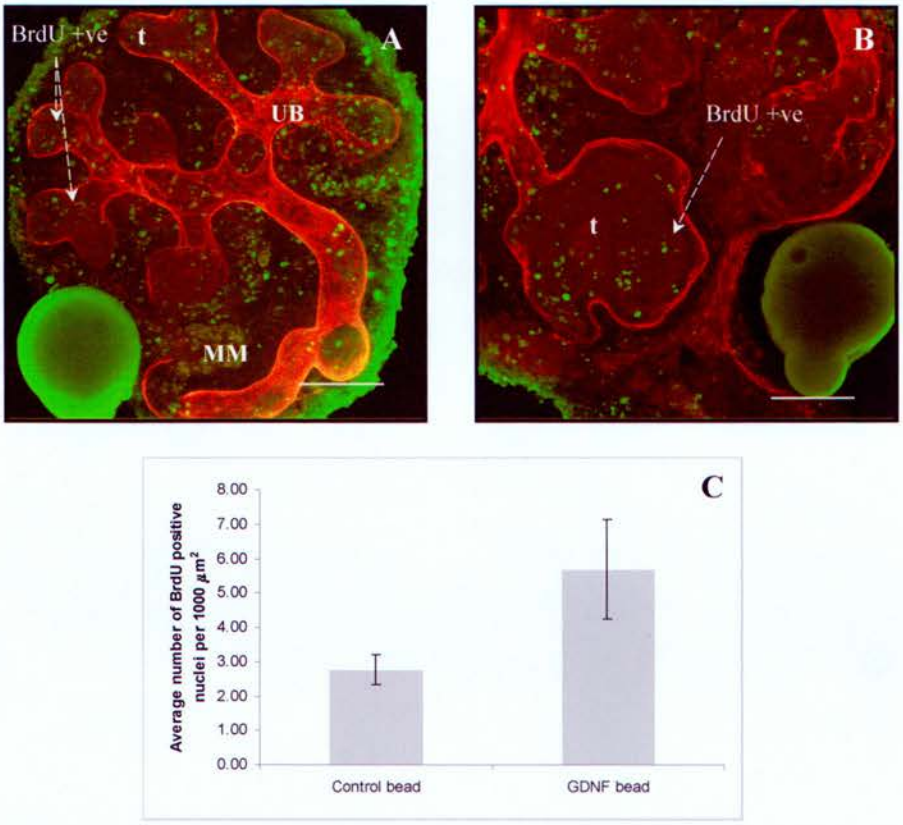

Figure 3.12: Local effect of GDNF on cell proliferation at the tips of the ureteric bud

(A) Control beads (1% BSA) at the tips of E11.5 kidneys in culture for 48 hours, **(B)** GDNF soaked beads (50 µg/ml). Arrows showing BrdU positive nuclei at the tips of the ureteric bud. Double staining: TRITC-anti laminin and FITC-anti BrdU. **(C)** Average number of BrdU positive nuclei per 1000 μm^2 at the tips of the epithelium (control bead: 2.76 ± 0.44, GDNF bead: 5.69 ± 1.43). Control bead n= 23, GDNF bead n= 8 (n values represent the number of tips). Data are shown as mean ± SEM. p= 0.05 UB: ureteric bud, MM: metanephric mesenchyme, t: terminal tip. Scale bars = 100 µm.

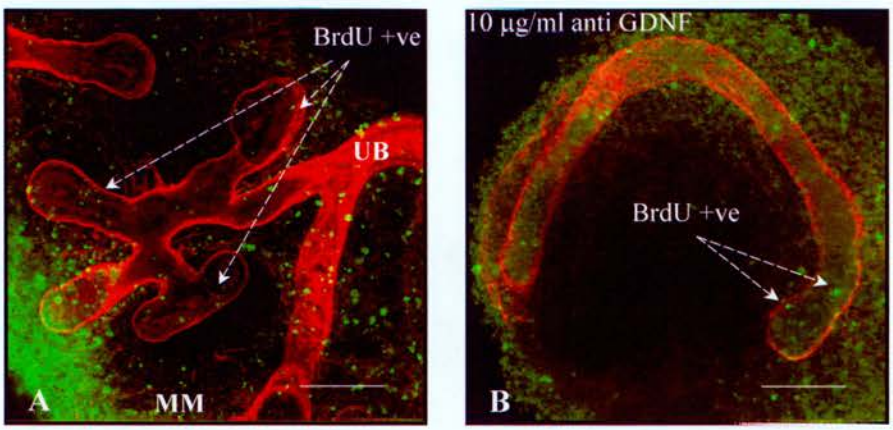

Figure 3.13: Effect of anti-GDNF antibody on cell proliferation at the tips of the ureteric bud

(A) A control kidney cultured for 48 hours, **(B)** kidney culture supplemented with 10 µg/ml function blocking antibody to GDNF for 48 hours. Arrows showing BrdU positive nuclei at the tips of the ureteric bud. Double staining: TRITC-anti laminin and FITC-anti BrdU. UB: ureteric bud, MM: metanephric mesenchyme. Scale bars = 100 µm.

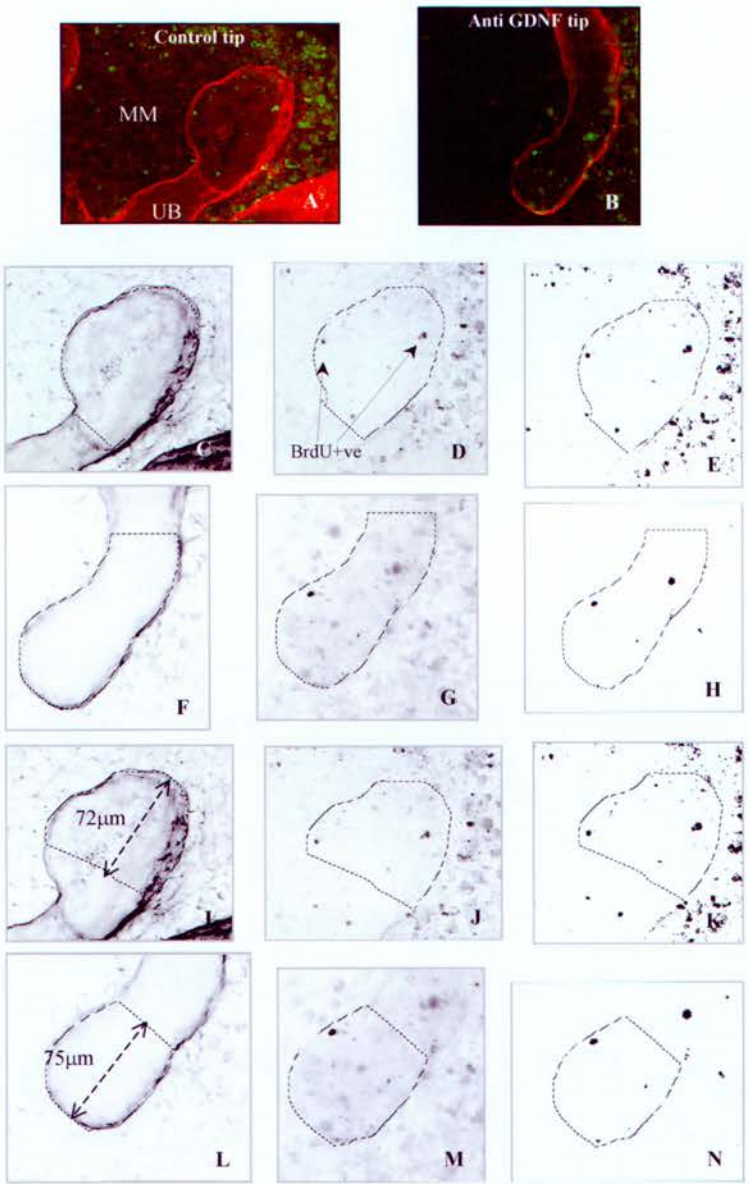

Figure 3.14: Quantification methods on the effect of 10 μg/ml anti GDNF antibody on cell proliferation at the tips of the ureteric epithelium

(A) Control, **(B)** 10 μg/ml anti GDNF in stack of three 3 μm thick confocal optical sections. Panels **(C-E)** and **(I-K)** show the same control tip, **(F-H)** and **(L-N)** show the same anti-GDNF tip viewed in Scion Image. Panels **(C, F, I, L)** show the epithelium (TRITC-anti laminin) in gray scale, **(D, G, J, M)** show the nuclei (FITC-anti BrdU) in gray scale, **(E, H, K, N)** show the positive BrdU nuclei for counting after adjustment of the fluorescence intensity 3x higher the threshold of the fluorescence background of the FITC-anti BrdU sections.

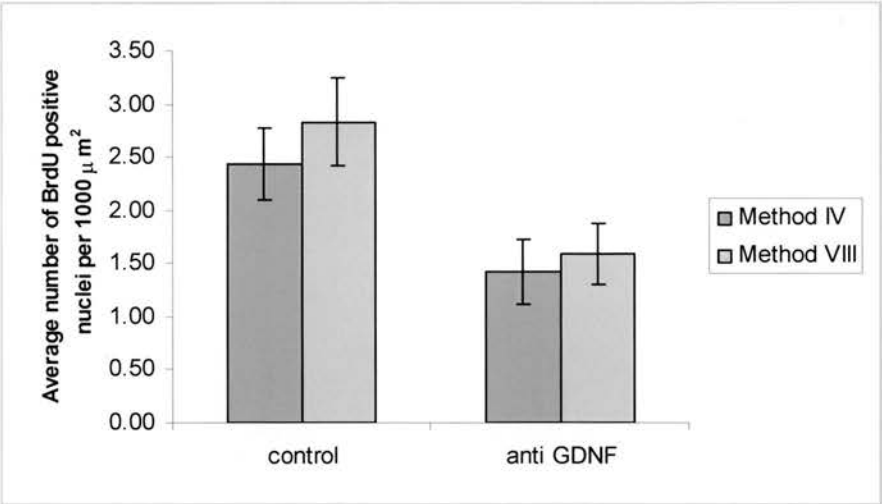

Figure 3.15: Blocking GDNF in culture results in reduction of cell proliferation at the tips of the branching ureteric bud

Comparison of the two counting methods described in figure 3.14. Data are shown as the mean of BrdU positive nuclei per 1000 μm^2 of epithelial tip (control (IV): 2.43 ± 0.34, anti-GDNF (IV): 1.41 ± 0.31, control (VIII): 2.83 ± 0.41, anti-GDNF (VIII): 1.59 ± 0.29). Control n= 15, anti-GDNF n= 4 (n values represent the number of tips). Error bars are the SEM, p= 0.048 (IV), p= 0.03 (VIII).

These results suggest that addition of GDNF in culture does not increase the cell proliferation at the ureteric bud tips. However, when GDNF is placed as a local source in close proximity to the ureteric bud tips, it might stimulate cell proliferation. Blocking GDNF in culture results in a reduction of cell proliferation at the terminal tips of the ureteric bud branches.

3.3.6 TGF-β effect on cell proliferation at the ureteric bud tips

TGF-β has been reported to exert an inhibitory effect on branching morphogenesis of the ureteric bud (Clark *et al.*, 2001; Ritvos *et al.*, 1995; Sakurai and Nigam, 1997). Ritvos and others (1995), showed that kidneys cultured in 1 nM TGF-β show abnormal branching with long UB branches in an arcade fashion which branch towards the periphery of the rudiment. The aim was to establish whether this inhibitory effect is due to regulation of cell proliferation at the tips of the epithelium.

Kidneys were cultured for 72 hours in 1 nM TGF-β which resulted in a reduction in branching morphogenesis (figure 3.17; control average number of tips: 15.71 ± 1.02; TGF-β: 8.17 ± 0.40; p= 0.00014 <0.01). The morphology of the ureteric buds fell into a range of phenotypes which included short branches emerging from the stalks (figure 3.16). In order to examine whether the inhibitory effect was due to regulation of cell proliferation at the bud tips, BrdU was incorporated in kidneys at 24 hours in culture (figure 3.18). After just 24 hours in culture, the TGF-β treated kidneys did not yet show a significant reduction in branching (figure 3.17; the control average number of tips was 4.33 ± 1.20 and the TGF-β average number was 2.67 ± 0.67 p= 0.30). However quantification of the proliferating cells showed that at the tips of the ureteric bud cultured in 1 nM of TGF-β, the average of proliferating cells is significantly lower (p= 1.59 $x10^{-5}$ <0.01) than the control tips (figure 3.19).

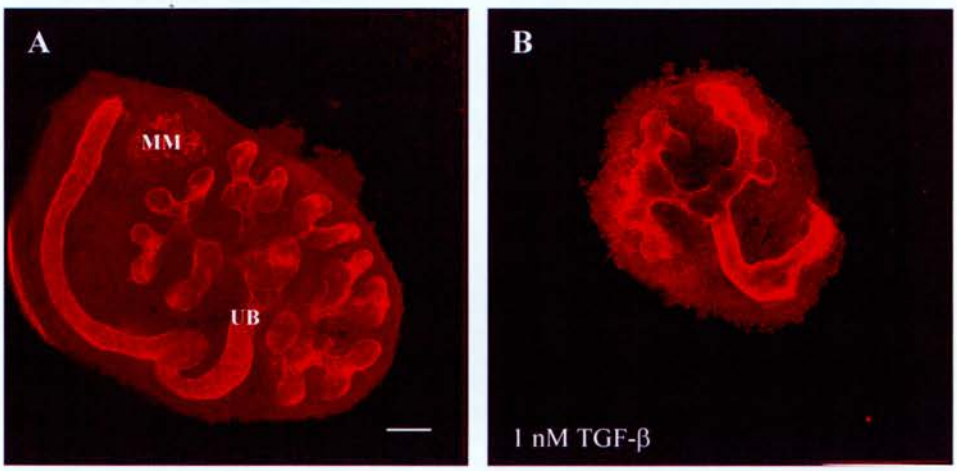

Figure 3.16: The effect of TGF-β on ureteric bud branching morphogenesis

(A) an E11.5 kidney in culture for 72 hours, **(B)** an E11.5 kidney in a culture supplemented with 1 nM TGF-β. Staining: TRITC-anti laminin. UB: ureteric bud, MM: metanephric mesenchyme. Scale bar = 100 μm.

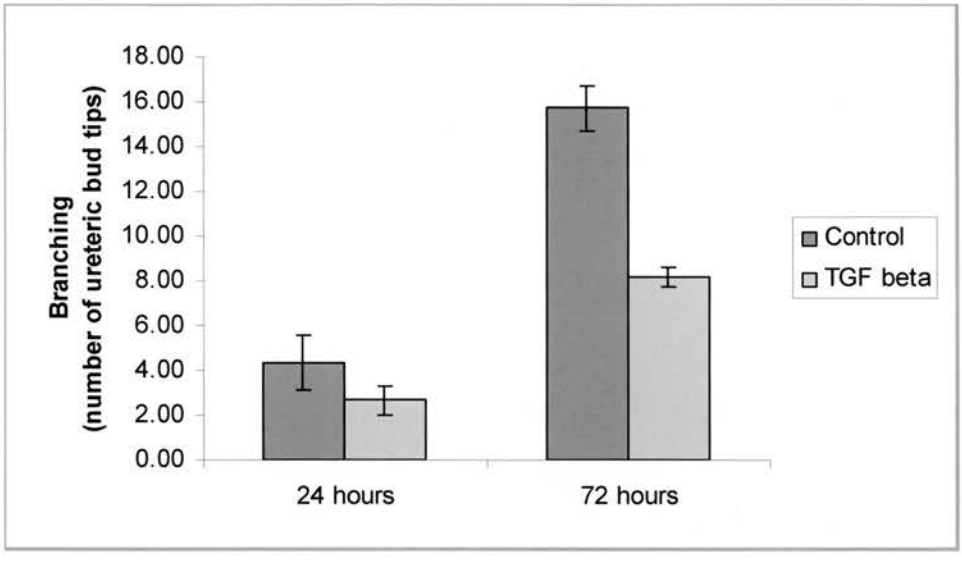

Figure 3.17: Effect of 1 nM TGF-β on ureteric bud branching morphogenesis in culture

E11.5 kidneys were cultured for 24 and 72 hours in 1 nM TGF-β. Branching is quantified as the number of terminal ureteric bud tips. Data shown represent the average number of ureteric bud tips, error bars are the SEM. For 24 hour culture control n= 3 , TGF-β n= 3. For 72 hours culture control n= 7 and TGF-β n= 6 (n values represent the number of kidneys).

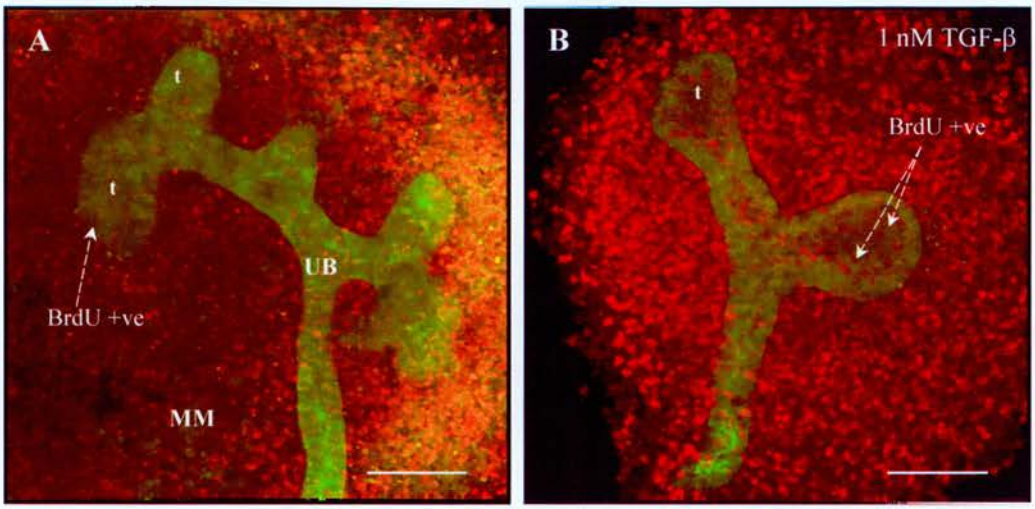

Figure 3.18: TGF-β effect on cell proliferation

(A) Control kidney in culture for 24 hours, **(B)** kidney in culture supplemented with 1 nM TGF-β for 24 hours. Arrows showing the BrdU positive nuclei on the epithelium. Double staining: FITC-anti calbindin D28k and TRITC-anti BrdU. UB: ureteric bud, MM: metanephric mesenchyme, **t**: terminal tip. Scale bars = 100 μm.

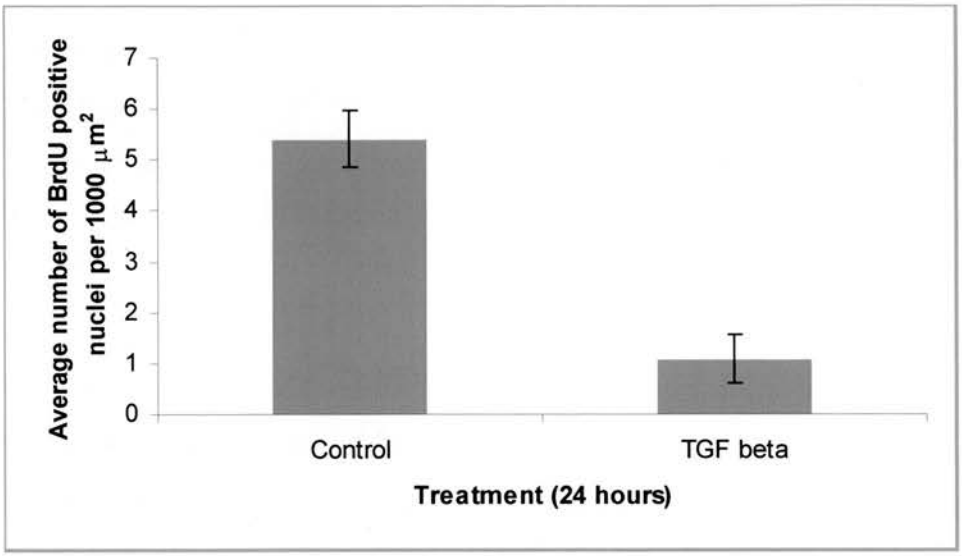

Figure 3.19: Effect of 1 nM TGF-β on cell proliferation at the tips of the branching ureteric bud

E11.5 kidneys cultured in 1 nM TGF-β for 24 hours. The graph represents the average number of BrdU positive nuclei per 1000 μm^2 of the epithelium (control: 5.40 ± 0.55, TGF-β: 1.09 ± 0.48). Control n= 13, TGF-β n= 7 (n values represent the number of tips). Data are shown as mean ± SEM. $p < 0.01$

3.4 Discussion

Localized cell proliferation is shown to be a feature of developmental shape changes during epithelial folding and branching morphogenesis (Goldin *et al.*, 1984; Jernvall and Thesleff, 2000). This chapter examines whether localized proliferation is present during branching morphogenesis of the ureteric bud. Cell proliferation was assessed by BrdU incorporation in organ cultures for 24 hours before fixation as previously described (Davies *et al.*, 1995; Fisher *et al.*, 2001; Tokuda *et al.*, 2003). In the experiments where the whole incubation period was 24 hours or less, BrdU was present throughout the culture period. The presence of BrdU for the whole culture period or the last 24 hours did not seem to have any toxic effect on the rudiments which grew and branched as normal. Other workers, such as Tokuda and others (Tokuda *et al.*, 2003), have also used 24 hour BrdU incubations in with no reported toxic effect.

In summary, the results show that during ureteric bud development, there is an increase in local proliferation at the ampullary tips of the growing epithelium, a specialization that correlates with branching activity. There is also evidence that local proliferation is the first sign of initiation of the ureteric bud. Two known regulators of ureteric bud branching morphogenesis (GDNF and TGF-β) were examined in relation to their possible positive or negative effect on the localized proliferation at the tips of the epithelium.

Localized cell proliferation at the UB tips and during UB outgrowth

During branching morphogenesis, the emergence of the new buds is an active process which is often associated with high cell proliferation. This is the case in the terminal endbud during branching morphogenesis of the pubertal mammary gland (Daniel *et al.*, 1984; Humphreys *et al.*, 1996). In the developing salivary gland in culture, initial cleft formation is independent of cell proliferation (Nakanishi *et al.*, 1987) however during branching morphogenesis labeling of

proliferating cells with [^{3}H]thymidine, shows specific localization on the distal areas of the salivary epithelial lobules (Bernfield and Banerjee, 1982) less proliferating cells in the interlobular areas and almost none in the center of the epithelium (Bernfield *et al.*, 1972).

The formation of new ureteric bud tips show higher localized cell proliferation when compared to the ureteric bud stalks, a specialization of the ampullary tips that is correlated with branching activity. When branching is arrested with sodium chlorate, the cell proliferation at the ureteric bud tips is greatly reduced. Previous proliferation studies in human embryonic kidneys support the current observations that the ampullary ureteric bud tips are highly proliferative (Nadasdy *et al.*, 1998; Winyard *et al.*, 1996). Other branching organs such as the developing pancreas and lung show intense localized cell proliferation in the areas of branching activity (Horb and Slack, 2000; Mollard and Dziadek, 1998). In the embryonic lung, the actively growing distal bud shows a greater BrdU labeling in comparison to interbud regions, an area that shows a relatively higher localization of basement membrane components (Mollard and Dziadek, 1998). Nogawa *et al.* showed that embryonic lung epithelia in culture show high bromodeoxyuridine (BrdU) incorporation in areas of budding, but none in the areas between the buds (Nogawa *et al.*, 1998). The same study has shown that even though lung bud formation is accompanied with differentials in localized cell proliferation once branching morphogenesis is initiated, the initial bud outgrowth is not triggered by induction of localized cell proliferation (Nogawa *et al.*, 1998). In culture (at around 8 hours), at the presumptive metanephric area there is an increased area of localized cell proliferation where the ureteric bud will evaginate, suggesting that localized cell proliferation might be one of the forces that drive the ureteric bud outgrowth.

TGF-β superfamily members on cell proliferation at UB tips

Members of the TGF-β superfamily are key regulators of metanephric development (*chapter 1*). GDNF binds to GPI-anchored GDNF family receptor α1, activates the receptor tyrosine kinase Ret and signals through the MAP kinase pathway (Saarma, 2000; Sariola and Sainio, 1997; Worby *et al.*, 1996). TGF-β family members signal through receptor serine/threonine protein kinases. TGF-β binds to type II receptor (TβR-II), the complex then interacts with type I receptor (TβR-I), type II receptor phosphorylates type I receptor, which then phosphorylates and activates Smad proteins which carry the signal to the nucleus (reviewed in (Massague, 1998).

The role of GDNF on the branching of the ureteric bud has already been introduced in *chapter 1*. GDNF is required for ureteric bud outgrowth from the nephric duct. It binds directly to the tips of the ureteric bud epithelium and induces the formation of supernumerary buds (Sainio *et al.*, 1997b). GDNF and its receptors (GFRα1, Ret) are also important for the development of enteric, sympathetic and sensory neurons. Mutations of either the ligand or its receptors have the same phenotype. Mice lacking GDNF, Ret or GFRα1 show abnormalities in enteric nervous system and kidneys (Enomoto *et al.*, 1998; Moore *et al.*, 1996; Sanchez *et al.*, 1996). The enteric nervous system is a complex network of interconnected neurons that regulates intestinal motility and mucosal secretion (Costa and Brookes, 1994). The majority of the precursors of the enteric nervous system are derived from the vagal and anterior truncal neural crest that migrate into the developing gut (Durbec *et al.*, 1996). In GDNF and Ret knockout mice, no enteric neurons or glia are found below the oesophagus and adjacent stomach (Chalazonitis *et al.*, 1998). GDNF is a potent survival and mitogenic factor of neural crest-derived progenitors of the enteric nervous system (Chalazonitis *et al.*, 1998; Heuckeroth *et al.*, 1998; Taraviras *et al.*, 1999; Worley *et al.*, 2000). GDNF is also found to be highly expressed in testis (Hu *et al.*, 1999). In rat, during the early postnatal period of testis development the total number of Sertoli cells is established and is characterized by active cell

proliferation in response to follicle-stimulating hormone (FSH) (Hu *et al.*, 1999). GDNF is found to stimulate the proliferation of Sertoli cells in combination with FSH (Hu *et al.*, 1999).

In the present study, the role of GDNF on cell proliferation at the tips of the ureteric bud epithelium was examined. Exogenous addition of GDNF in organ culture results in increased branching morphogenesis (Towers *et al.*, 1998). The hypothesis tested was whether the branch-promoting effect of GDNF is due to stimulation of cell proliferation at the ureteric bud epithelial tips. The present results show that when GDNF is blocked, there is a reduction in branching which is accompanied by a reduction in cell proliferation at the tips of the branching epithelium. However, the addition of exogenous GDNF in culture results in enlarged ampullary tip morphology without an increase in cell proliferation. The reason for the enlarged tip morphology observed might be due to a stimulatory effect of the growth factor on the epithelial cell size rather than in cell numbers. However the quantification method used in this thesis cannot determine whether this is the case. A different approach would be to examine the effect of exogenously added GDNF in tissue sections or on isolated ureteric bud cells in monolayers. BrdU incorporation upon addition of GDNF would be easier to quantify using the BrdU labeling index (percentage of BrdU positive nuclei/ 100 nuclei). Addition of GDNF to ureteric bud cells growing in certain extracellular matrix components has been shown to be mitogenic (Towers *et al.*, 1998).

When applied locally, GDNF might stimulate cell proliferation at the tips, but since the exact concentration of GDNF released from the beads is not known, the increase in cell proliferation observed might be due to high sensitivity to the gradient. In a similar study the effect of BMP-7 soaked beads on the cell proliferation in kidney organ cultures was examined (Piscione *et al.*, 2001). In that study, the effects of the ligand at specific positions relative to the bead were determined using composite images of the explant tissue sections. The composite images were subdivided into four concentric zones relative to the bead's

location. The radial distance between the perimeter of each concentric zone was 75 μm. The concentration of the ligand was predicted to be the highest in the zone area closest to the bead (zone 1) and was gradually less the further away from the local source of BMP-7 (bead) (Piscione *et al.*, 2001). The effect of BMP-7 on cell proliferation at each of these 75 μm radius zones (zone 1-4) was measured and expressed as percentage of BrdU incorporation. A similar approach could be addressed in the case of GDNF-soaked beads and quantification of BrdU incorporation in successive zones closer or farther to the bead would show whether high concentration of GDNF acting locally (in close proximity) is mitogenic. There is a potential problem with this approach, however, because kidney cultures spread and change shape as they grow, and measurement of the final position of a bead does not necessarily reflect where it was as the culture was growing.

Overall the results presented here show that GDNF does not affect cell proliferation at the tips of the actively growing ureteric bud, which is in accordance with earlier observations (Sainio *et al.*, 1997b). These contradict the results of Pepicelli *et al.* that suggest that GDNF-regulated growth and branching of the ureteric bud is due to the local regulation of ureter tip-specific factors and an increase in local proliferation (Pepicelli *et al.*, 1997). However, in the latter study the ampullary tips of the GDNF treated kidneys appear fused (Pepicelli *et al.*, 1997) a finding that is validated in the present study and might be probably due to the suggested effect of GDNF to increase cell adhesion (Sainio *et al.*, 1997b).

TGF-β itself as previously mentioned is a negative regulator of ureteric bud branching. In murine kidney cultures, TGF-β1 causes branching abnormalities; ureteric bud branches appear elongated in an arcade fashion (Ritvos *et al.*, 1995). The results in this chapter show that addition of TGF-β results in a reduction of branching after 72 hours in culture which is consistent with the findings of Clark *et al.* where TGF-β1 added to cultured rat metanephroi inhibits overall

metanephric and ureteric bud growth, leading to reduced nephron endowment (Clark *et al.*, 2001).

TGF-β can stimulate and inhibit cell proliferation in the same cell type, and is shown to be inhibitory on proliferation of almost all non-neoplastic epithelia in culture (reviewed in Moses *et al.*, 1990). TGF-β inhibits cell cycle progression by lengthening or arresting the G1 phase, through retaining the retinoblastoma gene product (Rb) in the underphosphorylated, growth suppressive state (reviewed in Laiho *et al.*, 1990; Massague, 1990).

In the current experimental system, BrdU incorporation in TGF-β treated kidneys for 24 hours shows a significant reduction in cell proliferation at the ampullary tips of the ureteric bud epithelium. This is similar to studies in other developing branching organs such as the lung, mammary gland and pancreas. In the lung organ culture, TGF-β1 reduces branching and overall lung size (Bragg *et al.*, 2001; Serra *et al.*, 1994). TGF-β1 treatment results in a reduction in the percent of [^{3}H]thymidine-labeled nuclei in the lung epithelium (Serra *et al.*, 1994) and BrdU incorporation (Bragg *et al.*, 2001). Local administration of TGF-β in mammary gland cultures results in inhibition on normal branching morphogenesis. The ducts of the treated glands do not elongate and closely resemble growth-quiescent thin-walled ducts with blunt-tipped terminal ends (Silberstein and Daniel, 1987). The effect of TGF-β is epithelium specific at the mammary end buds and results in a reduction of DNA synthesis to levels similar to the untreated growth-quiescent ducts (Daniel *et al.*, 1989; Silberstein and Daniel, 1987). In the embryonic pancreas in culture, addition of TGF-β results in a reduction in epithelial cell proliferation (at 6 days) (Sanvito *et al.*, 1994).

The branching phenotype obtained in the current study is not similar to the one documented by Ritvos *et al.* (Ritvos *et al.*, 1995) where the ureteric bud branches were elongated. The short UB branches observed are probably due to the reduced cell proliferation at the epithelial tips. It is also possible that TGF-β may

stimulate the deposition of extracellular matrix components or TIMP around the developing ureteric bud tips and consequently limiting the number of branches observed after 72 hours in culture. The action of TGF-β generally leads to up-regulation of cell adhesion, an action mediated by enhanced synthesis and deposition of extracellular matrix components and decreased pericellular proteolysis (reviewed in Massague, 1990). In the developing mammary gland, there is an elevated level of collagen type I at the end buds located near an implanted source of TGF-β (Daniel and Robinson, 1992).

To summarize, this chapter shows that localized cell proliferation is a specialization of the actively growing ureteric bud tips, which correlates with branching activity as it is lost when branching is blocked. Localized cell proliferation also appears to be the first sign of the ureteric bud as it emerges from the Wolffian duct in culture. The experiments were performed to investigate the pattern of cell proliferation during ureteric bud evagination and on the branching ureteric bud epithelium in culture. In principle, it would be possible to gain similar information *in vivo* by treating pregnant mice with BrdU at different time points (i.e. E10.5 before the UB emergence from the Wolffian duct, E11.5, E12.0 and E12.5 before mesenchyme has started forming epithelial structures of future nephrons (Bates *et al.*, 2000)).

The branch-promoting effect of GDNF did not cause an increase in cell proliferation at the tips of the ureteric bud, but instead caused expansion of the area of bud that had tip character, whereas the branch-inhibiting effect of TGF-β was found to be associated with less proliferation at the ureteric bud tips. GDNF heterozygous mice have similar body weights to wild-type mice (Cullen-McEwen *et al.*, 2001). However GDNF heterozygous kidneys are approximately 25% smaller than the wild-type kidneys, they have abnormal shape possibly due to defected branching morphogenesis, and they have 30% less nephrons (Cullen-McEwen *et al.*, 2001). It would be of interest to examine the cell proliferation

pattern in the GDNF heterozygous kidneys and compare with the wild type kidneys.

Chapter 4

The Cytoskeleton During Branching Morphogenesis of the Ureteric Bud

4.1 Introduction

Morphogenetic changes occur as the result of embryonic epithelial cells responding to signals and generating the activity that allows them to participate in organogenesis (for review see Bard, 1992). The cytoskeleton is responsible for much of the activity within the cell. In mammalian cells, the actin cytoskeleton provides the driving force for cell motility and surface remodeling (Kabsch and Vandekerckhove, 1992). The actin cytoskeleton is a highly dynamic structure that is reshaped during the cell cycle, in response to extracellular signals and controls cell-cell and cell-substrate interactions together with adhesion molecules (Hall, 1994). The main mechanism by which epithelial cells change their shape seems to be the contraction of rings of microfilaments in a purse-string mechanism (figure 4.1).

Epithelia form contiguous sheets of cells linked by cell-cell adhesion molecules and junctions on their lateral surfaces (for review Gumbiner, 1996). Adherens junctions are sites of strong adhesion between the cells just below their apical surface and are associated with actin filaments (Knust and Bossinger, 2002). Cadherins are the major adhesion receptors of the adherens junctions, where they colocalize with dense actin filament bundles (Gumbiner, 1996). The contractile ring of the purse-string mechanism is composed of actin and myosin-II that contracts resulting in wedge shaped cells (Kiehart, 1999).

During late *Drosophila* embryogenesis, the establishment of the dorsal ectoderm involves a process referred to as dorsal closure (Settleman, 1999). Earlier morphogenetic movements of the embryo leave a hole in the dorsal side of the embryo that is covered by a thin transient epithelial structure (amnioserosa) that ultimately degenerates (Settleman, 1999). Dorsal closure involves the movement of the lateral epidermal epithelial sheets from each side of the embryo that zip together at the dorsal midline to form one contiguous epithelial sheet (Grose and Martin, 1999; Settleman, 1999). This process involves cytoskeleton-mediated cell shape changes, by formation of an intracellular actin-purse string (Harden *et*

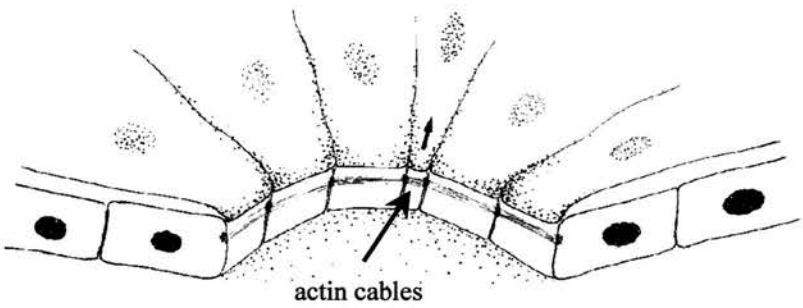

(From Nodder and Martin, 1997)

Figure 4.1: Purse-string mechanism

Intracellular actin filaments anchor into adherens junctions at the apices of epithelial cells. Contraction of the actin cables results in a change of the cell shape into wedges and a subsequent movement of the epithelial sheet.

al., 1999). Actin filaments and myosin are accumulated at the leading edge of the lateral epithelial cells and contraction leads to the epithelial sheets meeting and fusing at the dorsal midline (Grose and Martin, 1999). The process is mediated by members of the Rho family of small guanosine triphosphatases (GTPases) that are key regulators of the actin cytoskeleton (Harden *et al.*, 1999; Settleman, 2000).

Partial purse-string mechanism is common in invaginations of the epithelial sheets during morphogenesis (Kiehart, 1999). An example of this can be found in the morphogenetic changes during fold formation of the proximal rat colon (Colony and Conforti, 1993). During fold formation, actin microfilaments are observed in cells located at the apices of the developing folds (figure 4.2).

During branching morphogenesis in the developing salivary gland, the actin cytoskeleton is important for the epithelial cell shape changes (Hardman and Spooner, 1992b; Spooner, 1973). Actin microfilament contraction in the apices of the epithelial cells of the developing salivary gland is associated with tip formation. Disruption of the cytoskeleton results in loss of clefts and arrest of branching morphogenesis (Spooner, 1973).

Aim

The aim of this chapter is to find (i) whether the cytoskeleton has a special arrangement in the ureteric bud, which correlates with the branching activity and (ii) whether the cytoskeletal elements of the ureteric epithelium play an important role in branching morphogenesis.

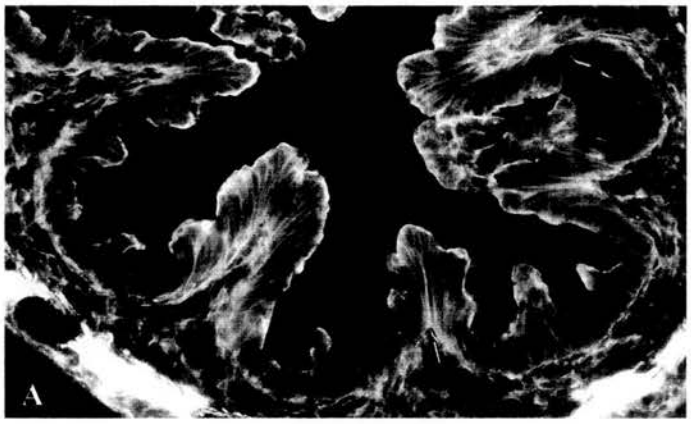

(From Colony and Conforti, 1993)

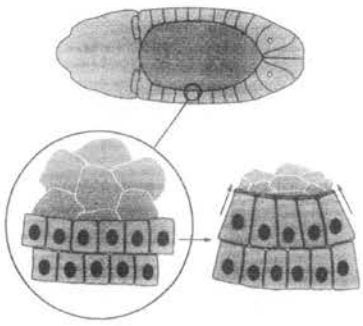

B

(From Grose and Martin, 1999)

Figure 4.2: Epithelial cell movement during development

(A) Actin filament localization in the apices of the folds of E_r20 proximal colon (arrow) **(B)** Dorsal closure in the late *Drosophila* embryo where a contractile actin cable in the leading edge cells draws the epidermis over the exposed amnioserosa.

4.2 Results

4.2.1 Localization of actin filaments at the ureteric bud tips during branching morphogenesis

In order to test whether the cytoskeleton shows special arrangement during the shape changes occurring during ureteric bud branching, the first step was to characterize the expression pattern of actin in the developing collecting duct. The localization of actin filaments was assessed using the mushroom toxin phalloidin which is extensively used to visualize actin filaments within cells (VanBuren *et al.*, 1998; Wulf *et al.*, 1979). Phalloidin binds to actin filaments, enhances polymerization of actin and stabilizes actin filaments (Cooper, 1987; Sampath and Pollard, 1991).

Isolated E11.5 kidney rudiments were cultured in standard medium for a time course of 24 to 72 hours and were stained using rhodamine conjugated phalloidin. As shown in figure 4.3, there was a strong phalloidin staining of the actin filaments concentrated on the ureteric bud epithelium in comparison to the mesenchyme which does not stain as much. The expression of actin filaments on the epithelium is concentrated at the apical ends of the ureteric bud tips throughout the culture period (figure 4.3).

To test whether the very strong expression of filamentous actin at the tips of the branching epithelium correlates with branching activity, branching was arrested using either sodium chlorate or a MAP kinase inhibitor (PD98059). E11.5 kidney rudiments were cultured for 24 hours in standard medium (control) or in the presence of 30 mM sodium chlorate which blocks branching morphogenesis of the ureteric bud as previously mentioned (Davies *et al.*, 1995). Rhodamine conjugated phalloidin staining in chlorate-treated kidneys shows a different actin filament distribution than in control kidneys. When ureteric bud branching is blocked, filamentous actin is uniformly distributed on the ureteric bud epithelium with loss of the specific localization of F-actin from the tips of the ureteric buds

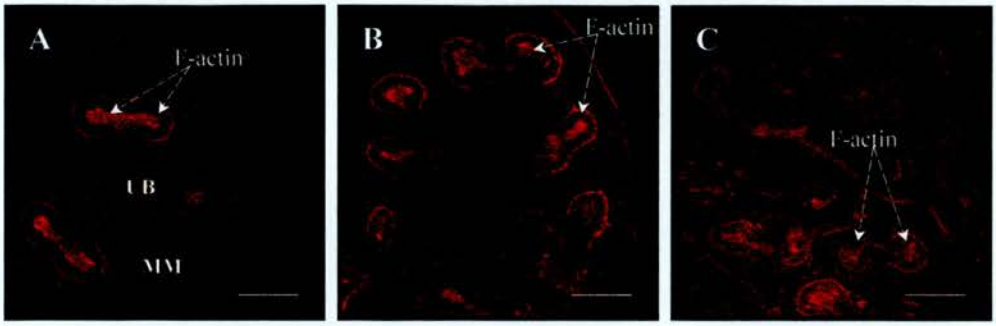

Figure 4.3: Localization of actin filaments at the tip ends of the branching ureteric bud in culture

(A) E11.5 kidney in culture for 24 hours, **(B)** 48 hours and **(C)** 72 hours. Kidneys are stained with TRITC-phalloidin which stabilizes the microfilaments. Filamentous actin is strongly expressed at the apical parts of the ureteric bud tips. Arrows show the localization of actin filaments at the epithelial tips. UB: ureteric bud, MM: metanephric mesenchyme, F-: filamentous. Scale bars = 100 μm.

(figure 4.4). This result suggests that the special arrangement of F-actin at the tips of the ureteric bud is present during branching activity and is lost when branching is blocked.

Kidneys were also cultured for 48 hours in the presence of 10 μM PD98059, a MAP kinase inhibitor that blocks the branching but not extension of the ureteric bud resulting in less but longer branches (Fisher *et al.*, 2001). Again, when branching is blocked, phalloidin staining differs from that in the controls (figure 4.5). The fluorescence is found higher at the ureteric bud tips but actin cables appear disrupted when compared to actin filaments in control tips.

The above results show that during branching activity there is a specialized arrangement of actin filaments at the apical areas of the ureteric bud tips. This specialization occurs during branching and is lost when branching is arrested.

4.2.2 Localization of actin filaments during ureteric bud outgrowth from the Wolffian duct

Ureteric bud appears as a "tip"-like outgrowth from the Wolffian duct. To test whether the shape changes, during the evagination process, are accompanied by changes in the cytoskeleton, Wolffian ducts and surrounding mesenchyme were isolated from E10.5 embryos before ureteric bud outgrowth. The Wolffian ducts and surrounding mesenchyme were cultured for 12 hours. In culture, by this time the ureteric bud has emerged from the duct but has not yet branched. Rhodamine conjugated phalloidin staining showed high expression of actin filaments at the apical part of the newly formed ureteric bud (figure 4.6).

This result suggests that the first ureteric bud branch from the Wolffian duct is like the ureteric bud branches inside the developing metanephros and that changes at the cytoskeletal arrangement may be driving the initial appearance of the ureteric bud.

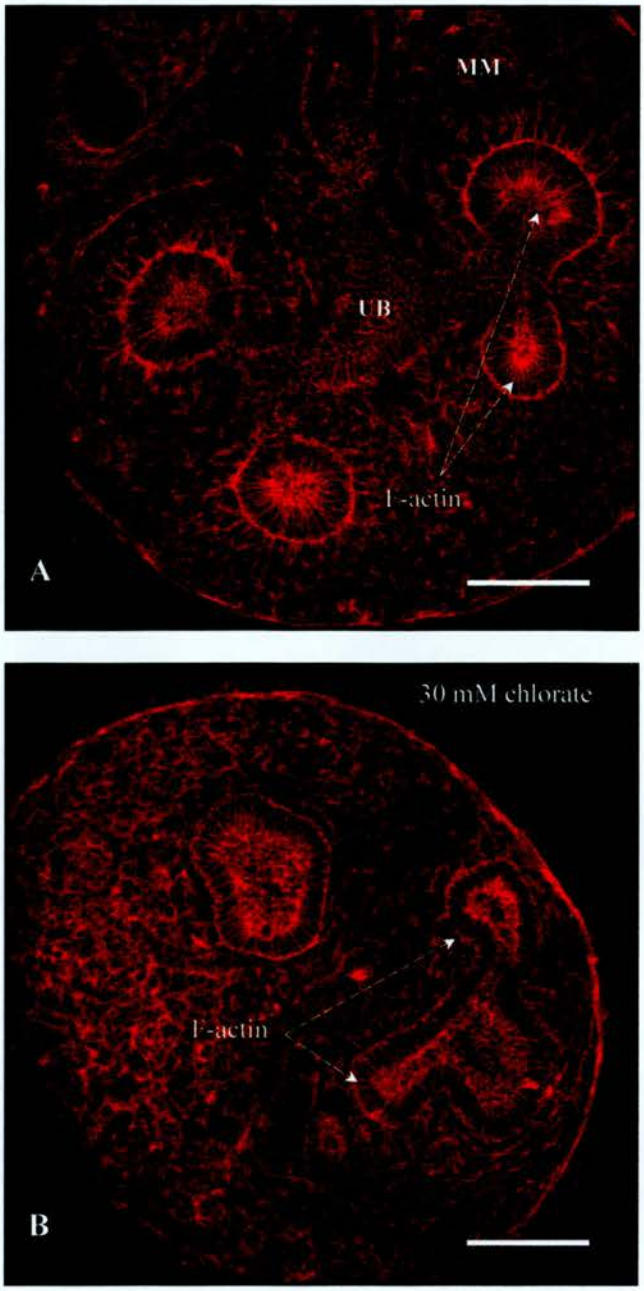

Figure 4.4: Localization of actin filaments in chlorate-treated kidneys where normal branching is disrupted

(A) An E11.5 metanephros in control culture for 24 hours showing normal branching and filamentous actin distribution at the apices of the ureteric bud tip cells (arrows), **(B)** an E11.5 metanephros in culture supplemented with 30 mM sodium chlorate showing disrupted branching morphogenesis. F-actin (arrows) on the chlorate-treated epithelium appears similar to the microfilament distribution in the control UB stalks. Staining: TRITC-phalloidin. UB: ureteric bud, MM: metanephric mesenchyme, F-: filamentous. Scale bars = 100 μm.

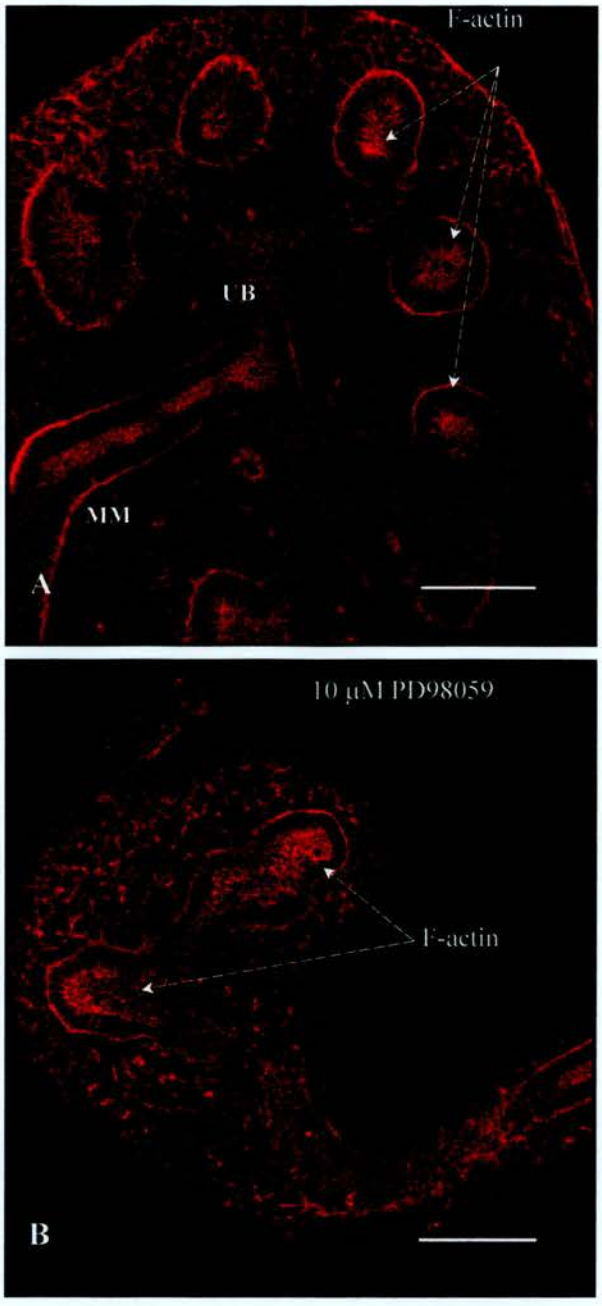

Figure 4.5: Localization of actin filaments in kidneys where branching is arrested through MAP kinase inhibition

(A) F-actin localization at the tips of the epithelium in a control kidney cultured for 48 hours, **(B)** F-actin distribution is altered on the epithelium of a kidney cultured for 48 hours at 10 μM PD98059. Arrows show the actin filaments. Staining: TRITC-phalloidin. UB: ureteric bud, MM: metanephric mesenchyme, F-: filamentous. Scale bars = 100 μm.

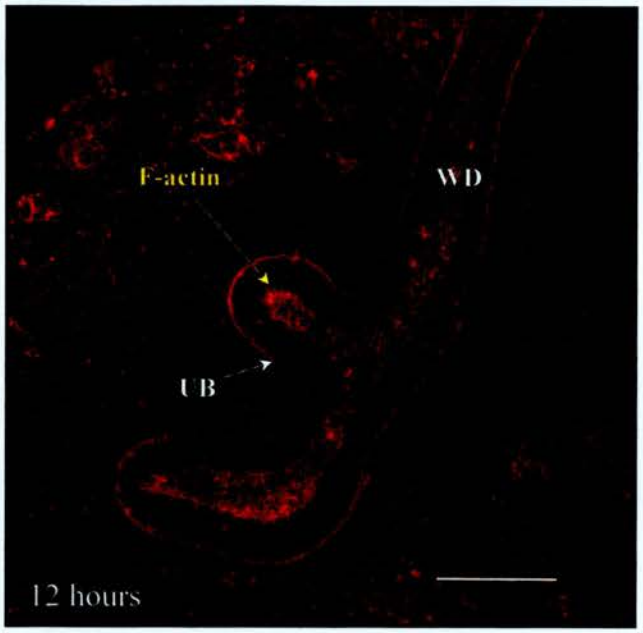

Figure 4.6: Actin localization during ureteric bud outgrowth from the Wolffian duct in culture

An E10.5 Wolffian duct in culture for 12 hours. White arrow shows the emerging ureteric bud at the caudal end of the duct, yellow arrow shows the filamentous actin localized at the outgrowing tip of the bud. Staining: TRITC-phalloidin. WD: Wolffian duct, UB: ureteric bud, F-: filamentous. Scale bar = 100 μm.

4.2.3 Inhibition of actin on ureteric bud branching morphogenesis

Rhodamine conjugated phalloidin staining has shown a special arrangement of actin filaments at the tip ends of the ureteric bud epithelium during branching, which is lost when branching is blocked. In order to examine whether this special arrangement of F-actin is important for branching, the effect of disrupting actin filaments on branching morphogenesis was investigated.

Cytochalasin D is a mold metabolite, which binds with high affinity to the barbed end of actin filaments (Cooper, 1987). It inhibits actin polymerization and disrupts actin organization (Cooper, 1987; Soong *et al.*, 1990). Cytochalasin D is used in various studies that investigate the effect of actin disruption in epithelial shape changes (Colony and Conforti, 1993; Soong *et al.*, 1990). The latter study shows that cytochalasin D at concentrations ranging from 1.0 μg/ml to 0.1 μg/ml has an inhibitory effect on corneal epithelial cell migration, with complete migration arrest at 0.5 μg/ml (Soong *et al.*, 1990). Therefore, I decided to start at this concentration in the present organ culture system.

Kidney rudiments were initially cultured for 72 hours at 0.5 μg/ml cytochalasin D. At this concentration, branching and growth of the epithelium was completely inhibited (figure 4.7). At lower concentrations (0.3 and 0.1 μg/ml), the effect was inhibitory and the morphology of the epithelium was distorted (figure 4.8). At 0.3 μg/ml cytochalasin D, the ureteric bud stalk branches appeared swollen, with minimal ramification at the terminal branches reflecting the importance of the intact cytoskeleton in ureteric bud tissue integrity. At the lowest concentration (0.1 μg/ml) which is a very low concentration, the morphology of the ureteric epithelium appeared swollen to a lesser extend than at 0.3 μg/ml without blocking branching morphogenesis (figure 4.8). The stalk branches appeared swollen and the ureteric bud tips were funnel-shaped. The effect of cytochalasin D was tested for reversibility at the lowest concentration 0.1 μg/ml. Kidneys were cultured for 24 hours at 0.1 μg/ml cytochalasin D and then they were

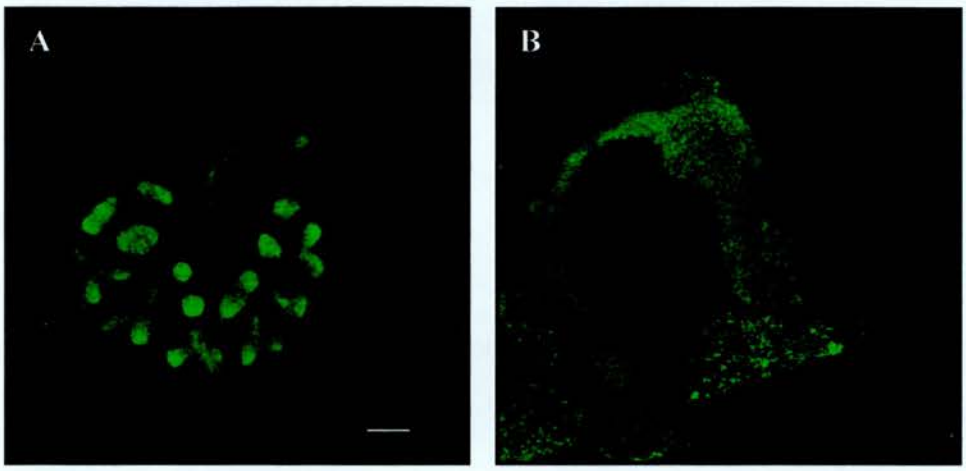

Figure 4.7: The effect of blocking actin polymerization on branching morphogenesis

(A) kidney cultured in 0.5% DMSO as control for 72 hours, **(B)** kidney cutlured in 0.5 μg/ml cytochalasin D. Staining: FITC-anti calbindin D28k. Scale bar = 100 μm.

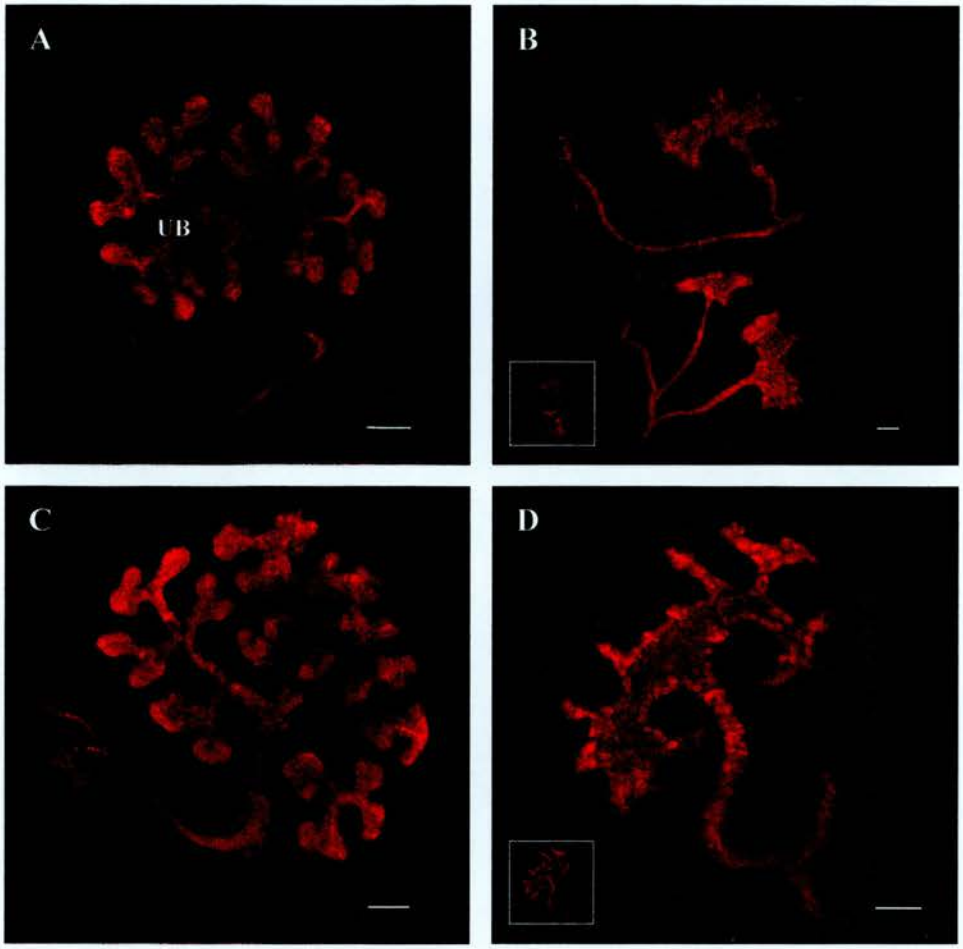

Figure 4.8: Effect of lower concentrations of cytochalasin D on branching morphogenesis in culture

Kidney rudiments were cultured for 72 hours in **(A)** 0.03% DMSO (control), **(B)** 0.3 μg/ml cytochalasin D (a double ureter is present), **(C)** 0.001% DMSO (control) and **(D)** 0.1 μg/ml cytochalasin D. In (B) and (D) the background fluorescence has been removed (using Adobe photoshop) for aesthetic purposes only and the originals have been included as small inserts at the bottom left of each picture. Staining: TRITC-anti calbindin D28k. Scale bars = 100 μm.

transferred to control culture medium for further 24 hours. Branching morphogenesis was resumed in control culture medium (figure 4.9).

The effect that 0.1 μg/ml cytochalasin D has on ureteric bud branching was investigated in a time course of 24, 48 and 72 hours (figure 4.10). At 24 hours, the ureteric bud tips showed an enlarged morphology (figure 4.10 A-F) in relation to the control tips. As branching morphogenesis progressed, this expanded tip morphology persisted at both culture times of 48 and 72 hours in relation to control tips (figure 4.10 G-L and M-R). The branching (that is, the number of ureteric bud tips) was reduced at all time points in relation to controls (figure 4.11). At 24 hours the average number of control tips was 6.3 ± 0.25 and the cytochalasin D treated kidney tips were 3.3 ± 0.63 ($p= 0.012$; < 0.05). At 48 hours, the average number of the control tips were 14.5 ± 1.89 whereas the cytochalasin D treated tips were 8 ± 1.05, ($p= 0.03$; <0.05). By 72 hours in culture, the average number of tips was 17.5 ± 2.40 for the control kidneys and 11 ± 1 ($p= 0.067$) for the kidneys cultured in 0.1 μg/ml cytochalasin D. The expanded morphology of the ureteric bud tips when kidneys were cultured for 48 and 72 hours in 0.1 μg/ml cytochalasin D was accompanied by scattering of some epithelial cells into the surrounding mesenchyme (figure 4.12).

Whether the scattering of the epithelial tip cells observed in kidneys cultured in cytochalasin D was a feature of the branching activity was investigated. Kidneys were cultured for 72 hours in 30 mM of sodium chlorate to block branching activity. Cytochalasin D (at 0.1 μg/ml) was added during the whole culture period to test whether the tip cells would scatter. The morphology of the ureteric bud was chlorate-like and there was no cell scattering observed at the tips of the branching arrested epithelium (figure 4.13). This suggests that the cells of the actively growing tips are probably in a less stable state in comparison to the cells of the ureteric bud stalks. This less stable state allows cells at the tips to scatter when actin cytoskeleton is mildly disrupted with 0.1 μg/ml Cyto D. When the tips are not active (as in chlorate treated kidneys) the cells are probably more

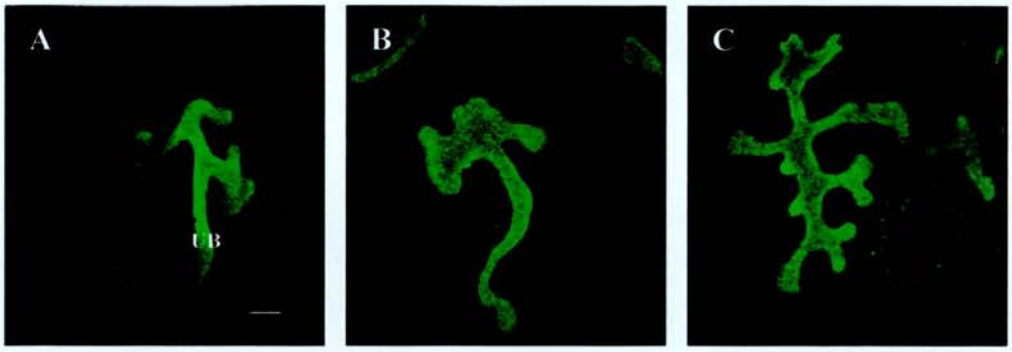

Figure 4.9: The effect of 0.1 μg/ml cytochalasin D on branching morphogenesis of the ureteric bud is reversible

(A) control E11.5 kidney after 24 hours in culture, **(B)** kidney cultured for 24 hours in the presence of 0.1 μg/ml cytochalasin D, **(C)** kidney cultured for 24 hours in 0.1 μg/ml cytochalasin D and transferred for further 24 hours in control culture medium. Branching morphogenesis was recovered. Staining: FITC-anti calbindin D28k. UB: ureteric bud. Scale bar = 100 μm.

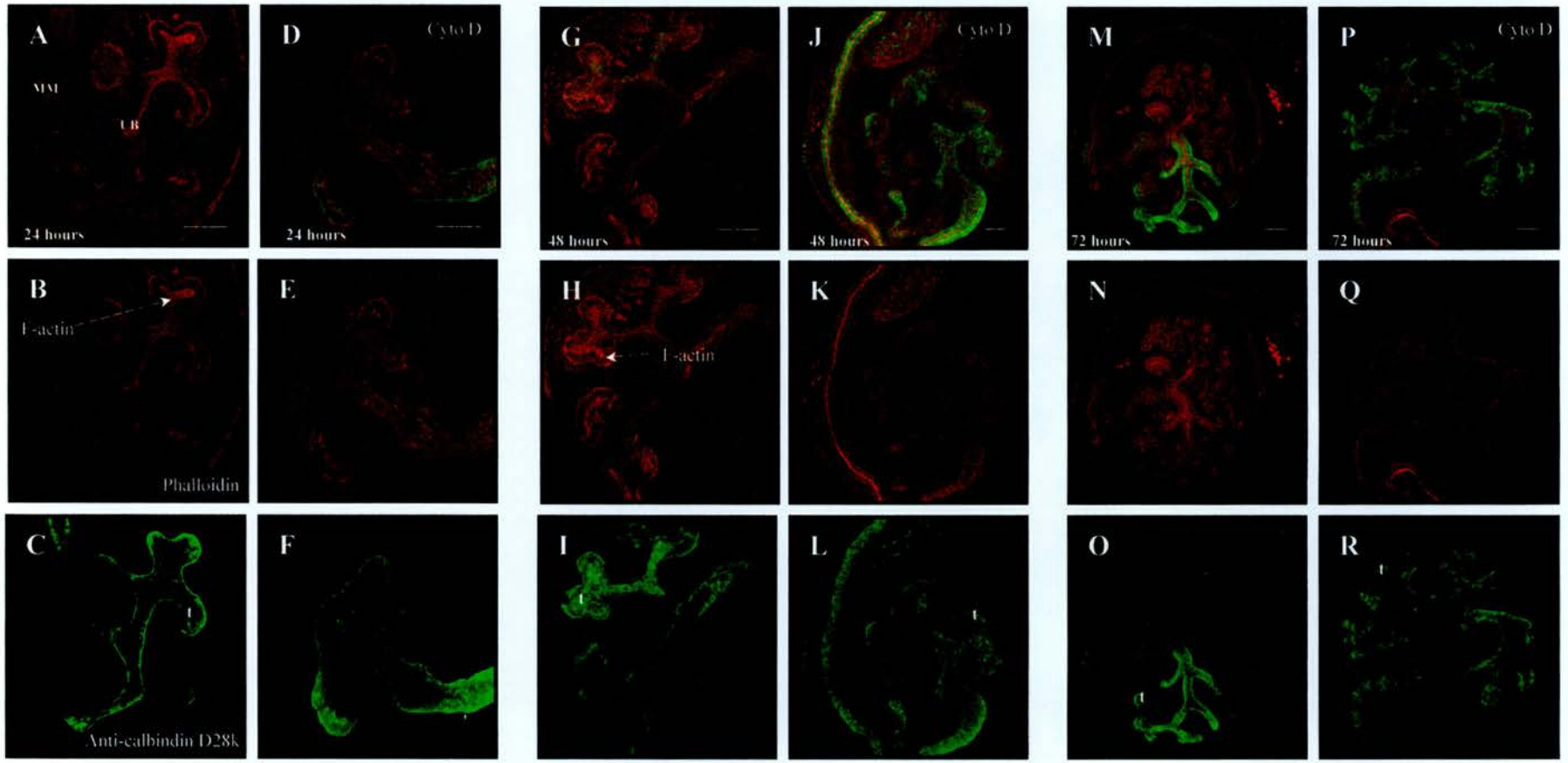

Figure 4.10: The effect of 0.1 μg/ml cytochalasin D on branching morphogenesis of the ureteric bud in culture

Panels **(A-C)**, **(G-H)** and **(M-O)** show E11.5 kidneys in control cultures (0.001% DMSO) for 24, 48 and 72 hours respectively. Panels **(D-F)**, **(J-L)** and **(P-R)** show E11.5 kidneys in cultures supplemented with 0.1 μg/ml cytochalasin D for 24, 48 and 72 hours respectively. Control red panels **(B, H, N)** and cytochalasin D red panels **(E, K, Q)** show the localization of actin filaments on the branching epithelium. Control green panels **(C, I, O)** and cytochalasin D green panels **(F, L, R)** show the branching epithelium. Panels **(A, D, G, J, M, P)** are merged confocal images. Staining: TRITC-phalloidin and FITC- anti calbindin D28k. UB: ureteric bud, MM: metanephric mesenchyme F-: filamentous, **t:** tip. Scale bars = 100 μm.

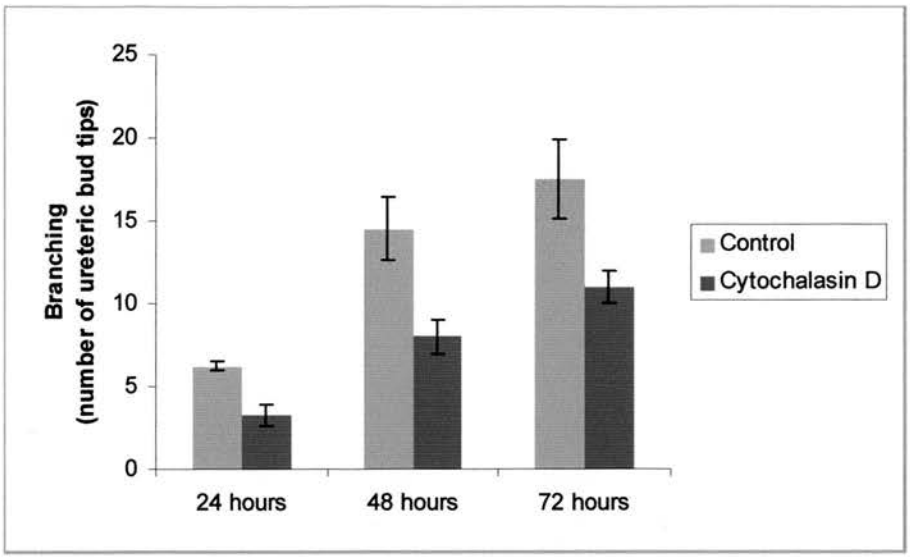

Figure 4.11: Low concentration of cytochalasin D (0.1 μg/ml) results in a decrease in ureteric bud branching in culture

E11.5 kidney rudiments were cultured for 24-72 hours in culture medium (control) or supplemented with 0.1 μg/ml cytochalasin D. Branching is quantified as the number of terminal ureteric bud tips under each treatment. Data shown represent the average number of ureteric bud tips, error bars are the SEM.

Control (24h) n= 4, Cyto D (24h) n= 4

Control (48h) n= 4, Cyto D (48h) n= 5

Control (72h) n= 4, Cyto D (72h) n= 3

(n values represent the number of kidneys)

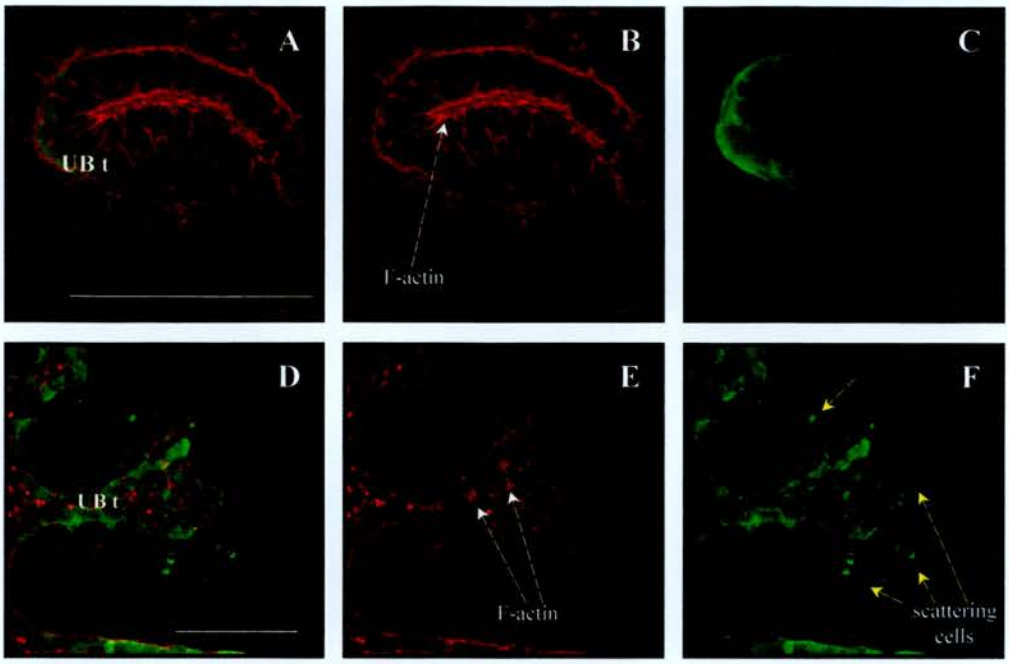

Figure 4.12: Low concentration of cytochalasin D causes cell scattering at the tips of the ureteric bud

(A-C) high magnification of a confocal image of a ureteric bud terminal tip after 72 hours in a control culture, **(B)** shows the localization of actin filaments at the tips, **(C)** shows the epithelium. **(D-F)** high magnification of a tip after 72 hours in a culture supplemented with 0.1 μg/ml cytochalasin D, **(E)** shows the disruption of the actin filaments at the tip ends, **(F)** shows the epithelial cells scattering (yellow arrows). Double staining: TRITC-phalloidin in (B) and (E), FITC- anti calbindin D28k in (C) and (F). Panels (A) and (D) are merged confocal images. Scale bars = 100 μm.

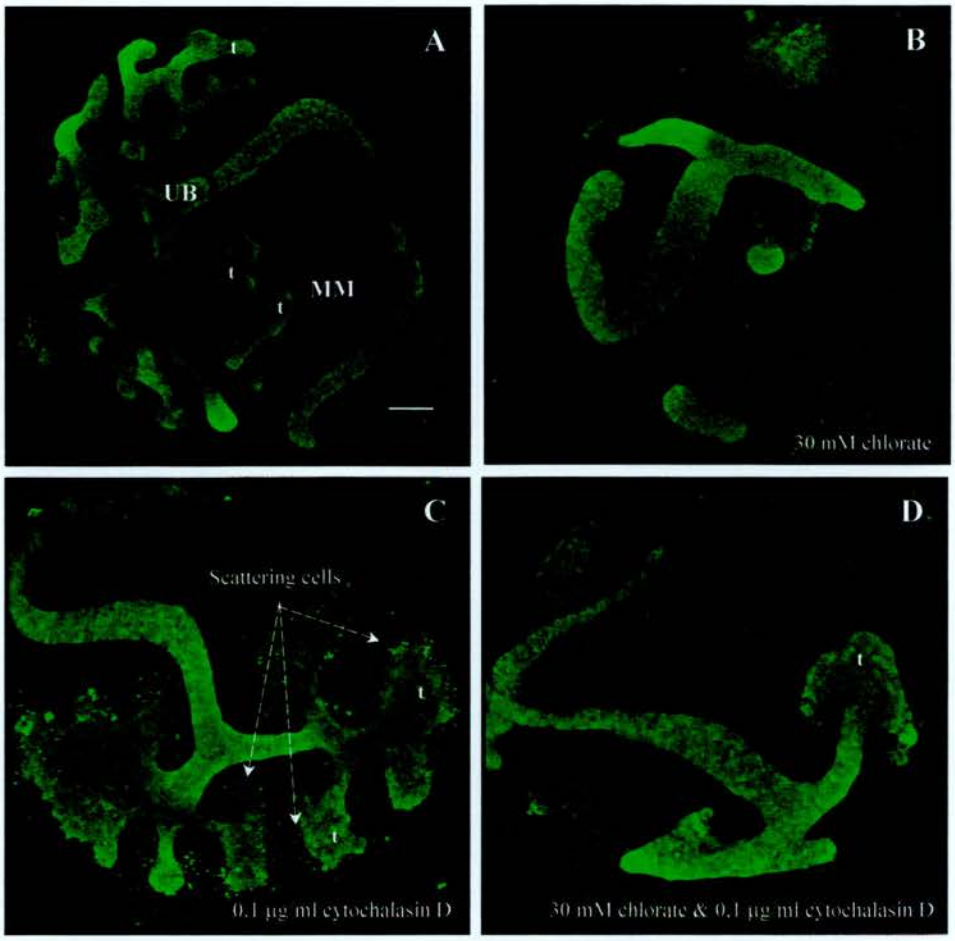

Figure 4.13: The cell scattering effect of cytochalasin D at the ureteric bud tips, occurs during branching morphogenesis

(A) a kidney in a control culture, **(B)** a kidney in a culture supplemented with 30 mM sodium chlorate, **(C)** a kidney in a culture supplemented with 0.1 µg/ml cytochalasin D, **(D)** a kidney in a culture supplemented with 30 mM sodium chlorate and 0.1 µg/ml cytochalasin D. All cultures were for 72 hours. In (**C**) the arrows show the scattering of the cells at the tip ends of the ureteric bud. Staining: FITC-anti calbindin D28k. UB: ureteric bud, MM: metanephric mesenchyme, t: terminal tip. Scale bar = 100 µm.

stable and mild disruption of the actin cytoskeleton does not result in scattering. Therefore, inhibiting actin filament formation at the very low concentration affects the stability of the cells at the ureteric bud tip ends, rather than the whole of the ureteric bud.

These results show that at very low concentrations, inhibition of actin filament polymerization sustains the branching of the ureteric bud epithelium and results in expanded tip morphology. The scattering of some of the epithelial cells from the tip ends which occur only when branching morphogenesis is taking place and not when branching is blocked, also suggests that during branching the cell junctions at the ureteric bud tips may be less stable and that the mild disruption of the actin cytoskeleton causes them to scatter.

4.2.4 Adherens junctions at the ureteric bud tips

Cell adhesion is crucial for the assembly, the structural integrity and the organization of epithelia into three-dimensional tissues of animals (Gumbiner, 1996). Adherens junctions are regions of the plasma membrane where E-cadherin molecules function as cell adhesion molecules and actin-based cytoskeleton is assembled where adjacent epithelial cells contact each other (Nagafuchi, 2001).

The scattering cells at the tips of the ureteric bud, when actin cytoskeleton is mildly disrupted, support the hypothesis that the cell-cell junctions at the tip ends may be less stable. In order to investigate this hypothesis, kidneys were cultured for 24 hours at 0.1 μg/ml cytochalasin D. They were then immunostained with anti E-cadherin antibody and the distribution of E-cadherin was compared to control tips. The results showed that there is a difference in the expression pattern of E-cadherin at the tips of the branching epithelium when actin filaments are disrupted (figure 4.14). The control kidneys show E-cadherin staining expressed at the apical parts of the tips in a similar localization pattern as seen

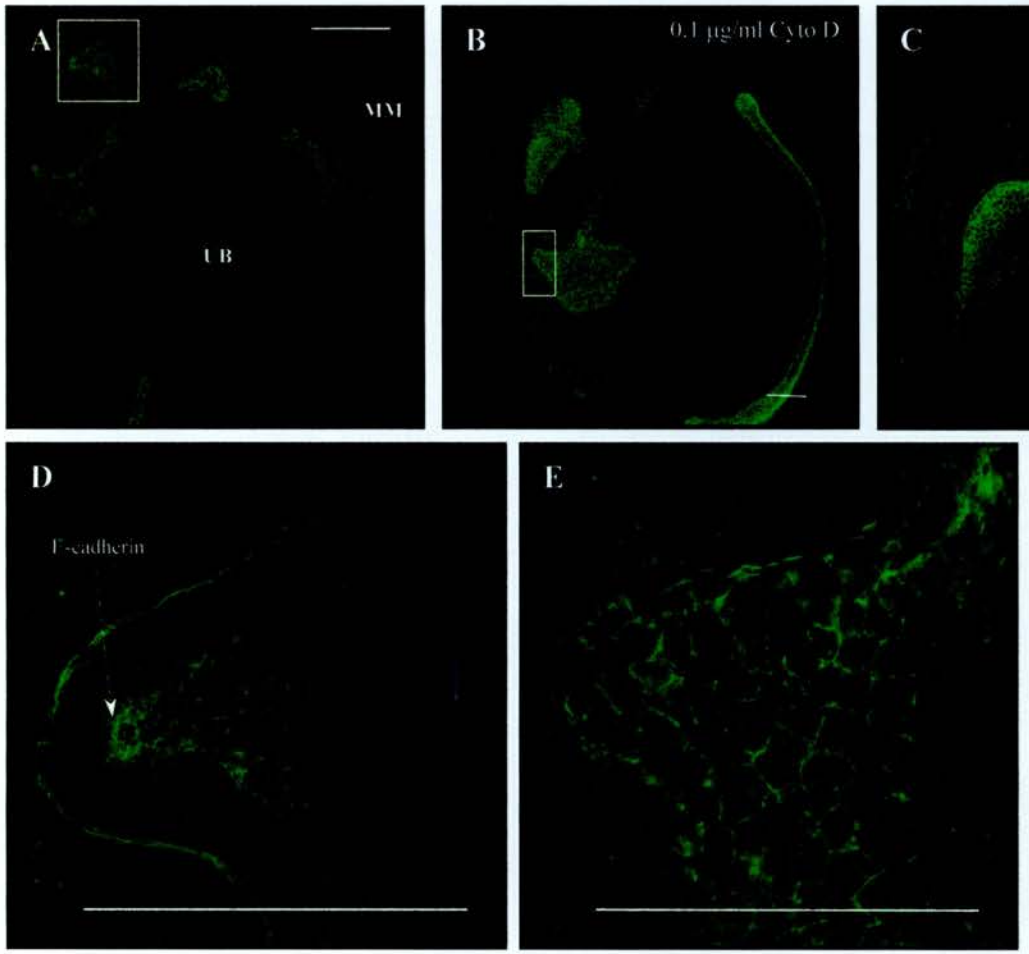

Figure 4.14: The effect of cytochalasin D on the adherens junctions at the tips of the epithelium

(A) control kidney in culture supplemented with 0.001% DMSO for 24 hours, **(B)** kidney in culture supplemented with 0.1 µg/ml cytochalasin D, **(C)** is a higher magnification of (B), **(D)** is a higher magnification of the control tip indicated in (A) and **(E)** is a higher magnification of the tip indicated in (B). In **(D)** E-cadherin is expressed at the apical part of a control UB tip (arrow), in **(E)** E-cadherin localization at the tip of a Cyto D treated kidney reveals loss of epithelial polarity. Staining: FITC-anti E-cadherin. UB: ureteric bud, MM: metanephric mesenchyme. Scale bars = 100 µm.

for actin filaments. In the kidneys treated with cytochalasin D, the cells of the ureteric bud appear to have lost their epithelial polarity. E-cadherin expression shows that it is not localized only at the apices of the tip cells but also to the basal surfaces. The cell layer at the tip edge (figure 4.14E) also shows weaker E-cadherin staining than the rest of the cyto D treated epithelial tip.

4.2.5 Role of myosin during ureteric bud branching morphogenesis

Filamentous actin and associated myosins take part in cellular processes like cell motility and contraction. A contractile actin-myosin purse-string mechanism may be involved during ureteric bud branching morphogenesis. In order to investigate this hypothesis, the acto-myosin contractility on ureteric bud branching morphogenesis was examined by inhibition of myosin.

Butanedione monoxime (BDM) is a general myosin ATPase inhibitor that acts directly on myosin molecules, inhibits actin-myosin interaction in vitro and is widely used as a non-muscle myosin inhibitor (Cramer and Mitchison, 1995; Herrmann *et al.*, 1992; Soeno *et al.*, 1999; Steinberg and McIntosh, 1998). Subsequently, pharmacological inhibition of myosin with BDM was used in the current organ culture system. E11.5 kidneys were cultured for 72 hours in the presence of 20 mM BDM. At this concentration, the effect was clearly inhibitory on branching and probably lethal (figure 4.15). Kidneys were then cultured at lower concentrations of BDM (10 mM and 5 mM) for 72 hours (figure 4.16). The effect of myosin inhibition on ureteric bud branching was inhibitory and dose dependent (figure 4.17). Inhibiting myosin resulted in less branching. The average number of ureteric bud tips at 10 mM was 15.2 ± 2.3, at 5 mM it was 23.3 ± 2.5 in comparison to the controls which was 34.5 ± 2.9. The morphology of the branching epithelium from the BDM treated kidneys appeared similar to the controls. The inhibitory effect of BDM was reversible. To demonstrate this, kidneys were cultured for 24 hours in 5 mM BDM and then transferred to control

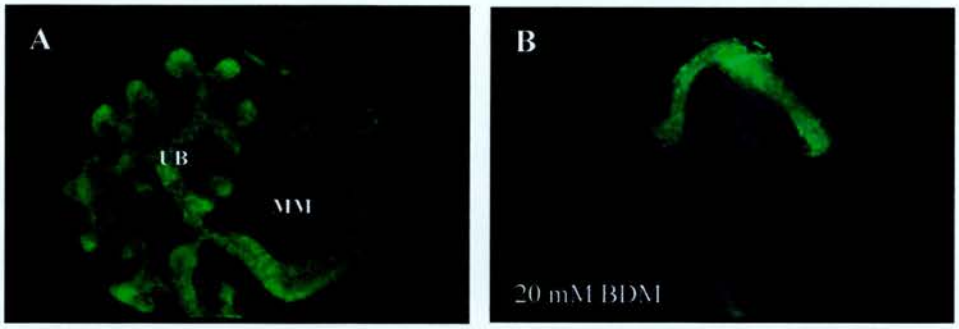

Figure 4.15: The effect of myosin inhibition on branching morphogenesis

(A) E11.5 kidney in culture for 72 hours, **(B)** kidney in culture supplemented with 20 mM BDM. Staining: FITC-anti calbindin D28k. UB: ureteric bud, MM: metanephric mesenchyme.

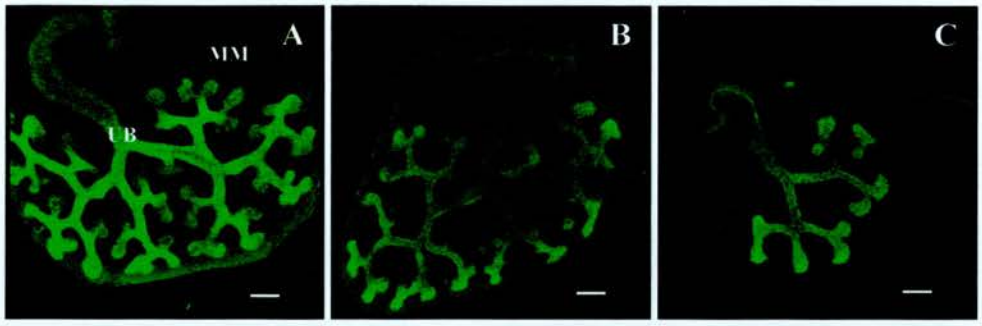

Figure 4.16: The inhibition of myosin reduces branching morphogenesis of the ureteric bud

(A) Control kidney in culture for 72 hours, **(B)** supplemented with 5 mM BDM, **(C)** 10 mM BDM. Staining: FITC-anti calbindin D28k. UB: ureteric bud, MM: metanephric mesenchyme. Scale bars = 100 μm.

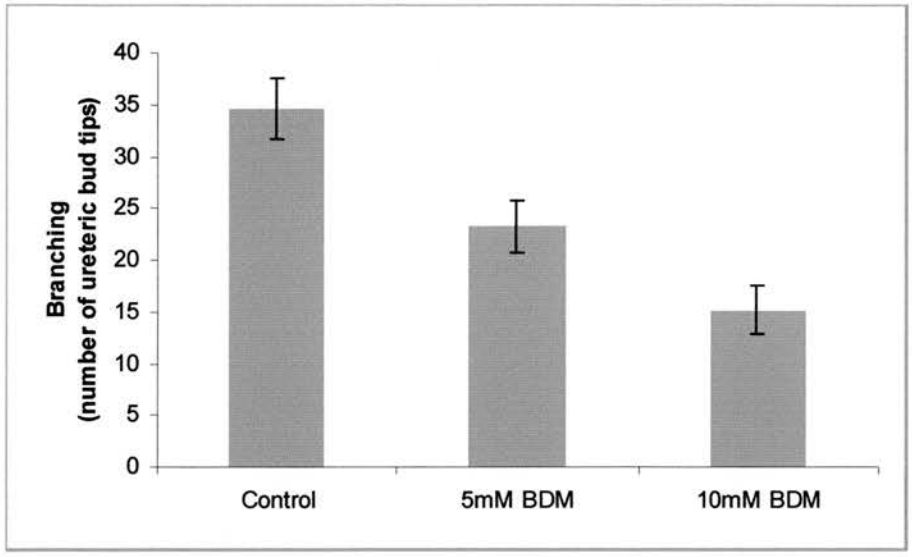

Figure 4.17: Myosin inhibition results in a decrease in branching morphogenesis

E11.5 kidney rudiments were cultured for 72 hours in culture medium (control) or supplemented with 5 mM, 10 mM BDM. Branching is quantified as the number of terminal ureteric bud tips under each treatment: control: 34.5 ± 2.9, BDM (5 mM) : 23.3 ± 2.5, BDM (10 mM) : 15.2 ± 2.3. P= 0.007 <0.01 between control and BDM (5mM), p= $2.59 \times 10^{-5} < 0.01$ between control and BDM (10 mM). Control n= 16, BDM (5 mM) n= 11, BDM (10 mM) n= 11 (n values represent the number of kidneys). Data shown represent the average number of ureteric bud tips, error bars are the SEM.

culture medium for further 24 hours and 48 hours. By that period the branching was recovered (figure 4.18).

These results suggest that actin-myosin contractility is important for efficient ureteric bud branching morphogenesis.

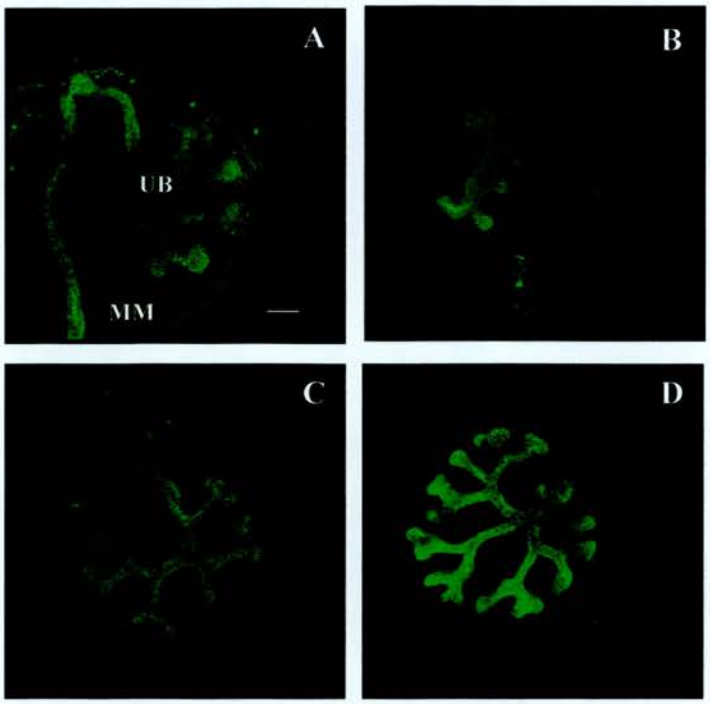

Figure 4.18: The effect of 5 mM BDM on ureteric bud branching morphogenesis is reversible

(A) Control kidney culture for 24 hours, **(B)** culture supplemented with 5 mM BDM for 24 hours, **(C)** a kidney cultured for 24 hours at 5 mM BDM and further 24 hours under control conditions, **(D)** a kidney cultured for 24 hours at 5 mM BDM and 48 hours under control conditions. Staining: FITC-anti calbindin D28k. UB: ureteric bud, MM: metanephric mesenchyme. Scale bar = 100 μm.

4.3 Discussion

The rearrangement of the cytoskeleton is responsible for the epithelial shape changes that occur during embryonic development. Healing of wounds in single cells or embryonic tissues requires actomyosin contraction (Bement *et al.*, 1999; Grose and Martin, 1999; Kiehart, 1999). During single-cell wound healing in *Xenopus* oocytes, actin filaments and myosin are recruited independently to the wound borders (Bement *et al.*, 1999). Their purse string contraction results in wound edges constriction, a process dependent on a Rho GTPase (Bement *et al.*, 1999). Small skin wounds in embryos heal by contraction of an actin cable that is assembled on the front row of epidermal cells (Martin and Lewis, 1992). At the wound margins, myosin II is localized at the sites of the actin cables, as well as cadherins are clustered where actin cables are linked in adjacent cells via adherens junctions (Brock *et al.*, 1996). The cells at the wound margins become wedge shaped, via the contractile force which pulls the wound edges together (Brock *et al.*, 1996; Nodder and Martin, 1997).

The formation of tubes and branching structures during organogenesis is accompanied with a great deal of shape change that involves rearrangement of the cytoskeleton. During ureteric bud branching morphogenesis in culture, phalloidin staining shows a strong localization of the actin filaments at the apical areas in the tips of the epithelium. This special localization of actin filaments is present when the ureteric bud evaginates as a single tip from the Wolffian duct and persists at the newly formed tips throughout the culture period examined (24-72 hours). This special arrangement of the microfilaments in the UB tips is present during branching activity and disappears when branching is arrested either in chlorate-treated kidneys or when branching is blocked with the MAPK inhibitor PD98059. In the latter treatment, phalloidin staining reveals focal aggregates of actin present in the ureteric bud tips and at the stalks. In the developing lung in culture, at the postbudding stage (48 hours), when the buds have elongated, actin filaments show a strong localization at the tips of the

branches in comparison to the clefts, a specialization associated with branching activity (Miura and Shiota, 2000). However, in contrast with the high actin localization at the apical part of the evaginating ureteric bud (24 hours in culture), no specific localization of actin is present at the prebudding stage of the developing lung (6 hours in culture) when no clefts are present yet (Miura and Shiota, 2000). Also, there is no specific actin arrangement in the clefts or the bud tips at the onset-budding stage (24 hours in culture), when clefts have started to form (Miura and Shiota, 2000).

Cytochalasin D is a specific actin filament depolymerization agent that does not appear to disrupt other cell functions significantly (Colony and Conforti, 1993; Cooper, 1987). It is widely used in studies to reversibly disrupt the actin cytoskeleton (Bement *et al.*, 1999; Colony and Conforti, 1993; McCluskey and Martin, 1995; Soong *et al.*, 1990; Stevenson and Begg, 1994). In embryonic epidermal wound healing, addition of Cyto D blocks formation of the actin cable at the wound margins and leads to failure of reepithelialisation (McCluskey and Martin, 1995). In single-cell wounds in *Xenopus* oocytes, cytochalasin D also prevents wound closure (Bement *et al.*, 1999).

In the developing ureteric bud, addition of cytochalasin D results in an arrest of branching morphogenesis at concentration 0.5 μg/ml and a disruption of ureteric bud branching morphology at lower concentrations 0.3 and 0.1 μg/ml. The effect of 0.1 μg/ml cytochalasin D, a very low concentration, is reversible and does not affect branching activity which takes place as revealed in the time course of 24 to 72 hours. At this concentration of the actin disrupting agent, the UB tips show an enlarged morphology with funnel-shaped ampullary ends. Some cells at the enlarged tips scatter in comparison to the stalk cells and reflect a probable less stable state of cell-cell contacts at the newly formed tips (sites of branching activity). This is not observed when branching activity is arrested in chlorate-treated kidneys. The cells at the stalks of the ureteric bud, cultured in very low concentration of cytochalasin D, do not show any signs of scattering reflecting

that, as branching progresses, the cells at the stalks establish mature cell-cell contacts that are not subject to mild disruption of the actin cytoskeleton. The cell scattering at the newly formed tips observed after mild disruption of the actin filaments suggest that the cell-cell contacts might not be stable yet.

The majority of F-actin in epithelial cells localizes in adhesive belts that encircles the cell just below the apical surface at the adherens junctions (Gumbiner, 1996; Knust and Bossinger, 2002). The transmembrane core of adherens junctions consists of cadherins that are transmembrane Ca^{2+}-dependent homotypic adhesion receptors (Gumbiner, 1996; Vasioukhin and Fuchs, 2001). During embryonic wound healing, E-cadherin molecules are associated with actin filament cable at the leading edge (Danjo and Gipson, 1998). Disruption of E-cadherin caused disruption of the actin filaments at the wound margins and subsequent torn uneven epithelial wound margin (Danjo and Gipson, 1998).

Immunostaining of E-cadherin in the developing ureteric bud shows localization at the apical parts of the UB tip cells in a similar expression to actin filaments, as seen with phalloidin staining. Disruption of actin filaments with the lowest cytochalasin D concentration (0.1 μg/ml) alters E-cadherin distribution throughout the ureteric bud epithelium, with weaker staining at the cell-cell contacts in the cell layer at the edge of the tips. In primary keratinocytes, addition of cytochalasin D also results in disruption of the adhesion contacts between cells, even though some cadherin is still localized to cell borders (Vasioukhin *et al.*, 2000). In MDCK epithelia cells, new cell-cell contacts are not formed upon addition of cytochalasin D; the young contacts disassemble whereas the more mature cell-cell contacts are not disrupted (Adams *et al.*, 1998).

Rho family of small GTPases are known regulators of the actin cytoskeleton (Ridley, 1999; Settleman, 2000; Van Aelst and D'Souza-Schorey, 1997) and mediate cell signaling responses to direct rearrangement of the actin cytoskeleton during development (Settleman, 1999). In epithelial cells, members of the Rho GTPases such as Rho and Rac are required for the establishment of cadherin

mediated cell-cell adhesion and the actin cytoskeleton (Braga *et al.*, 1997; Evers *et al.*, 2000). Blocking the function of endogenous Rho and Rac prevents the establishment of cadherin-mediated cell-cell contacts and blocking Rac function prevents actin recruitment to cadherin complex in keratinocytes (Braga *et al.*, 1997). In the *Drosophila* tracheal system, dominant negative Rac results in an increase in E-cadherin levels, loss of distinction between the apical-basolateral domains in cell contact, in addition with expanded F-actin distribution, and an increase of the amount of cytoplasmic actin (Chihara *et al.*, 2003). Hyperactivation of Rac, in the same system, disrupts the cell adhesion in the epithelium resulting in detachment of cells from the tracheal cell cluster (Chihara *et al.*, 2003). In the Rac mutant embryos, the tracheal terminal branches are lost (Chihara *et al.*, 2003). It would be of interest to examine the role of the Rho family of small GTPases at the cytoskeletal organization and cell-cell contacts at the tips of the developing ureteric epithelium.

Myosin II co-localizes along the actin filaments in wound margin during wound healing and its inhibition results in inhibiting wound closure (Bement *et al.*, 1999; Danjo and Gipson, 1998). I was unable to identify the precise localization of myosin on the ureteric bud epithelium by immunohistochemistry in whole mounts due to the presence of both UB and mesenchymal components. Myosin was reversibly inhibited using butanedione monoxime (BDM), a general myosin ATPase inhibitor, which resulted in reduced branching morphogenesis in a dose dependent manner. At 20 mM, the effect of BDM on the ureteric bud epithelium was probably lethal as no morphogenesis took place in accordance with a previous study in fission yeast where at concentrations above 15 mM the effect of the drug was lethal (Steinberg and McIntosh, 1998). BDM (10 mM) reversibly inhibits postmitotic epithelial cell spreading without directly disrupting actin filaments at this concentration (Cramer and Mitchison, 1995). In *Xenopus* oocytes, wound healing actin is accumulated at the wound closure margins in the presence of much higher BDM concentrations suggesting that actin is not directly affected from the drug (Bement *et al.*, 1999; Kiehart, 1999).

The experiments described above, were performed using the metanephric organ culture that allows the manipulation of organotypic branching morphogenesis. Pharmacological disruption of the cytoskeletal elements in this experimental model system allows direct visualization of the effects on the branching architecture. However, the drawback of the results in this chapter is the presence of both epithelial and mesenchymal compartments and the experimental disruption of the actin or myosin might be affecting the mesenchyme. Hence, the effects of cytochalasin D or BDM on the epithelial branching morphogenesis observed might also be due to their indirect effects on the mesenchymal cells. The isolated ureteric bud three-dimensional tubulogenesis model, recently developed after the above experiments were complete, would be a more appropriate system to study the questions addressed here as it displays an organotypic ureteric bud branching morphogenesis without the presence of the mesenchyme (Sakurai *et al.*, 2001).

To summarize, this chapter focuses on the cytoskeletal elements involved during branching morphogenesis of the ureteric epithelium. It shows that branching morphogenesis is dependent on actin-myosin contractility. Blocking either actin microfilament formation or myosin results in a disrupted epithelial morphology or a reduction of branching, respectively. Actin filaments show a strong expression at the tips of the branching ureteric buds, a special arrangement correlated with branching activity. Mild disruption of the actin cytoskeleton results in expanded tip morphology and altered cell junctions.

Chapter 5

Specializations at the Tip of the Branching Ureteric Bud Revealed by Lectin Histochemistry and Differential Display

5.1 Introduction

Plant lectin binding studies have offered information regarding the presence and compartmentalization of sugar residues in tissues. They have been used to reveal tissue-bound glycocongugates during limb development, or development of organs including the pancreas and kidney (Laitinen *et al.*, 1987; Maylie-Pfenninger and Jamieson, 1980; Milaire, 1991). *Dolichos Biflorus* Agglutinin (DBA) is a plant lectin which recognizes α-linked *N*-acetylgalactosamine and has been extensively used as a tissue marker for the collecting duct epithelia (Qiao *et al.*, 2001; Qiao *et al.*, 1999b).

The evidence for the DBA reacting with collecting ducts in adult kidneys of many species including mouse, rat, rabbit and human comes from a comparative study of 14 species (Holthofer, 1983). In adult rat kidney collecting ducts, DBA binds to the apical cell membranes of the principal cells along the entire length of the collecting duct (Brown *et al.*, 1985). It also stains the intercalated cells (Murata *et al.*, 1983) in a heterogeneous pattern so that DBA binds strongly to their apical plasma membranes from the cortex and outer stripe of the outer medulla (Brown *et al.*, 1985). In adult mouse kidneys, DBA shows strong reactivity with the intercalated cells of the collecting duct (Laitinen *et al.*, 1987).

In embryonic rat kidneys (E_r 18), DBA shows binding to most cells of the collecting duct (Holthofer, 1988). In embryonic mouse kidneys, DBA shows specific reactivity with the developing collecting ducts from at least as early as embryonic day 13 (Laitinen *et al.*, 1987). At around E15, cells with the respective morphology of principal and intercalated cells evolve in the deep cortical part, and here there is a heterogeneous DBA staining on the epithelial cells as early as E13 (Laitinen *et al.*, 1987).

In the present study, I show that DBA binding shows a specialized expression pattern at the developing ureteric bud epithelium at an even earlier stage, and this pattern again emphasizes that the tip cells differ from those of the stalks.

5.2 Results

5.2.1 Lack of DBA binding to the ureteric bud tips during branching morphogenesis

Kidney rudiments were cultured for 24, 48 and 72 hours and stained with fluorescein labeled *Dolichos Biflorus* agglutinin. At each of these time-points, they showed a distinct expression pattern: the binding of the lectin was absent from the tips of the ureteric bud although the stalks stained strongly (figure 5.1). DBA binding in the stalks appears to stain the basement membrane as the lectin staining is similar to the anti-laminin staining.

5.2.2 Changes in DBA binding at the ureteric bud tips when branching is regulated

In order to examine whether the absence of DBA staining at the tips of the ureteric bud is a special feature of the actively growing epithelium, the effects of exogenous GDNF or a function-blocking antibody to GDNF on DBA staining were studied.

As described in *chapter 3,* the addition of exogenous GDNF increases the ureteric bud terminal tip area and induces the appearance of ectopic tips from the ureteric bud stalk. Therefore 100 ng/ml of recombinant GDNF were added to the cultures for 48 hours and ureteric buds were double stained with TRITC anti-laminin and FITC-DBA. The GDNF-enlarged ureteric bud tips lacked DBA binding (figure 5.2). The ectopic buds emerging from the stalk also showed lack of binding to the lectin (figure 5.2 J-L), but the stalks themselves still bound lectin strongly.

Blocking GDNF signaling in culture results in a reduction of branching morphogenesis. Kidneys were cultured at 10 μg/ml anti GDNF function blocking antibody for 48 hours. Under these conditions binding of DBA was found

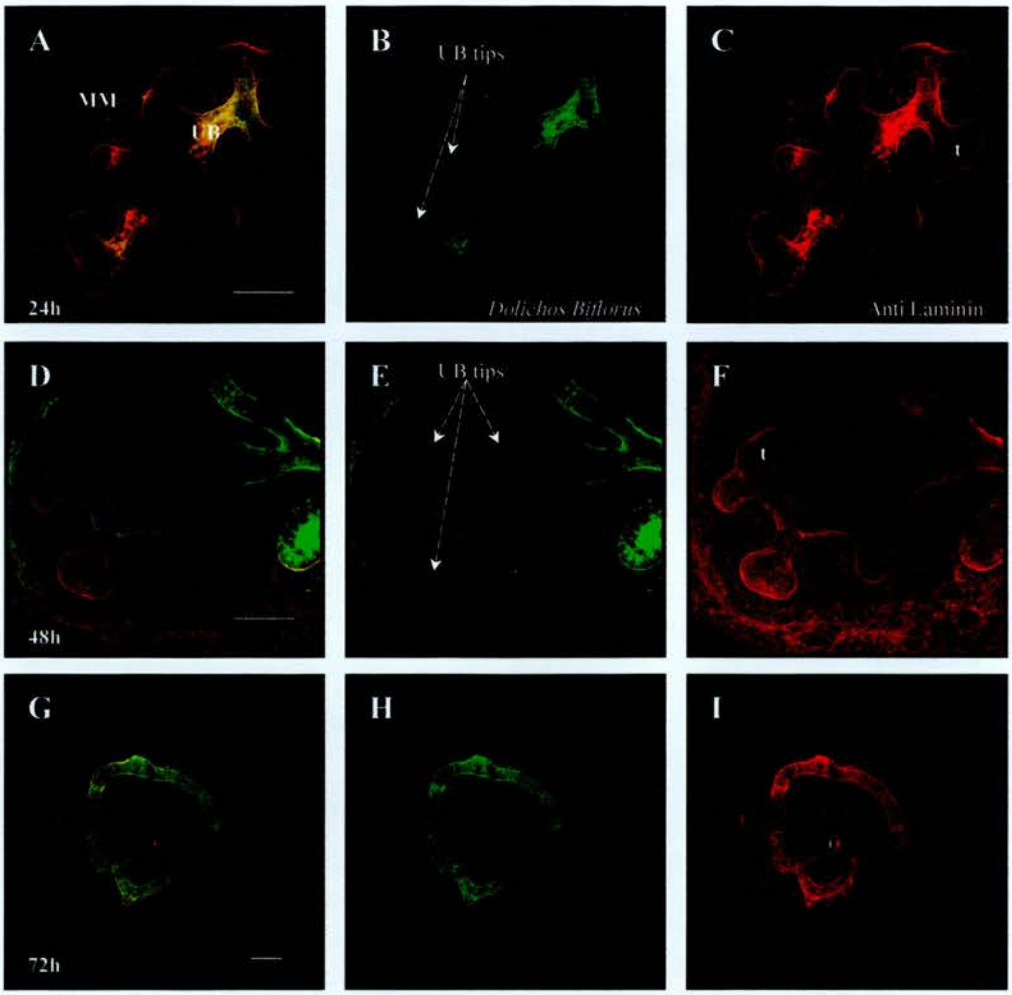

Figure 5.1: *Dolichos Biflorus* agglutinin binding on the ureteric bud epithelium during branching morphogenesis in culture

Kidney rudiments in culture for 24 hours shown in **(A-C)**, 48 hours in **(D-F)** and 72 hours in **(G-I)** double stained for FITC-*Dolichos Biflorus* Agglutinin **(B, E, H)** and TRITC- anti laminin **(C, F, I)**. Arrows show the exclusion of the DBA from the tips of the ureteric epithelium. Panels **(A, D, G)** show the merged confocal pictures. UB: ureteric bud, MM: metanephric mesenchyme, **t**: Ureteric bud terminal tip. Scale bars = 100 μm.

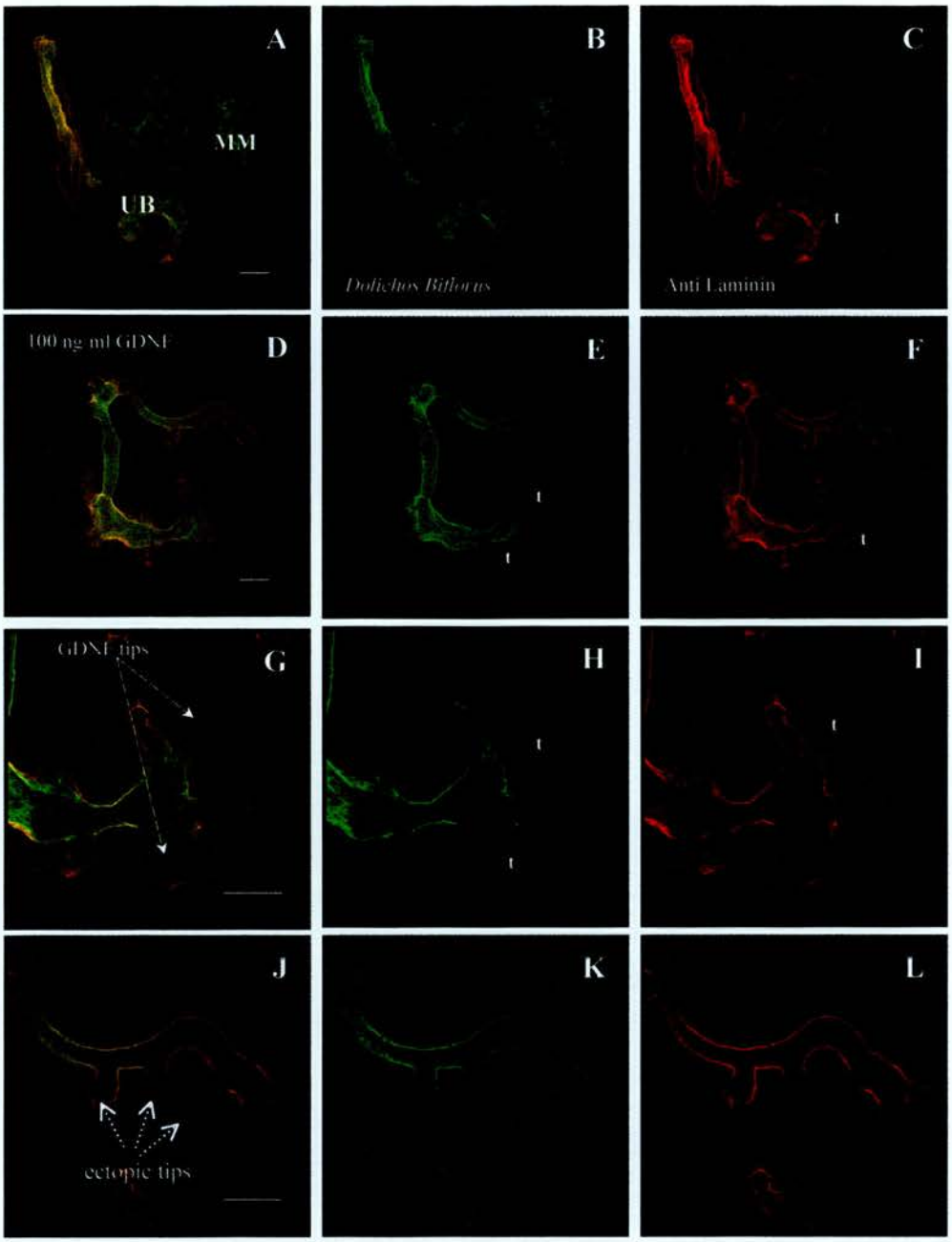

Figure 5.2: The effect of exogenous GDNF on *Dolichos Biflorus* agglutinin binding at the terminal tips of the ureteric epithelium

(A-C) a kidney cultured under control conditions for 48 hours, **(D-L)** a kidney cultured in medium supplemented with 100 ng/ml GDNF for 48 hours. Panels **(G-I)** show a higher magnification of confocal picture **(D)**, the arrows show the enlarged ureteric bud tips after exogenous GDNF administration in culture. In panels **(J-L)** the open arrows show the presence of ectopic tips along the stalk of the epithelium. Double staining: FITC-DBA **(B, E, H, K)** and TRITC-anti laminin **(C, F, I, L)**, panels **(A, D, G, J)** are merged confocal pictures. UB: ureteric bud, MM: metanephric mesenchyme, **t**: terminal tip. Scale bars = 100 μm.

throughout the epithelium including the tips (figure 5.3). These results suggest that absence of DBA staining correlates with branching activity, and DBA-negativity might be a marker of active ureteric bud tips.

5.2.3 The transition between tip and stalk is reversible

The ureteric bud evaginates from the Wolffian duct as a tip-like outgrowth which then elongates and divides dichotomously, initially to form a T-shape structure with two tips 180° apart. During branching, the first two tips become stalks as their tips continue to grow and bifurcate. In the normal course of events, therefore, tips give rise to stalk cells.

In culture, newly formed tips show a characteristic lack of DBA binding as do ectopic buds emerging from the ureteric bud stalks where tips are not normally formed (see above). To test whether stalks that are DBA-positive are able to form tips which lack DBA binding, we developed a method to induce new tip formation from established stalks. E11.5 isolated kidneys were further microdissected as shown in figure 2.3 (*chapter 2*). One tip was removed mechanically from the T-shape stage ureteric buds and extra metanephric mesenchyme was placed next to the resulting Γ-shape ureteric buds. The control kidneys were cultured for 24 hours whereas the amputated Γ-shape ureteric buds were cultured for 48 hours to achieve equal branching. Lectin histochemistry showed that the newly formed tips emerging from the stalk did not stain for DBA (figure 5.4).

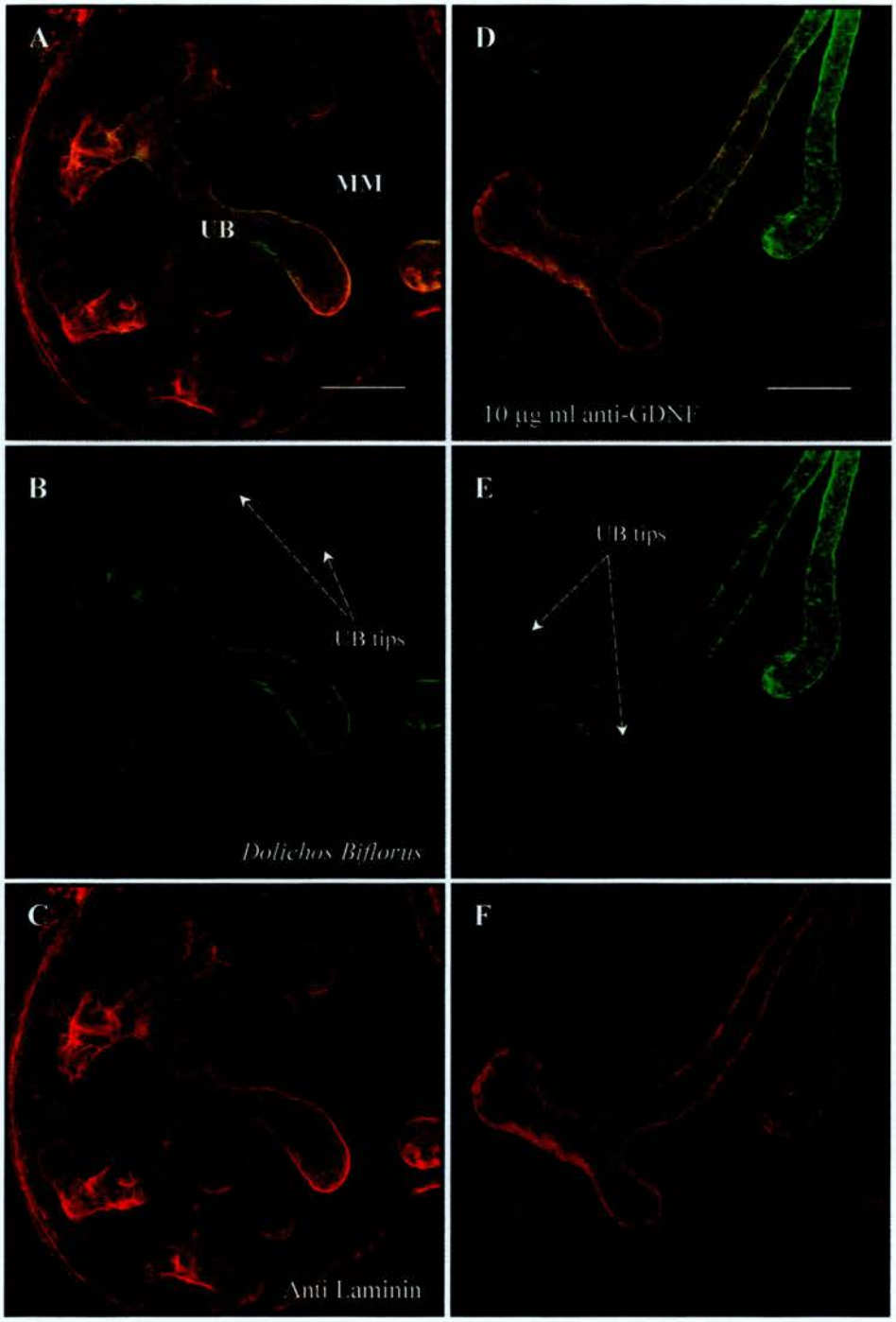

Figure 5.3: The effect of a function blocking antibody to GDNF on *Dolichos Biflorus* agglutinin binding at the terminal tips of the ureteric epithelium

(A-C) a control E11.5 kidney in culture for 48 hours, **(D-F)** a kidney in culture supplemented with 10 μg/ml function blocking anti-GDNF for 48 hours. **(B)** shows DBA binding missing from terminal tips in control organ, **(E)** shows DBA binding throughout the epithelium in experimental rudiment, arrows show the terminal tips. Double staining: FITC-DBA **(B, E)** and TRITC-anti laminin **(C, F)**. Merged confocal images **(A, D)**. UB: ureteric bud, MM: metanephric mesenchyme. Scale bars = 100 μm.

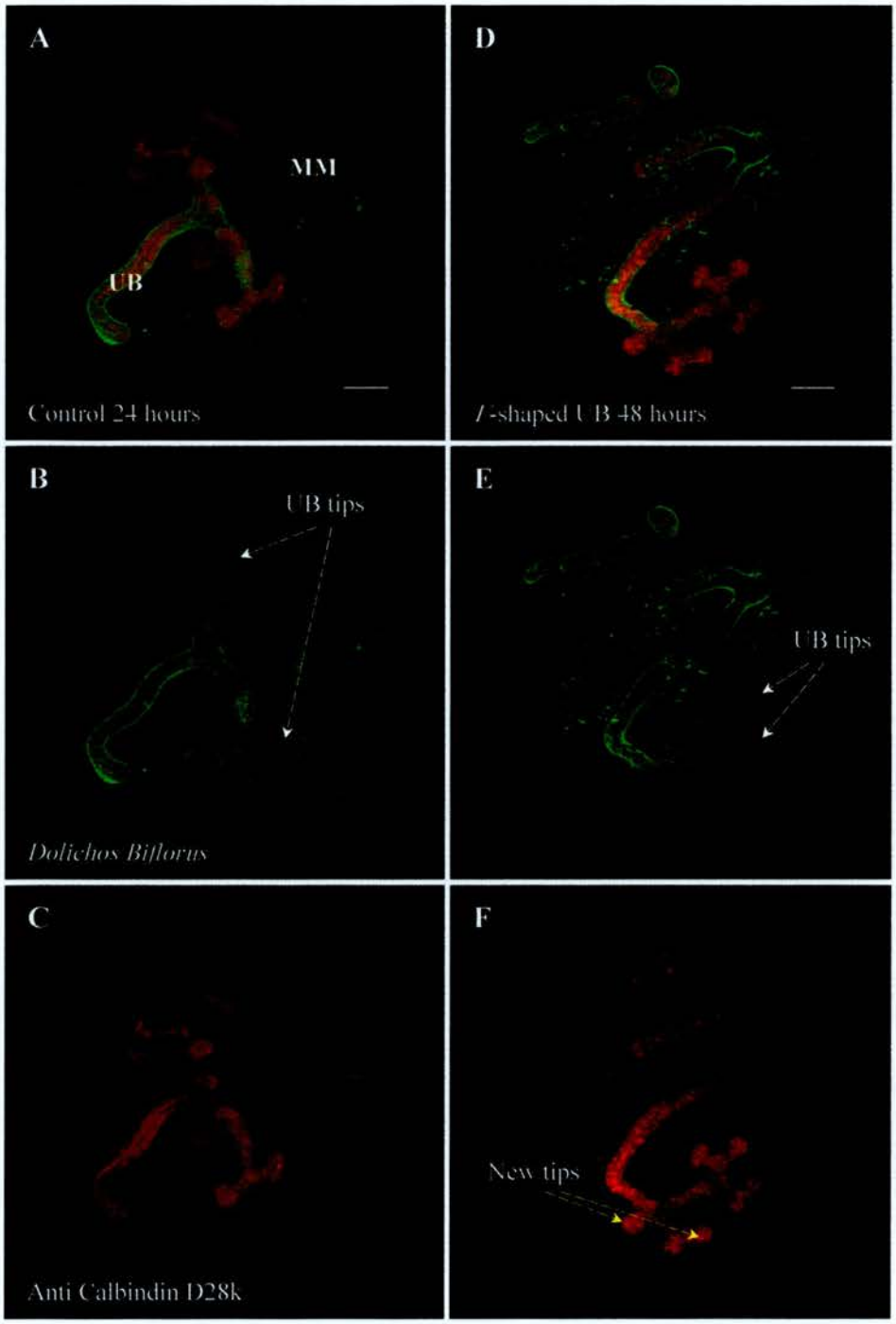

Figure 5.4: *Dolichos Biflorus* agglutinin binding at the newly formed tips of the ureteric epithelium

(A-C) a control kidney in culture for 24 hours, **(D-F)** a Γ-shaped ureteric bud in culture for 48 hours which has formed new branches (yellow arrows). **(B)** and **(E)** show DBA staining missing from terminal epithelial tips (white arrows). Double staining: FITC-DBA **(B, E)** and TRITC-anti calbindin D28k **(C, F)**. Merged confocal images **(A, D)**. UB: ureteric bud, MM: metanephric mesenchyme. Scale bars = 100 μm.

5.3 Are tips different from stalks in other ways?

The previous two chapters have shown that during branching the ureteric bud tips display specializations such as increased local cell proliferation and special cytoskeletal rearrangement. The results of the previous section also suggest that they differ in respect to glycoconjugate expression as revealed by the lack of DBA binding in the ampullary tips. They also show that subsequent to tip amputation at the T-shape stage, the stalks have the ability to form new tips. The question addressed here is whether the ureteric bud tips differ from the stalks at the molecular level, which is examined by means of differential display PCR on the early T-shape stage ureteric epithelium.

Differential display is a powerful molecular tool which permits the identification and subsequent isolation of transcripts differentially expressed between undifferentiated and differentiated cells or in one tissue at different developmental stages (Liang and Pardee, 1992; Miele *et al.*, 1998). In a differential display (figure 5.5), each RNA sample is first reverse transcribed with an anchored oligo(dT) primer that is modified at the 3′-end (two extra bases are included) to ensure that it anneals at the start of the poly(A) tail of mRNA rather than non specifically within the poly(A) tail. The objective is to obtain a tag of a few hundred bases, which is sufficiently long to uniquely identify a mRNA but short enough to be separated from others by size (Liang and Pardee, 1997). Polyacrylamide gel electrophoresis can separate DNA molecules that differ in a range of 1 to 500 bp. In order to amplify fragments of each cDNA within 500 bp of the mRNA poly(A) tail, short arbitrary 5′ primers of 10 nucleotides in length are used (Liang and Pardee, 1992). Incorporation of a radiolabeled nucleotide into the display reactions allows the resulting PCR products to be visualized by autoradiography following polyacrylamide electrophoresis (Miele *et al.*, 1998). For differential display, generally a final polyacrylamide concentration of 6% is considered appropriate with an effective separation range of between 25 to 500 bp (McPherson and Moller, 2000). This

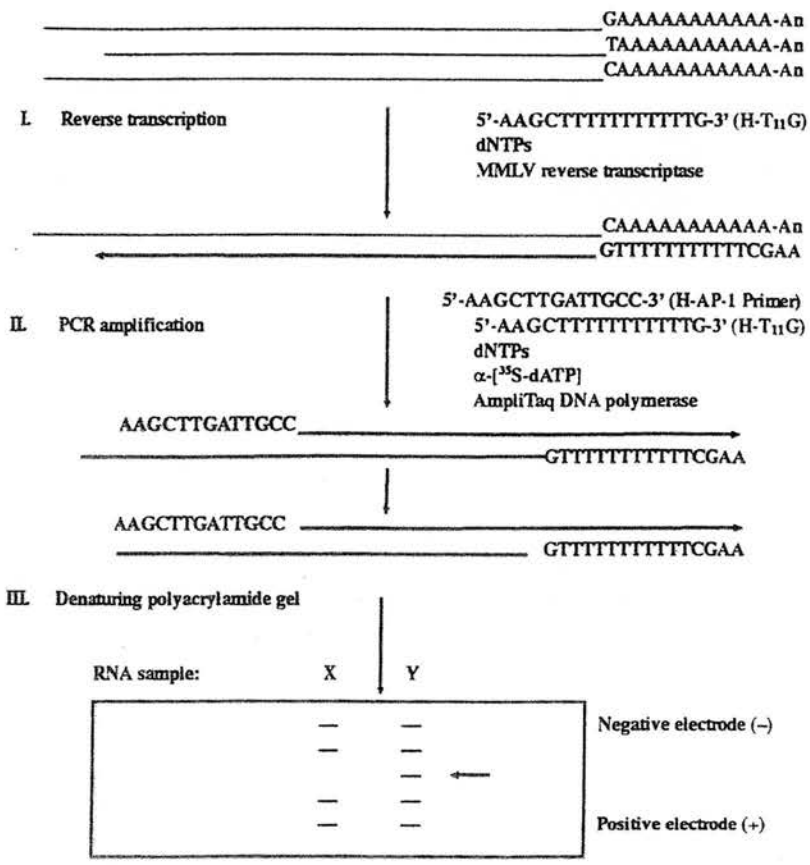

Figure 5.5 : Schematic representation of differential display

(From Liang and Pardee, 1997)

procedure allows amplification of an mRNA subpopulation without knowledge of sequence information.

During kidney development, the mesenchymal to epithelial transition (MET) is accompanied by dramatic changes in gene expression (for reviews see Davies, 1996; Patterson and Dressler, 1994). Differential display has been used to identify these changes in gene expression between uninduced and induced mesenchymal cells (Leimeister *et al.*, 1999) as well as to identify genes that are upregulated during MET either by comparing the gene profiles of E10.5 and E13 metanephroi (Rosenblum and Yager, 1997) or during ex vivo condensation and tubulogenesis (Plisov *et al.*, 2000).

Here I describe pilot experiments to the hypothesis that in the early stages of ureteric bud development (E11.5) tips differ from the stalks in the molecular level.

5.4 Differential display results

For the experiments, tips and stalks of the T-shape stage ureteric buds of E11.5 metanephroi were isolated by microdissection and were subjected to gene expression analysis using the differential display technique (Miele *et al.*, 1998). Approximately 2 μg of total RNA (estimated from the intensity of ethidium bromide staining) was prepared from 20 isolated ureteric bud tips and 20 stalks, and three different anchor oligo-dT-containing primers were used to produce total cDNA for differential display analysis. Amplified fragments were separated by high-resolution electophoresis. Most of the amplified cDNA fragments appeared in both tracks that is did not differ from the tips and stalks. However few differentially displayed cDNA bands were found – some of these were specific to tips, and others were specific to stalks. (figure 5.6). Figure 5.6B shows the presence of differentially expressed cDNA bands both in the stalk and the tip.

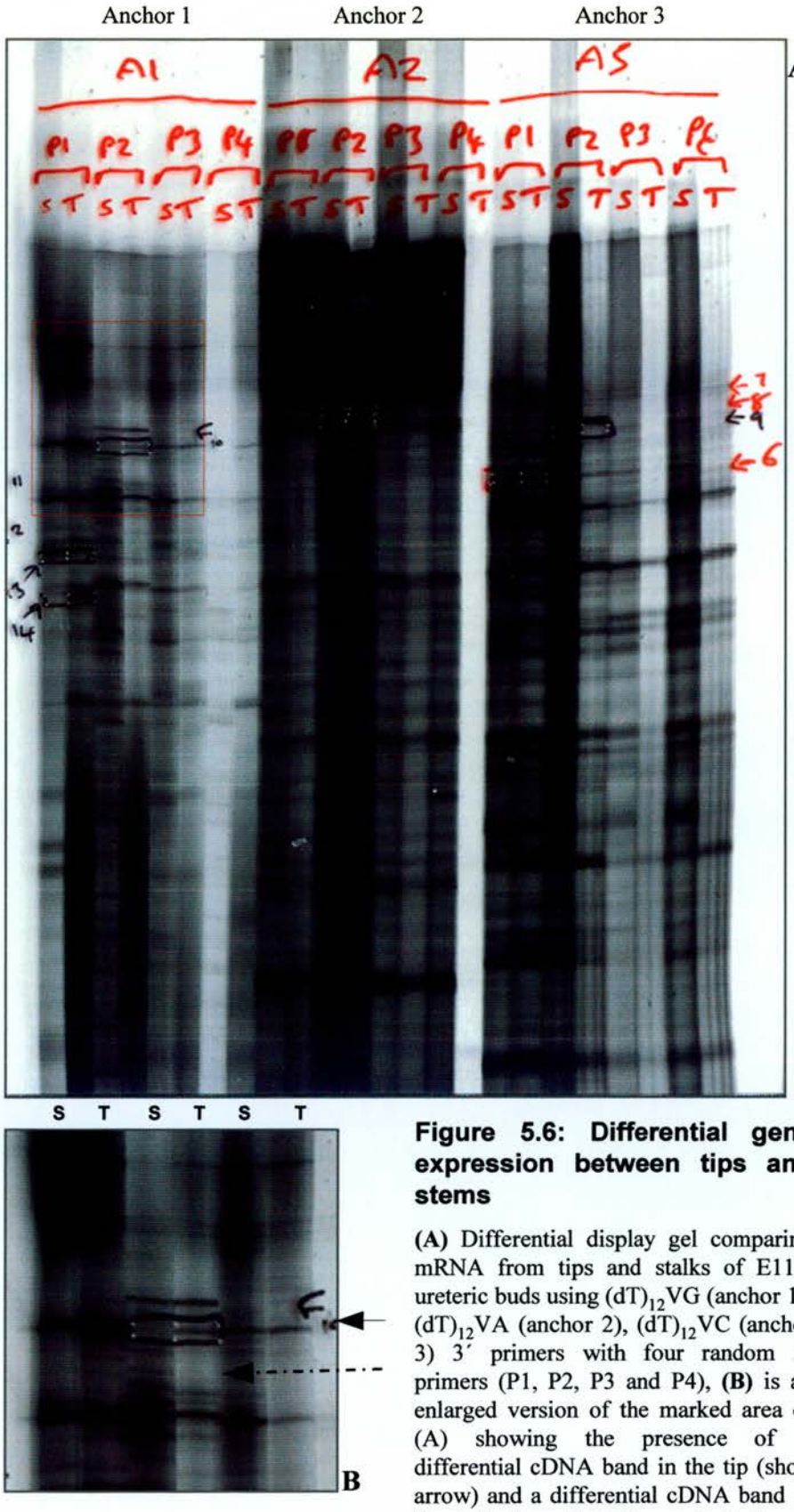

Figure 5.6: Differential gene expression between tips and stems

(A) Differential display gel comparing mRNA from tips and stalks of E11.5 ureteric buds using $(dT)_{12}VG$ (anchor 1), $(dT)_{12}VA$ (anchor 2), $(dT)_{12}VC$ (anchor 3) 3′ primers with four random 5′ primers (P1, P2, P3 and P4), **(B)** is an enlarged version of the marked area of (A) showing the presence of a differential cDNA band in the tip (short arrow) and a differential cDNA band in the stalk (long dashed arrow). T: tip, S: stalk

The results presented here are a preliminary attempt to identify differentially expressed genes in the ureteric bud epithelium at the early stages of branching morphogenesis. Even though the sequences of the differential cDNA bands are not known yet (because the samples were physically destroyed by a colleague in error), this pilot study suggests that there are differences in gene expression between tips and stalks in the ureteric bud epithelium at the initial stages of branching morphogenesis. The stalk-specific bands might have been expected from known directions of differentiation (as collecting duct cells mature) but tip specific genes may be novel.

These pilot experiments form the foundation for further analytical work that can identify the genes involved. This would involve the excision of the differentially expressed transcripts from the dried gel, cDNA recovery, PCR amplification for single-stranded conformation polymorphism (SSCP) analysis in order to isolate with confidence the precise differential bands (Miele *et al.*, 1998). Following excision of the differential bands, cDNA recovery and PCR re-amplification using the original primer combination, the fragments will be sequenced for identification. *In situ* hybridization will reveal whether the gene in question is expressed in the epithelium or the surrounding mesenchyme, and will confirm differential expression in either the tip or the stalk.

These experiments could not be pursued further in the present thesis due to this project's time limitations that did not allow the complete experiment to be restarted, following loss of the samples mentioned above.

5.5 Discussion

5.5.1 Branching correlates with lack of DBA binding from the tips

During ureteric bud branching morphogenesis, the developing epithelium induces the formation of nephrons and determines the architecture of the kidney. The nephrons are formed at the terminal tips of the developing ureteric epithelium, the ampullae, suggesting an important role for this region of the epithelium. This leads to the hypothesis that the ampullary UB tip might show differences and specializations throughout its development, specializations that are important for the branching pattern and eventually the nephron induction. The two previous chapters have shown that tips differ from stalks in respect to proliferation and cytoskeletal organization; this chapter shows that they also differ in respect to glycoconjugate and gene expression.

A lack of DBA binding from the ureteric ampullary tips is observed in E11.5 murine embryonic kidneys cultured for 24 hours and persists at least until 72 hours (figure 5.1) whereas there is strong binding of DBA in the basement membranes of the stalks. This is in accordance with a previous finding in embryonic rat ureteric bud where at $E_r12.5$ DBA staining is excluded from the terminal tip (Herzlinger *et al.*, 1993). Further evidence comes from the neonatal rabbit kidney, which since it completes its development within 3-5 weeks after birth, at the time of birth the collecting duct system continues to develop (Kloth *et al.*, 1998). In the neonatal rabbit kidney, fully embryonic collecting duct ampullae are found in the outer cortex and more mature tissue is found in the midcortical and medullary regions (Kloth *et al.*, 1998). A recent lectin histochemical study revealed a complete lack of DBA labeling from the ampullary tip of the neonatal rabbit kidney (Schumacher *et al.*, 2002).

The identity of the glycoconjugate that *Dolichos Biflorus* agglutinin recognizes is currently unknown. Recently, a first attempt to identify the glycoconjugate that DBA recognizes showed that it probably belongs to a group of

glycosaminoglycans (Schumacher *et al.*, 2002). If this turns out to be the case, it is possible that the DBA-binding glycoconjugate is directly involved in branching morphogenesis as removal of all glycosaminoglycans blocks ureteric bud branching (Davies *et al.*, 1995; plus all chlorate data in this thesis). Lectin histochemistry studies have shown that DBA is associated with cell differentiation as it recognizes postmitotic differentiating epidermal cells (Hrdlickova-Cela *et al.*, 2001) and it binds specifically fully differentiated trophoblast cells (Nakano *et al.*, 2002). It is possible therefore that the cells at the ureteric bud stalks that show DBA staining are entering a differentiating stage.

In order to establish whether this specialization at the terminal tip of the ureteric bud is a special feature of the actively growing epithelium, the effects of exogenous GDNF (as a branching promoter) or a function-blocking antibody to GDNF (as a branching inhibitor) on DBA binding were examined. The enlarged GDNF-treated tips retained their "tip"-phenotype and lacked DBA reactivity, as did the ectopic-buds emerging from the stalk. The latter finding is surprising as the "new" outgrowths (ectopic) emerge from an area that does not normally give rise to new tips and where the differentiation process has started suggesting that differentiation from tip to stalk is reversible.

Ureteric bud development is arrested when GDNF is blocked with a function blocking antibody (Davies *et al.*, 1999; Towers *et al.*, 1998). In kidneys treated with anti-GDNF, DBA staining is present throughout the epithelium with no specialized compartmentalization. This is also the case in kidneys treated with chlorate where block of branching is accompanied with loss of specialization at the tips as seen with the lack of DBA binding (Davies, unpublished observation). This suggests that lack of DBA binding correlates with branching activity and most likely rescue of branching would also result in compartmentalization in the lectin binding.

Collagen XVIII is a heparan sulphate proteoglycan (Halfter *et al.*, 1998) that in the developing ureteric bud shows a specific lack of expression from the terminal

tips (Lin *et al.*, 2001b) similar to the one observed with DBA. Local application of GDNF is shown to cause loss of the type XVIII collagen expression from the ureteric bud tips (Lin *et al.*, 2001b). Type XVIII collagen might be a candidate for DBA, and this could explain the reason why GDNF-enlarged tips were DBA-negative and why blocking of GDNF shows a uniform DBA reactivity on the branching-arrested ureteric bud.

5.5.2 Tip generation from stalk

The ability of the stalk to generate new tips (DBA-negative) from locations where naturally cells form only stalks (DBA-positive) is seen when kidneys are treated with exogenous GDNF. This is also the case in the generation of new "tips" from an amputated T-stage ureteric bud. The Γ-shape UB is able to form new tips that show a slight disturbed branching pattern orientation but are DBA-negative suggesting that the differentiation of the stalk is reversible and is able to generate less mature epithelium (DBA-negative) in order to compensate for the loss and eventually resume the "right" number of terminal ampullae for efficient nephron formation. Also there is the possibility that stalks might have the ability to form tips from any part of them. However as soon as new tips are formed they might exert a negative signal to the neighbouring stalk cells that prevent them from forming more tips in a way of controlling their emergence to the most efficient number or space orientation and thus establishing the architecture of the developing ureteric bud tree (which allows enough space for "correct" nephron number).

5.5.3 Differential gene expression

Up to date, several genes have identified to show spatial expression in the ureteric bud such as the c-ret and c-ros protooncogenes and members of the Wnt

family (Carroll and McMahon, 2000; Kispert *et al.*, 1996; Pachnis *et al.*, 1993). The protooncogenes c-ret and c-ros are reported to be expressed at the distal ends of the ureteric bud branches. More specifically, c-ret expression is restricted at the ureteric bud tips at E13.5-E17.5 metanephroi (Pachnis *et al.*, 1993), however at the earlier stage of E11.5 it is expressed throughout the ureteric bud epithelium (Fisher *et al.*, 2001). Ros shows a similar expression pattern at the E11.5 ureteric bud epithelium (Fisher *et al.*, 2001; Kanwar *et al.*, 1995). Another gene that is expressed at the branches of the E12.5 ureteric bud epithelium is *Sox9* (Kent *et al.*, 1996) and is used as a marker of the ureteric bud tips (Lin *et al.*, 2001a; Pepicelli *et al.*, 1997).

The Wnt gene family encode secreted glycoproteins that regulate key developmental processes including kidney development (for reviews see Carroll and McMahon, 2000; Vainio *et al.*, 1999; Vainio and Uusitalo, 2000). In the developing ureteric bud members of the Wnt family reveal a sequential and non-overlaping expression (Vainio *et al.*, 1999). Wnt-6 and Wnt-11 are both expressed at the ureteric bud tips (Lin *et al.*, 2001a). Wnt-11 expression is confined to the tips of the ureteric bud from as early as E11.5 and continues to be expressed at the tips of the newly formed branches of the growing ureteric bud tree (Kispert *et al.*, 1996). Wnt-7b expression is detected in the ureteric bud epithelium and it is confined to the stalks being excluded completely from the tip area where Wnt-11 is expressed (Kispert *et al.*, 1996; Vainio *et al.*, 1999). However, Wnt-7b is first detected in the stalks of the ureteric bud at E13.5 (Vainio *et al.*, 1999).

Extracellular matrix components such as collagen type IV and XVIII are excluded from the ureteric bud tips. Collagen type IV is present at the proximal parts of the ureteric bud excluded from the tips (Barasch *et al.*, 1999). Endostatin a carboxyl-terminal proteolytic cleavage product of collagen XVIII is found to be prominent at the branch points and the ureteric bud stalk (Karihaloo *et al.*, 2001a).

Recent studies have looked at either the gene expression of cells of ureteric bud origin cultured in monolayers vs. in extracellular matrix (3D tubulogenesis model) or the global gene expression patterns during the course of kidney development (Pavlova *et al.*, 1999; Stuart *et al.*, 2001). In the former study, branching morphogenesis was accompanied with differential expression of transcription factors with previously described roles in morphogenesis and downregulation of pro-apoptotic genes accompanied with upregulation of anti-apoptotic genes (Pavlova *et al.*, 1999). In the same study, a number of genes were found upregulated in conditions favouring branching morphogenesis such as c-met, basic fibrobast growth factor (bFGF) receptor and three homeobox genes, Hox-B5, -B8 and –B9 (Pavlova *et al.*, 1999). In the latter study, gene expression patterns were examined during kidney organogenesis (Stuart *et al.*, 2001). In the early embryonic kidney, genes that function in protein synthesis, DNA replication or structure and RNA synthesis were upregulated consistent with an actively proliferating tissue (Stuart *et al.*, 2001). The genes for structural proteins of the extracellular matrix or cytoskeleton were upregulated during midembryogenesis (Stuart *et al.*, 2001).

To date the evidence of spatiotemporal pattern of gene expression in the ureteric bud epithelium comes from expression studies. The information obtained herein is the initial step toward the identification of genes differentially regulated in the ureteric bud during the emergence of new tips and the establishment of the more stable stalk epithelium in the course of the formation of the ureteric bud tree.

Further studies are necessary in order to identify which are the genes that are differentially expressed in the tip of the ureteric bud epithelium. At present only hypotheses of possible up- or down- regulation of genes can be made. A possible up-regulation of genes with role in DNA replication would support the observations described in *chapter 3* that the ampullary tips are highly mitogenic during branching. Another possibility would be the up-regulation of extracellular proteinases at the tips that would support the observations of other researchers on

the lack of basement membrane components such as collagen type IV and XVIII at the tips.

Chapter 6

Conclusion

The metanephric kidney has received great attention as it is an excellent model to study reciprocal epithelial-mesenchymal tissue interactions between the branching ureteric bud and its surrounding metanephric mesenchyme during development. To date a wide knowledge exists on the molecular regulation, secreted molecules and signaling pathways involved in aspects of metanephric development especially nephrogenesis, whereas the ureteric epithelium component that itself develops into the collecting duct system has received little research attention. The formation of an epithelial organ via branching morphogenesis from a preexisting epithelial tube is currently getting more interest during organogenesis of a variety of internal organs. The main focus of my investigation is on the branching morphogenesis of the ureteric bud epithelium.

The aim of my thesis was to investigate whether the sites of branching activity namely the ureteric bud tips show specializations in relation to the rest of the epithelium during development of the collecting duct system.

As an experimental model system, I used the murine metanephric kidney. Isolated E11.5 metanephroi develop well in organ culture and undergo organotypic branching morphogenesis. This allowed manipulation of the branching morphology by pharmacological agents. The use of immunohistochemistry in combination with confocal laser scanning microscopy, which allowed visualization of whole mount organs, provided powerful techniques for examining with great definition the manipulation effects on the tubular branching structures during renal organogenesis.

Branching morphogenesis is a result of coordination between mechanical forces and the processes of cell growth, proliferation, differentiation and death (Hogan, 1999). Hence, the ureteric bud tips were examined for specializations on the intrinsic mechanisms that drive morphogenesis such as the pattern of cell proliferation (assessed by BrdU incorporation), cytoskeletal organization

(localization and inhibition studies) and gene expression (revealed by lectin histochemistry and differential display).

The results showed that increased localized cell proliferation is a feature of the actively growing ureteric bud tips in relation to the stalks. When branching morphogenesis of the ureteric bud was blocked, the cell proliferation at the tips was greatly reduced suggesting that the newly formed tips are mitogenic. The ureteric bud during evagination emerges as a single tip from the nephric duct; BrdU incorporation revealed an increase on cell proliferation at the presumptive metanephric area suggesting that localized cell proliferation might be the first sign of ureteric bud. Two known regulators of metanephric development were examined on their roles on cell proliferation on ureteric bud tips. The branch-promoting effect of GDNF resulted in an enlargement of the tip area with no effect on cell proliferation, whereas the branch-inhibiting effect of TGF-β resulted in a reduction in branching, which was also accompanied with a reduction in cell proliferation at the tips. Additional work is needed for identifying further the secreted paracrine factor(s) regulating cell proliferation at the tips of the branching epithelium and the UB as it evaginates from the Wollfian duct.

The dramatic shape changes of a developing branching epithelium are a result of cytoskeletal rearrangement. This is also the case during branching activity of the ureteric bud epithelium, as revealed with localization and inhibition of actin filaments and myosin. Phalloidin staining showed a strong expression of actin microfilaments at the ureteric bud tips during branching activity which was lost when branching was inhibited. Two widely used drugs, cytochalasin D and butanedione monoxime for inhibition of actin and myosin respectively, resulted in reduced ureteric bud branching, confirming that acto-myosin contractility is necessary for branching activity. Mild pharmacological inhibition of actin polymerization with cytochalasin D resulted in disrupted epithelial tip morphology with altered cell junctions as shown with E-cadherin

immunostaining. Further work will elucidate the signaling pathways regulating the cytoskeletal rearrangement in the branching epithelium, as well as the role and turnover of cell junction proteins in the ureteric bud tips.

Lectin histochemistry studies revealed a difference in expression of lectin binding glycoconjugates at the ureteric bud tips. The *Dolichos Biflorus* agglutinin (DBA), which is widely used as collecting duct marker, showed lack of binding to the ureteric bud tips. This specialization persisted throughout branching morphogenesis at the culture times studied and was lost when branching was blocked. Organ recombination studies showed that the ureteric bud stalks are able to form new tips when one UB tip is amputated from the T-shape stage ureteric bud. These newly formed tips regain their tip state as revealed with the lack of DBA binding. The differential expression of lectin binding glycoconjugates, along the actively growing epithelium, suggested the possibility that other genes than the currently known (such as *Wnt-11*) might be expressed in the E11.5 ureteric bud tip epithelium that might be identified as tip (or even stalk) markers. This hypothesis was tested in a pilot study using differential display. The preliminary results showed the presence of differentially expressed bands between the UB tips and stalks at the early stages of branching morphogenesis. Further studies are required on identifying the differential genes expressed between the two epithelial compartments, their expression and their role on UB development.

The key conclusion of my work is that several aspects of cell biology of the ureteric bud tips (proliferation, cytoskeleton, molecular expression) differ from that of stalks in response to the effects of the surrounding mesenchyme, but only when the tips are actively growing and branching. One possible limitation of the approach that I have taken is that due to the reciprocal interactions between the ureteric epithelium and surrounding metanephric mesenchyme, there is always the possibility of an indirect effect emanating from the mesenchyme during *in vitro* morphogenesis and manipulation. In principle, this limitation could be

addressed by separating epithelium and mesenchyme, subjecting them to different experimental treatments (such as transfection of dominant negative mutants) and recombining them.

The results presented in this thesis link the morphogenetic mechanisms that drive changes during embryogenesis with the organogenesis of the collecting duct system. Ureteric bud branching morphogenesis is a process of considerable interest as it plays a major role in determining the nephron number in the kidney and hence its functionality. In essence, abnormal or defective ureteric bud branching is implicated in the genesis of human renal diseases.

References

Abrahamson, D. R., Robert, B., Hyink, D. P., St John, P. L., and Daniel, T. O. (1998). Origins and formation of microvasculature in the developing kidney. *Kidney Int Suppl* **67,** S7-11.

Adams, C. L., Chen, Y. T., Smith, S. J., and Nelson, W. J. (1998). Mechanisms of epithelial cell-cell adhesion and cell compaction revealed by high-resolution tracking of E-cadherin-green fluorescent protein. *J Cell Biol* **142,** 1105-19.

Airenne, T., Lin, Y., Olsson, M., Ekblom, P., Vainio, S., and Tryggvason, K. (2000). Differential expression of mouse laminin gamma2 and gamma2* chain transcripts. *Cell Tissue Res* **300,** 129-37.

al-Awqati, Q., and Goldberg, M. R. (1998). Architectural patterns in branching morphogenesis in the kidney. *Kidney Int* **54,** 1832-42.

Balkovetz, D. F. (1998). Hepatocyte growth factor and Madin-Darby canine kidney cells: in vitro models of epithelial cell movement and morphogenesis. *Microsc Res Tech* **43,** 456-63.

Barasch, J., Yang, J., Qiao, J., Tempst, P., Erdjument-Bromage, H., Leung, W., and Oliver, J. A. (1999). Tissue inhibitor of metalloproteinase-2 stimulates mesenchymal growth and regulates epithelial branching during morphogenesis of the rat metanephros. *J Clin Invest* **103,** 1299-307.

Bard, J. (1992). "Morphogenesis: the cellular and molecular processes of developmental anatomy." Cambridge University Press, Cambridge.

Barnes, J. D., Crosby, J. L., Jones, C. M., Wright, C. V., and Hogan, B. L. (1994). Embryonic expression of Lim-1, the mouse homolog of Xenopus Xlim-1, suggests a role in lateral mesoderm differentiation and neurogenesis. *Dev Biol* **161,** 168-78.

Barnett, M. W., Fisher, C. E., Perona-Wright, G., and Davies, J. A. (2002). Signalling by glial cell line-derived neurotrophic factor (GDNF) requires heparan sulphate glycosaminoglycan. *J Cell Sci* **115,** 4495-503.

Bates, C. M., Kharzai, S., Erwin, T., Rossant, J., and Parada, L. F. (2000). Role of N-myc in the developing mouse kidney. *Dev Biol* **222,** 317-25.

Batourina, E., Gim, S., Bello, N., Shy, M., Clagett-Dame, M., Srinivas, S., Costantini, F., and Mendelsohn, C. (2001). Vitamin A controls epithelial/mesenchymal interactions through Ret expression. *Nat Genet* **27,** 74-8.

Bellusci, S., Grindley, J., Emoto, H., Itoh, N., and Hogan, B. L. (1997). Fibroblast growth factor 10 (FGF10) and branching morphogenesis in the embryonic mouse lung. *Development* **124,** 4867-78.

Bement, W. M., Mandato, C. A., and Kirsch, M. N. (1999). Wound-induced assembly and closure of an actomyosin purse string in Xenopus oocytes. *Curr Biol* **9,** 579-87.

Bernfield, M., and Banerjee, S. D. (1982). The turnover of basal lamina glycosaminoglycan correlates with epithelial morphogenesis. *Dev Biol* **90,** 291-305.

Bernfield, M., Gotte, M., Park, P. W., Reizes, O., Fitzgerald, M. L., Lincecum, J., and Zako, M. (1999). Functions of cell surface heparan sulfate proteoglycans. *Annu Rev Biochem* **68,** 729-77.

Bernfield, M. R., Banerjee, S. D., and Cohn, R. H. (1972). Dependence of salivary epithelial morphology and branching morphogenesis upon acid mucopolysaccharide-protein (proteoglycan) at the epithelial surface. *J Cell Biol* **52,** 674-89.

Birchmeier, C., and Gherardi, E. (1998). Developmental roles of HGF/SF and its receptor, the c-Met tyrosine kinase. *Trends Cell Biol* **8,** 404-10.

Boccaccio, C., Ando, M., Tamagnone, L., Bardelli, A., Michieli, P., Battistini, C., and Comoglio, P. M. (1998). Induction of epithelial tubules by growth factor HGF depends on the STAT pathway. *Nature* **391,** 285-8.

Braga, V. M., Machesky, L. M., Hall, A., and Hotchin, N. A. (1997). The small GTPases Rho and Rac are required for the establishment of cadherin-dependent cell-cell contacts. *J Cell Biol* **137,** 1421-31.

Bragg, A. D., Moses, H. L., and Serra, R. (2001). Signaling to the epithelium is not sufficient to mediate all of the effects of transforming growth factor beta and bone morphogenetic protein 4 on murine embryonic lung development. *Mech Dev* **109,** 13-26.

Brandli, A. W. (1999). Towards a molecular anatomy of the Xenopus pronephric kidney. *Int J Dev Biol* **43,** 381-95.

Bresciani, F. (1968). Topography of DNA synthesis in the mammary gland of the C3H mouse and its control by ovarian hormones: an autoradiographic study. *Cell Tissue Kinet* **1,** 51-63.

Brock, J., Midwinter, K., Lewis, J., and Martin, P. (1996). Healing of incisional wounds in the embryonic chick wing bud: characterization of the actin purse-string and demonstration of a requirement for Rho activation. *J Cell Biol* **135,** 1097-107.

Brophy, P. D., Ostrom, L., Lang, K. M., and Dressler, G. R. (2001). Regulation of ureteric bud outgrowth by Pax2-dependent activation of the glial derived neurotrophic factor gene. *Development* **128,** 4747-56.

Brown, D., Roth, J., and Orci, L. (1985). Lectin-gold cytochemistry reveals intercalated cell heterogeneity along rat kidney collecting ducts. *Am J Physiol* **248,** C348-56.

Bullock, S. L., Fletcher, J. M., Beddington, R. S., and Wilson, V. A. (1998). Renal agenesis in mice homozygous for a gene trap mutation in the gene encoding heparan sulfate 2-sulfotransferase. *Genes Dev* **12,** 1894-906.

Cacalano, G., Farinas, I., Wang, L. C., Hagler, K., Forgie, A., Moore, M., Armanini, M., Phillips, H., Ryan, A. M., Reichardt, L. F., Hynes, M., Davies, A., and Rosenthal, A. (1998). GFRalpha1 is an essential receptor component for GDNF in the developing nervous system and kidney. *Neuron* **21,** 53-62.

Cadigan, K. M., and Nusse, R. (1997). Wnt signaling: a common theme in animal development. *Genes Dev* **11,** 3286-305.

Cancilla, B., Ford-Perriss, M. D., and Bertram, J. F. (1999). Expression and localization of fibroblast growth factors and fibroblast growth factor receptors in the developing rat kidney. *Kidney Int* **56,** 2025-39.

Cano-Gauci, D. F., Song, H. H., Yang, H., McKerlie, C., Choo, B., Shi, W., Pullano, R., Piscione, T. D., Grisaru, S., Soon, S., Sedlackova, L., Tanswell, A. K., Mak, T. W., Yeger, H., Lockwood, G. A., Rosenblum, N. D., and Filmus, J. (1999). Glypican-3-deficient mice exhibit developmental overgrowth and some of the abnormalities typical of Simpson-Golabi-Behmel syndrome. *J Cell Biol* **146,** 255-64.

Carroll, T. J., and McMahon, A. P. (2000). Secreted molecules in metanephric induction. *J Am Soc Nephrol* **11,** S116-9.

Chalazonitis, A., Rothman, T. P., Chen, J., and Gershon, M. D. (1998). Age-dependent differences in the effects of GDNF and NT-3 on the development of neurons and glia from neural crest-derived precursors immunoselected from the fetal rat gut: expression of GFRalpha-1 in vitro and in vivo. *Dev Biol* **204,** 385-406.

Chihara, T., Kato, K., Taniguchi, M., Ng, J., and Hayashi, S. (2003). Rac promotes epithelial cell rearrangement during tracheal tubulogenesis in Drosophila. *Development* **130,** 1419-1428.

Clark, A. T., Young, R. J., and Bertram, J. F. (2001). In vitro studies on the roles of transforming growth factor-beta 1 in rat metanephric development. *Kidney Int* **59,** 1641-53.

Colony, P. C., and Conforti, J. C. (1993). Morphogenesis in the fetal rat proximal colon: effects of cytochalasin D. *Anat Rec* **235,** 241-52.

Cooper, J. A. (1987). Effects of cytochalasin and phalloidin on actin. *J Cell Biol* **105,** 1473-8.

Costa, M., and Brookes, S. J. (1994). The enteric nervous system. *Am J Gastroenterol* **89,** S129-37.

Cramer, L. P., and Mitchison, T. J. (1995). Myosin is involved in postmitotic cell spreading. *J Cell Biol* **131,** 179-89.

Cullen-McEwen, L. A., Drago, J., and Bertram, J. F. (2001). Nephron endowment in glial cell line-derived neurotrophic factor (GDNF) heterozygous mice. *Kidney Int* **60,** 31-6.

Daniel, C. W., and Robinson, S. D. (1992). Regulation of mammary growth and function by TGF-beta. *Mol Reprod Dev* **32,** 145-51.

Daniel, C. W., Silberstein, G. B., and Strickland, P. (1984). Reinitiation of growth in senescent mouse mammary epithelium in response to cholera toxin. *Science* **224,** 1245-7.

Daniel, C. W., Silberstein, G. B., Van Horn, K., Strickland, P., and Robinson, S. (1989). TGF-beta 1-induced inhibition of mouse mammary ductal growth: developmental specificity and characterization. *Dev Biol* **135,** 20-30.

Danjo, Y., and Gipson, I. K. (1998). Actin 'purse string' filaments are anchored by E-cadherin-mediated adherens junctions at the leading edge of the epithelial wound, providing coordinated cell movement. *J Cell Sci* **111,** 3323-32.

Davies, J. (1993). How to build a kidney. *Semin Cell Biol* **4,** 213-9.

Davies, J. (1994). Control of calbindin-D28K expression in developing mouse kidney. *Dev Dyn* **199,** 45-51.

Davies, J. (2001). Intracellular and extracellular regulation of ureteric bud morphogenesis. *J Anat* **198,** 257-64.

Davies, J., Lyon, M., Gallagher, J., and Garrod, D. (1995). Sulphated proteoglycan is required for collecting duct growth and branching but not nephron formation during kidney development. *Development* **121,** 1507-17.

Davies, J. A. (1996). Mesenchyme to epithelium transition during development of the mammalian kidney tubule. *Acta Anat (Basel)* **156,** 187-201.

Davies, J. A. (2002). Do different branching epithelia use a conserved developmental mechanism? *Bioessays* **24,** 937-48.

Davies, J. A., and Bard, J. B. (1998). The development of the kidney. *Curr Top Dev Biol* **39,** 245-301.

Davies, J. A., and Davey, M. G. (1999). Collecting duct morphogenesis. *Pediatr Nephrol* **13,** 535-41.

Davies, J. A., and Fisher, C. E. (2002). Genes and proteins in renal development. *Exp Nephrol* **10,** 102-13.

Davies, J. A., Fisher, C. E., and Barnett, M. W. (2001). Glycosaminoglycans in the study of mammalian organ development. *Biochem Soc Trans* **29,** 166-71.

Davies, J. A., Millar, C. B., Johnson, E. M., Jr., and Milbrandt, J. (1999). Neurturin: an autocrine regulator of renal collecting duct development. *Dev Genet* **24,** 284-92.

De Archangelis, A., Mark, M., Kreidberg, J., Sorokin, L., and Georges-Labouesse, E. (1999). Synegistic activities of alpha3 and alpha6 integrins are required during apical ectodermal ridge formation and organogenesis in the mouse. *Development* **126,** 3957-68.

Debas, H. T. (1997). Molecular insights into the development of the pancreas. *Am J Surg* **174,** 227-31.

Dressler, G. R. (1997). Genetic control of kidney development. *Adv Nephrol Necker Hosp* **26,** 1-17.

Dressler, G. R., Deutsch, U., Chowdhury, K., Nornes, H. O., and Gruss, P. (1990). Pax2, a new murine paired-box-containing gene and its expression in the developing excretory system. *Development* **109,** 787-95.

Dressler, G. R., and Woolf, A. S. (1999). Pax2 in development and renal disease. *Int J Dev Biol* **43,** 463-8.

Dudley, A. T., Lyons, K. M., and Robertson, E. J. (1995). A requirement for bone morphogenetic protein-7 during development of the mammalian kidney and eye. *Genes Dev* **9,** 2795-807.

Durbec, P. L., Larsson-Blomberg, L. B., Schuchardt, A., Costantini, F., and Pachnis, V. (1996). Common origin and developmental dependence on c-ret of subsets of enteric and sympathetic neuroblasts. *Development* **122,** 349-58.

Durbeej, M., and Ekblom, P. (1997). Dystroglycan and laminins: glycoconjugates involved in branching epithelial morphogenesis. *Exp Lung Res* **23,** 109-18.

Eccles, M., Bockett, N., and Stayner, C. (2003). PAX2 and Renal-Coloboma Syndrome. *In* "The Kidney: From normal development to congenital disease" (P. D. Vize, A. S. Woolf, and J. B. L. Bard, Eds.), pp. 411-432. Accademic Press, London.

Ehrenfels, C. W., Carmillo, P. J., Orozco, O., Cate, R. L., and Sanicola, M. (1999). Perturbation of RET signaling in the embryonic kidney. *Dev Genet* **24,** 263-72.

Ekblom, M., Falk, M., Salmivirta, K., Durbeej, M., and Ekblom, P. (1998). Laminin isoforms and epithelial development. *Ann N Y Acad Sci* **857,** 194-211.

Ekblom, P., Ekblom, M., Fecker, L., Klein, G., Zhang, H. Y., Kadoya, Y., Chu, M. L., Mayer, U., and Timpl, R. (1994). Role of mesenchymal nidogen for epithelial morphogenesis in vitro. *Development* **120,** 2003-14.

Enomoto, H., Araki, T., Jackman, A., Heuckeroth, R. O., Snider, W. D., Johnson, E. M., Jr., and Milbrandt, J. (1998). GFR alpha1-deficient mice have deficits in the enteric nervous system and kidneys. *Neuron* **21,** 317-24.

Evers, E. E., Zondag, G. C., Malliri, A., Price, L. S., ten Klooster, J. P., van der Kammen, R. A., and Collard, J. G. (2000). Rho family proteins in cell adhesion and cell migration. *Eur J Cancer* **36,** 1269-74.

Fisher, C. E., Michael, L., Barnett, M. W., and Davies, J. A. (2001). Erk MAP kinase regulates branching morphogenesis in the developing mouse kidney. *Development* **128,** 4329-38.

Godin, R. E., Robertson, E. J., and Dudley, A. T. (1999). Role of BMP family members during kidney development. *Int J Dev Biol* **43,** 405-11.

Godin, R. E., Takaesu, N. T., Robertson, E. J., and Dudley, A. T. (1998). Regulation of BMP7 expression during kidney development. *Development* **125,** 3473-82.

Golden, J. P., DeMaro, J. A., Osborne, P. A., Milbrandt, J., and Johnson, E. M., Jr. (1999). Expression of neurturin, GDNF, and GDNF family-receptor mRNA in the developing and mature mouse. *Exp Neurol* **158,** 504-28.

Goldin, G. V., Hindman, H. M., and Wessells, N. K. (1984). The role of cell proliferation and cellular shape change in branching morphogenesis of the embryonic mouse lung: analysis using aphidicolin and cytochalasins. *J Exp Zool* **232,** 287-96.

Goldin, G. V., and Opperman, L. A. (1980). Induction of supernumerary tracheal buds and the stimulation of DNA synthesis in the embryonic chick lung and trachea by epidermal growth factor. *J Embryol Exp Morphol* **60,** 235-43.

Grobstein, C. (1953a). Inductive epithelio-mesenchymal interaction in cultured organ rudiments of the mouse. *Science* , 52-5.

Grobstein, C. (1953b). Morphogenetic interaction between embryonic mouse tissues separated by a membrane filter. *Nature* **172,** 869-71.

Grose, R., and Martin, P. (1999). Parallels between wound repair and morphogenesis in the embryo. *Semin Cell Dev Biol* **10,** 395-404.

Gumbiner, B. M. (1996). Cell adhesion: the molecular basis of tissue architecture and morphogenesis. *Cell* **84,** 345-57.

Gupta, I. R., Macias-Silva, M., Kim, S., Zhou, X., Piscione, T. D., Whiteside, C., Wrana, J. L., and Rosenblum, N. D. (2000). BMP-2/ALK3 and HGF signal in parallel to regulate renal collecting duct morphogenesis. *J Cell Sci* **113,** 269-78.

Gupta, I. R., Piscione, T. D., Grisaru, S., Phan, T., Macias-Silva, M., Zhou, X., Whiteside, C., Wrana, J. L., and Rosenblum, N. D. (1999). Protein kinase A is a negative regulator of renal branching morphogenesis and modulates inhibitory and stimulatory bone morphogenetic proteins. *J Biol Chem* **274,** 26305-14.

Halfter, W., Dong, S., Schurer, B., and Cole, G. J. (1998). Collagen XVIII is a basement membrane heparan sulfate proteoglycan. *J Biol Chem* **273,** 25404-12.

Hall, A. (1994). Small GTP-binding proteins and the regulation of the actin cytoskeleton. *Annu Rev Cell Biol* **10,** 31-54.

Harden, N., Ricos, M., Ong, Y. M., Chia, W., and Lim, L. (1999). Participation of small GTPases in dorsal closure of the Drosophila embryo: distinct roles for Rho subfamily proteins in epithelial morphogenesis. *J Cell Sci* **112,** 273-84.

Hardman, P., and Spooner, B. S. (1992a). Localization of extracellular matrix components in developing mouse salivary glands by confocal microscopy. *Anat Rec* **234,** 452-9.

Hardman, P., and Spooner, B. S. (1992b). Salivary epithelium branching morphogenesis. *In* "Epithelial organization and development" (T. P. Fleming, Ed.), pp. 353-375. Chapman & Hall, London.

Hatini, V., Huh, S. O., Herzlinger, D., Soares, V. C., and Lai, E. (1996). Essential role of stromal mesenchyme in kidney morphogenesis revealed by targeted disruption of Winged Helix transcription factor BF-2. *Genes Dev* **10,** 1467-78.

Hennighausen, L., and Robinson, G. W. (1998). Think globally, act locally: the making of a mouse mammary gland. *Genes Dev* **12,** 449-55.

Herrmann, C., Wray, J., Travers, F., and Barman, T. (1992). Effect of 2,3-butanedione monoxime on myosin and myofibrillar ATPases. An example of an uncompetitive inhibitor. *Biochemistry* **31,** 12227-32.

Herzlinger, D., Abramson, R., and Cohen, D. (1993). Phenotypic conversions in renal development. *J Cell Sci Suppl* **17,** 61-4.

Heuckeroth, R. O., Lampe, P. A., Johnson, E. M., and Milbrandt, J. (1998). Neurturin and GDNF promote proliferation and survival of enteric neuron and glial progenitors in vitro. *Dev Biol* **200,** 116-29.

Hilfer, S. R. (1996). Morphogenesis of the lung: control of embryonic and fetal branching. *Annu Rev Physiol* **58,** 93-113.

Hogan, B. L. (1999). Morphogenesis. *Cell* **96,** 225-33.

Hogan, B. L., Grindley, J., Bellusci, S., Dunn, N. R., Emoto, H., and Itoh, N. (1997). Branching morphogenesis of the lung: new models for a classical problem. *Cold Spring Harb Symp Quant Biol* **62,** 249-56.

Holthofer, H. (1983). Lectin binding sites in kidney. A comparative study of 14 animal species. *J Histochem Cytochem* **31,** 531-7.

Holthofer, H. (1988). Cell type-specific glycoconjugates of collecting duct cells during maturation of the rat kidney. *Cell Tissue Res* **253,** 305-9.

Horb, L. D., and Slack, J. M. (2000). Role of cell division in branching morphogenesis and differentiation of the embryonic pancreas. *Int J Dev Biol* **44,** 791-6.

Horster, M. F., Braun, G. S., and Huber, S. M. (1999). Embryonic renal epithelia: induction, nephrogenesis, and cell differentiation. *Physiol Rev* **79,** 1157-91.

Hrdlickova-Cela, E., Plzak, J., Holikova, Z., Dvorankova, B., and Smetana, K., Jr. (2001). Postmitotic basal cells in squamous cell epithelia are identified with Dolichos biflorus agglutinin--functional consequences. *Apmis* **109,** 714-20.

Hu, J., Shima, H., and Nakagawa, H. (1999). Glial cell line-derived neurotropic factor stimulates sertoli cell proliferation in the early postnatal period of rat testis development. *Endocrinology* **140,** 3416-21.

Huang, S., and Ingber, D. E. (1999). The structural and mechanical complexity of cell-growth control. *Nat Cell Biol* **1,** E131-8.

Humphreys, R. C., Krajewska, M., Krnacik, S., Jaeger, R., Weiher, H., Krajewski, S., Reed, J. C., and Rosen, J. M. (1996). Apoptosis in the terminal endbud of the murine mammary gland: a mechanism of ductal morphogenesis. *Development* **122,** 4013-22.

Hynes, R. O. (1992). Integrins: versatility, modulation, and signaling in cell adhesion. *Cell* **69,** 11-25.

Jaskoll, T., and Melnick, M. (1999). Submandibular gland morphogenesis: stage-specific expression of TGF-alpha/EGF, IGF, TGF-beta, TNF, and IL-6 signal transduction in normal embryonic mice and the phenotypic effects of TGF-beta2, TGF-beta3, and EGF-r null mutations. *Anat Rec* **256,** 252-68.

Jernvall, J., and Thesleff, I. (2000). Reiterative signaling and patterning during mammalian tooth morphogenesis. *Mech Dev* **92,** 19-29.

Jing, S., Wen, D., Yu, Y., Holst, P. L., Luo, Y., Fang, M., Tamir, R., Antonio, L., Hu, Z., Cupples, R., Louis, J. C., Hu, S., Altrock, B. W., and Fox, G. M. (1996). GDNF-induced activation of the ret protein tyrosine kinase is mediated by GDNFR-alpha, a novel receptor for GDNF. *Cell* **85,** 1113-24.

Juliano, R. L., and Haskill, S. (1993). Signal transduction from the extracellular matrix. *J Cell Biol* **120,** 577-85.

Kabsch, W., and Vandekerckhove, J. (1992). Structure and function of actin. *Annu Rev Biophys Biomol Struct* **21,** 49-76.

Kadoya, Y., and Yamashina, S. (1989). Intracellular accumulation of basement membrane components during morphogenesis of rat submandibular gland. *J Histochem Cytochem* **37,** 1387-92.

Kanwar, Y. S., Liu, Z. Z., Kumar, A., Wada, J., and Carone, F. A. (1995). Cloning of mouse c-ros renal cDNA, its role in development and relationship to extracellular matrix glycoproteins. *Kidney Int* **48,** 1646-59.

Kanwar, Y. S., Ota, K., Yang, Q., Wada, J., Kashihara, N., Tian, Y., and Wallner, E. I. (1999). Role of membrane-type matrix metalloproteinase 1 (MT-1-MMP), MMP-2, and its inhibitor in nephrogenesis. *Am J Physiol* **277,** F934-47.

Karihaloo, A., Karumanchi, S. A., Barasch, J., Jha, V., Nickel, C. H., Yang, J., Grisaru, S., Bush, K. T., Nigam, S., Rosenblum, N. D., Sukhatme, V. P., and Cantley, L. G. (2001a). Endostatin regulates branching morphogenesis of renal epithelial cells and ureteric bud. *Proc Natl Acad Sci U S A* **98,** 12509-14.

Karihaloo, A., O'Rourke, D. A., Nickel, C., Spokes, K., and Cantley, L. G. (2001b). Differential MAPK pathways utilized for HGF- and EGF-dependent renal epithelial morphogenesis. *J Biol Chem* **276,** 9166-73.

Katz, B. Z., and Yamada, K. M. (1997). Integrins in morphogenesis and signaling. *Biochimie* **79,** 467-76.

Kent, J., Wheatley, S. C., Andrews, J. E., Sinclair, A. H., and Koopman, P. (1996). A male-specific role for SOX9 in vertebrate sex determination. *Development* **122,** 2813-22.

Khwaja, A., Lehmann, K., Marte, B. M., and Downward, J. (1998). Phosphoinositide 3-kinase induces scattering and tubulogenesis in epithelial cells through a novel pathway. *J Biol Chem* **273,** 18793-801.

Kiehart, D. P. (1999). Wound healing: The power of the purse string. *Curr Biol* **9,** R602-5.

Kispert, A., Vainio, S., Shen, L., Rowitch, D. H., and McMahon, A. P. (1996). Proteoglycans are required for maintenance of Wnt-11 expression in the ureter tips. *Development* **122,** 3627-37.

Kjellen, L., and Lindahl, U. (1991). Proteoglycans: structures and interactions. *Annu Rev Biochem* **60,** 443-75.

Kloth, S., Gmeiner, T., Aigner, J., Jennings, M. L., Rockl, W., and Minuth, W. W. (1998). Transitional stages in the development of the rabbit renal collecting duct. *Differentiation* **63,** 21-32.

Knust, E., and Bossinger, O. (2002). Composition and formation of intercellular junctions in epithelial cells. *Science* **298,** 1955-9.

Kreidberg, J. A., Donovan, M. J., Goldstein, S. L., Rennke, H., Shepherd, K., Jones, R. C., and Jaenisch, R. (1996). Alpha 3 beta 1 integrin has a crucial role in kidney and lung organogenesis. *Development* **122,** 3537-47.

Kreidberg, J. A., Sariola, H., Loring, J. M., Maeda, M., Pelletier, J., Housman, D., and Jaenisch, R. (1993). WT-1 is required for early kidney development. *Cell* **74,** 679-91.

Kulkarni, A. B., and Karlsson, S. (1993). Transforming growth factor-beta 1 knockout mice. A mutation in one cytokine gene causes a dramatic inflammatory disease. *Am J Pathol* **143,** 3-9.

Kume, T., Deng, K., and Hogan, B. L. (2000). Murine forkhead/winged helix genes Foxc1 (Mf1) and Foxc2 (Mfh1) are required for the early organogenesis of the kidney and urinary tract. *Development* **127,** 1387-95.

Laiho, M., DeCaprio, J. A., Ludlow, J. W., Livingston, D. M., and Massague, J. (1990). Growth inhibition by TGF-beta linked to suppression of retinoblastoma protein phosphorylation. *Cell* **62,** 175-85.

Laitinen, L., Virtanen, I., and Saxen, L. (1987). Changes in the glycosylation pattern during embryonic development of mouse kidney as revealed with lectin conjugates. *J Histochem Cytochem* **35,** 55-65.

Lehnert, S. A., and Akhurst, R. J. (1988). Embryonic expression pattern of TGF beta type-1 RNA suggests both paracrine and autocrine mechanisms of action. *Development* **104,** 263-73.

Leimeister, C., Bach, A., Woolf, A. S., and Gessler, M. (1999). Screen for genes regulated during early kidney morphogenesis. *Dev Genet* **24,** 273-83.

Lelongt, B., Trugnan, G., Murphy, G., and Ronco, P. M. (1997). Matrix metalloproteinases MMP2 and MMP9 are produced in early stages of kidney morphogenesis but only MMP9 is required for renal organogenesis in vitro. *J Cell Biol* **136,** 1363-73.

Liang, P., and Pardee, A. B. (1992). Differential display of eukaryotic messenger RNA by means of the polymerase chain reaction. *Science* **257,** 967-71.

Liang, P., and Pardee, A. B. (1997). Differential display. A general protocol. *Methods Mol Biol* **85,** 3-11.

Lin, Y., Liu, A., Zhang, S., Ruusunen, T., Kreidberg, J. A., Peltoketo, H., Drummond, I., and Vainio, S. (2001a). Induction of ureter branching as a response to Wnt-2b signaling during early kidney organogenesis. *Dev Dyn* **222,** 26-39.

Lin, Y., Zhang, S., Rehn, M., Itaranta, P., Tuukkanen, J., Heljasvaara, R., Peltoketo, H., Pihlajaniemi, T., and Vainio, S. (2001b). Induced repatterning of type XVIII collagen expression in ureter bud from kidney to lung type: association with sonic hedgehog and ectopic surfactant protein C. *Development* **128,** 1573-85.

Luo, G., Hofmann, C., Bronckers, A. L., Sohocki, M., Bradley, A., and Karsenty, G. (1995). BMP-7 is an inducer of nephrogenesis, and is also required for eye development and skeletal patterning. *Genes Dev* **9,** 2808-20.

Maas, R., Elfering, S., Glaser, T., and Jepeal, L. (1994). Deficient outgrowth of the ureteric bud underlies the renal agenesis phenotype in mice manifesting the limb deformity (ld) mutation. *Dev Dyn* **199,** 214-28.

Martin, P., and Lewis, J. (1992). Actin cables and epidermal movement in embryonic wound healing. *Nature* **360,** 179-83.

Martinez, G., Cullen-McEwen, L. A., and Bertram, J. F. (2001). Transforming growth factor-beta superfamily members: roles in branching morphogenesis in the kidney. *Nephrology* **6,** 274-284.

Massague, J. (1990). The transforming growth factor-beta family. *Annu Rev Cell Biol* **6,** 597-641.

Massague, J. (1998). TGF-beta signal transduction. *Annu Rev Biochem* **67,** 753-91.

Masure, S., Geerts, H., Cik, M., Hoefnagel, E., Van Den Kieboom, G., Tuytelaars, A., Harris, S., Lesage, A. S., Leysen, J. E., Van Der Helm, L., Verhasselt, P., Yon, J., and Gordon, R. D. (1999). Enovin, a member of the glial cell-line-derived neurotrophic

factor (GDNF) family with growth promoting activity on neuronal cells. Existence and tissue-specific expression of different splice variants. *Eur J Biochem* **266,** 892-902.

Maylie-Pfenninger, M. F., and Jamieson, J. D. (1980). Development of cell surface saccharides on embryonic pancreatic cells. *J Cell Biol* **86,** 96-103.

McCluskey, J., and Martin, P. (1995). Analysis of the tissue movements of embryonic wound healing--DiI studies in the limb bud stage mouse embryo. *Dev Biol* **170,** 102-14.

McPherson, M. J., and Moller, S. G. (2000). "PCR." BIOS Scientific Publishers Limited, Oxford.

Mendelsohn, C., Batourina, E., Fung, S., Gilbert, T., and Dodd, J. (1999). Stromal cells mediate retinoid-dependent functions essential for renal development. *Development* **126,** 1139-48.

Mendelsohn, C., Lohnes, D., Decimo, D., Lufkin, T., LeMeur, M., Chambon, P., and Mark, M. (1994). Function of the retinoic acid receptors (RARs) during development (II). Multiple abnormalities at various stages of organogenesis in RAR double mutants. *Development* **120,** 2749-71.

Metzger, R. J., and Krasnow, M. A. (1999). Genetic control of branching morphogenesis. *Science* **284,** 1635-9.

Miele, G., MacRae, L., McBride, D., Manson, J., and Clinton, M. (1998). Elimination of false positives generated through PCR re-amplification of differential display cDNA. *Biotechniques* **25,** 138-44.

Milaire, J. (1991). Lectin binding sites in developing mouse limb buds. *Anat Embryol (Berl)* **184,** 479-88.

Milbrandt, J., de Sauvage, F. J., Fahrner, T. J., Baloh, R. H., Leitner, M. L., Tansey, M. G., Lampe, P. A., Heuckeroth, R. O., Kotzbauer, P. T., Simburger, K. S., Golden, J. P., Davies, J. A., Vejsada, R., Kato, A. C., Hynes, M., Sherman, D., Nishimura, M., Wang, L. C., Vandlen, R., Moffat, B., Klein, R. D., Poulsen, K., Gray, C., Garces, A., Johnson, E. M., Jr., and et al. (1998). Persephin, a novel neurotrophic factor related to GDNF and neurturin. *Neuron* **20,** 245-53.

Mitsiadis, T. A., Salmivirta, M., Muramatsu, T., Muramatsu, H., Rauvala, H., Lehtonen, E., Jalkanen, M., and Thesleff, I. (1995). Expression of the heparin-binding cytokines, midkine (MK) and HB-GAM (pleiotrophin) is associated with epithelial-mesenchymal interactions during fetal development and organogenesis. *Development* **121,** 37-51.

Miura, T., and Shiota, K. (2000). Time-lapse observation of branching morphogenesis of the lung bud epithelium in mesenchyme-free culture and its relationship with the localization of actin filaments. *Int J Dev Biol* **44,** 899-902.

Miyamoto, N., Yoshida, M., Kuratani, S., Matsuo, I., and Aizawa, S. (1997). Defects of urogenital development in mice lacking Emx2. *Development* **124,** 1653-64.

Miyazaki, M. (1990). Branching morphogenesis in the embryonic mouse submandibular gland: a scanning electron microscopic study. *Arch Histol Cytol* **53,** 157-65.

Miyazaki, Y., Oshima, K., Fogo, A., Hogan, B. L., and Ichikawa, I. (2000). Bone morphogenetic protein 4 regulates the budding site and elongation of the mouse ureter. *J Clin Invest* **105,** 863-73.

Mollard, R., and Dziadek, M. (1998). A correlation between epithelial proliferation rates, basement membrane component localization patterns, and morphogenetic potential in the embryonic mouse lung. *Am J Respir Cell Mol Biol* **19,** 71-82.

Montesano, R., Matsumoto, K., Nakamura, T., and Orci, L. (1991a). Identification of a fibroblast-derived epithelial morphogen as hepatocyte growth factor. *Cell* **67,** 901-8.

Montesano, R., Schaller, G., and Orci, L. (1991b). Induction of epithelial tubular morphogenesis in vitro by fibroblast-derived soluble factors. *Cell* **66,** 697-711.

Moore, M. W., Klein, R. D., Farinas, I., Sauer, H., Armanini, M., Phillips, H., Reichardt, L. F., Ryan, A. M., Carver-Moore, K., and Rosenthal, A. (1996). Renal and neuronal abnormalities in mice lacking GDNF. *Nature* **382,** 76-9.

Morita, K., and Nogawa, H. (1999). EGF-dependent lobule formation and FGF7-dependent stalk elongation in branching morphogenesis of mouse salivary epithelium in vitro. *Dev Dyn* **215,** 148-54.

Moritz, K. M., and Wintour, E. M. (1999). Functional development of the meso- and metanephros. *Pediatr Nephrol* **13,** 171-8.

Moses, H. L., Yang, E. Y., and Pietenpol, J. A. (1990). TGF-beta stimulation and inhibition of cell proliferation: new mechanistic insights. *Cell* **63,** 245-7.

Muller, U., Wang, D., Denda, S., Meneses, J. J., Pedersen, R. A., and Reichardt, L. F. (1997). Integrin alpha8beta1 is critically important for epithelial-mesenchymal interactions during kidney morphogenesis. *Cell* **88,** 603-13.

Murata, F., Tsuyama, S., Suzuki, S., Hamada, H., Ozawa, M., and Muramatsu, T. (1983). Distribution of glycoconjugates in the kidney studied by use of labeled lectins. *J Histochem Cytochem* **31,** 139-44.

Nadasdy, T., Lajoie, G., Laszik, Z., Blick, K. E., Molnar-Nadasdy, G., and Silva, F. G. (1998). Cell proliferation in the developing human kidney. *Pediatr Dev Pathol* **1,** 49-55.

Nagafuchi, A. (2001). Molecular architecture of adherens junctions. *Curr Opin Cell Biol* **13,** 600-3.

Nakamura, E., Kadomatsu, K., Yuasa, S., Muramatsu, H., Mamiya, T., Nabeshima, T., Fan, Q. W., Ishiguro, K., Igakura, T., Matsubara, S., Kaname, T., Horiba, M., Saito, H., and Muramatsu, T. (1998). Disruption of the midkine gene (Mdk) resulted in altered expression of a calcium binding protein in the hippocampus of infant mice and their abnormal behaviour. *Genes Cells* **3,** 811-22.

Nakanishi, Y., Morita, T., and Nogawa, H. (1987). Cell proliferation is not required for the initiation of early cleft formation in mouse embryonic submandibular epithelium in vitro. *Development* **99,** 429-37.

Nakano, H., Shimada, A., Imai, K., Takahashi, T., and Hashizume, K. (2002). Association of Dolichos biflorus lectin binding with full differentiation of bovine trophoblast cells. *Reproduction* **124,** 581-92.

Nishinakamura, R., Matsumoto, Y., Nakao, K., Nakamura, K., Sato, A., Copeland, N. G., Gilbert, D. J., Jenkins, N. A., Scully, S., Lacey, D. L., Katsuki, M., Asashima, M., and Yokota, T. (2001). Murine homolog of SALL1 is essential for ureteric bud invasion in kidney development. *Development* **128,** 3105-15.

Nodder, S., and Martin, P. (1997). Wound healing in embryos: a review. *Anat Embryol (Berl)* **195,** 215-28.

Nogawa, H., Morita, K., and Cardoso, W. V. (1998). Bud formation precedes the appearance of differential cell proliferation during branching morphogenesis of mouse lung epithelium in vitro. *Dev Dyn* **213,** 228-35.

Ota, K., Stetler-Stevenson, W. G., Yang, Q., Kumar, A., Wada, J., Kashihara, N., Wallner, E. I., and Kanwar, Y. S. (1998). Cloning of murine membrane-type-1-matrix metalloproteinase (MT-1-MMP) and its metanephric developmental regulation with respect to MMP-2 and its inhibitor. *Kidney Int* **54,** 131-42.

Owen, F., and Jones, R. (1994). "Statistics." PITMAN Publishing, London.

Pachnis, V., Mankoo, B., and Costantini, F. (1993). Expression of the c-ret proto-oncogene during mouse embryogenesis. *Development* **119,** 1005-17.

Patterson, L. T., and Dressler, G. R. (1994). The regulation of kidney development: new insights from an old model. *Curr Opin Genet Dev* **4,** 696-702.

Patterson, L. T., Pembaur, M., and Potter, S. S. (2001). Hoxa11 and Hoxd11 regulate branching morphogenesis of the ureteric bud in the developing kidney. *Development* **128,** 2153-61.

Pavlova, A., Stuart, R. O., Pohl, M., and Nigam, S. K. (1999). Evolution of gene expression patterns in a model of branching morphogenesis. *Am J Physiol* **277,** F650-63.

Pellegrini, M., Pantano, S., Lucchini, F., Fumi, M., and Forabosco, A. (1997). Emx2 developmental expression in the primordia of the reproductive and excretory systems. *Anat Embryol (Berl)* **196,** 427-33.

Pelton, R. W., Saxena, B., Jones, M., Moses, H. L., and Gold, L. I. (1991). Immunohistochemical localization of TGF beta 1, TGF beta 2, and TGF beta 3 in the mouse embryo: expression patterns suggest multiple roles during embryonic development. *J Cell Biol* **115,** 1091-105.

Pepicelli, C. V., Kispert, A., Rowitch, D. H., and McMahon, A. P. (1997). GDNF induces branching and increased cell proliferation in the ureter of the mouse. *Dev Biol* **192,** 193-8.

Piscione, T. D., Phan, T., and Rosenblum, N. D. (2001). BMP7 controls collecting tubule cell proliferation and apoptosis via Smad1-dependent and -independent pathways. *Am J Physiol Renal Physiol* **280,** F19-33.

Piscione, T. D., Yager, T. D., Gupta, I. R., Grinfeld, B., Pei, Y., Attisano, L., Wrana, J. L., and Rosenblum, N. D. (1997). BMP-2 and OP-1 exert direct and opposite effects on renal branching morphogenesis. *Am J Physiol* **273,** F961-75.

Plisov, S. Y., Ivanov, S. V., Yoshino, K., Dove, L. F., Plisova, T. M., Higinbotham, K. G., Karavanova, I., Lerman, M., and Perantoni, A. O. (2000). Mesenchymal-epithelial transition in the developing metanephric kidney: gene expression study by differential display. *Genesis* **27,** 22-31.

Pohl, M., Sakurai, H., Stuart, R. O., and Nigam, S. K. (2000). Role of hyaluronan and CD44 in in vitro branching morphogenesis of ureteric bud cells. *Dev Biol* **224,** 312-25.

Potter, E. L. (1972). "Normal and Abnormal Development of the Kidney." Year Book Medical Publishers, Inc., Chicago.

Qiao, J., Bush, K. T., Steer, D. L., Stuart, R. O., Sakurai, H., Wachsman, W., and Nigam, S. K. (2001). Multiple fibroblast growth factors support growth of the ureteric bud but have different effects on branching morphogenesis. *Mech Dev* **109,** 123-35.

Qiao, J., Sakurai, H., and Nigam, S. K. (1999a). Branching morphogenesis independent of mesenchymal-epithelial contact in the developing kidney. *Proc Natl Acad Sci U S A* **96,** 7330-5.

Qiao, J., Uzzo, R., Obara-Ishihara, T., Degenstein, L., Fuchs, E., and Herzlinger, D. (1999b). FGF-7 modulates ureteric bud growth and nephron number in the developing kidney. *Development* **126,** 547-54.

Rauchman, M. (2000). The role of homeobox genes in kidney development. *Curr Opin Nephrol Hypertens* **9,** 37-42.

Ridley, A. J. (1999). Rho family proteins and regulation of the actin cytoskeleton. *Prog Mol Subcell Biol* **22,** 1-22.

Ridley, A. J., Comoglio, P. M., and Hall, A. (1995). Regulation of scatter factor/hepatocyte growth factor responses by Ras, Rac, and Rho in MDCK cells. *Mol Cell Biol* **15,** 1110-22.

Ritvos, O., Tuuri, T., Eramaa, M., Sainio, K., Hilden, K., Saxen, L., and Gilbert, S. F. (1995). Activin disrupts epithelial branching morphogenesis in developing glandular organs of the mouse. *Mech Dev* **50,** 229-45.

Rogers, S. A., Ryan, G., Purchio, A. F., and Hammerman, M. R. (1993). Metanephric transforming growth factor-beta 1 regulates nephrogenesis in vitro. *Am J Physiol* **264,** F996-1002.

Rosen, E. M., Nigam, S. K., and Goldberg, I. D. (1994). Scatter factor and the c-met receptor: a paradigm for mesenchymal/epithelial interaction. *J Cell Biol* **127,** 1783-7.

Rosenblum, N. D., and Yager, T. D. (1997). Changing patterns of gene expression in developing mouse kidney, as probed by differential mRNA display combined with cDNA library screening. *Kidney Int* **51,** 920-5.

Rosenthal, A. (1999). The GDNF protein family: gene ablation studies reveal what they really do and how. *Neuron* **22,** 201-3.

Saarma, M. (2000). GDNF - a stranger in the TGF-beta superfamily? *Eur J Biochem* **267,** 6968-71.

Sainio, K., Hellstedt, P., Kreidberg, J. A., Saxen, L., and Sariola, H. (1997a). Differential regulation of two sets of mesonephric tubules by WT-1. *Development* **124,** 1293-9.

Sainio, K., Suvanto, P., Davies, J., Wartiovaara, J., Wartiovaara, K., Saarma, M., Arumae, U., Meng, X., Lindahl, M., Pachnis, V., and Sariola, H. (1997b). Glial-cell-line-derived neurotrophic factor is required for bud initiation from ureteric epithelium. *Development* **124,** 4077-87.

Sakurai, H., Barros, E. J., Tsukamoto, T., Barasch, J., and Nigam, S. K. (1997). An in vitro tubulogenesis system using cell lines derived from the embryonic kidney shows dependence on multiple soluble growth factors. *Proc Natl Acad Sci U S A* **94,** 6279-84.

Sakurai, H., Bush, K. T., and Nigam, S. K. (2001). Identification of pleiotrophin as a mesenchymal factor involved in ureteric bud branching morphogenesis. *Development* **128,** 3283-93.

Sakurai, H., and Nigam, S. K. (1997). Transforming growth factor-beta selectively inhibits branching morphogenesis but not tubulogenesis. *Am J Physiol* **272,** F139-46.

Sakurai, H., and Nigam, S. K. (2000). Molecular and cellular mechanisms of kidney development. *In* "The kidney: physiology and pathophysiology" (D. W. Seldin, Ed.), pp. 685-702. Lippincott Williams and Wilkins, Philadelphia.

Samakovlis, C., Hacohen, N., Manning, G., Sutherland, D. C., Guillemin, K., and Krasnow, M. A. (1996). Development of the Drosophila tracheal system occurs by a series of morphologically distinct but genetically coupled branching events. *Development* **122,** 1395-407.

Sampath, P., and Pollard, T. D. (1991). Effects of cytochalasin, phalloidin, and pH on the elongation of actin filaments. *Biochemistry* **30,** 1973-80.

Sanchez, M. P., Silos-Santiago, I., Frisen, J., He, B., Lira, S. A., and Barbacid, M. (1996). Renal agenesis and the absence of enteric neurons in mice lacking GDNF. *Nature* **382,** 70-3.

Sanicola, M., Hession, C., Worley, D., Carmillo, P., Ehrenfels, C., Walus, L., Robinson, S., Jaworski, G., Wei, H., Tizard, R., Whitty, A., Pepinsky, R. B., and Cate, R. L. (1997). Glial cell line-derived neurotrophic factor-dependent RET activation can be mediated by two different cell-surface accessory proteins. *Proc Natl Acad Sci U S A* **94,** 6238-43.

Santos, O. F., Barros, E. J., Yang, X. M., Matsumoto, K., Nakamura, T., Park, M., and Nigam, S. K. (1994). Involvement of hepatocyte growth factor in kidney development. *Dev Biol* **163,** 525-9.

Santos, O. F., Moura, L. A., Rosen, E. M., and Nigam, S. K. (1993). Modulation of HGF-induced tubulogenesis and branching by multiple phosphorylation mechanisms. *Dev Biol* **159,** 535-48.

Santos, O. F., and Nigam, S. K. (1993). HGF-induced tubulogenesis and branching of epithelial cells is modulated by extracellular matrix and TGF-beta. *Dev Biol* **160,** 293-302.

Sanvito, F., Herrera, P. L., Huarte, J., Nichols, A., Montesano, R., Orci, L., and Vassalli, J. D. (1994). TGF-beta 1 influences the relative development of the exocrine and endocrine pancreas in vitro. *Development* **120,** 3451-62.

Sariola, H., and Sainio, K. (1997). The tip-top branching ureter. *Curr Opin Cell Biol* **9,** 877-84.

Saxen, L. (1987). "Organogenesis of the Kidney." Cambridge University Press, Cambridge.

Scharfmann, R. (2000). Control of early development of the pancreas in rodents and humans: implications of signals from the mesenchyme. *Diabetologia* **43,** 1083-92.

Schuchardt, A., D'Agati, V., Pachnis, V., and Costantini, F. (1996). Renal agenesis and hypodysplasia in ret-k- mutant mice result from defects in ureteric bud development. *Development* **122,** 1919-29.

Schumacher, K., Strehl, R., and Minuth, W. W. (2002). Detection of glycosylated sites in embryonic rabbit kidney by lectin chemistry. *Histochem Cell Biol* **118,** 79-87.

Serra, R., Pelton, R. W., and Moses, H. L. (1994). TGF beta 1 inhibits branching morphogenesis and N-myc expression in lung bud organ cultures. *Development* **120,** 2153-61.

Settleman, J. (1999). Rho GTPases in development. *Prog Mol Subcell Biol* **22,** 201-29.

Settleman, J. (2000). Getting in shape with Rho. *Nat Cell Biol* **2,** E7-9.

Shawlot, W., and Behringer, R. R. (1995). Requirement for Lim1 in head-organizer function. *Nature* **374,** 425-30.

Shilo, B. Z., Gabay, L., Glazer, L., Reichman-Fried, M., Wappner, P., Wilk, R., and Zelzer, E. (1997). Branching morphogenesis in the Drosophila tracheal system. *Cold Spring Harb Symp Quant Biol* **62,** 241-7.

Silberstein, G. B., and Daniel, C. W. (1987). Reversible inhibition of mammary gland growth by transforming growth factor-beta. *Science* **237,** 291-3.

Slack, J. M. (1995). Developmental biology of the pancreas. *Development* **121,** 1569-80.

Smuts, M. S., Hilfer, S. R., and Searls, R. L. (1978). Patterns of cellular proliferation during thyroid organogenesis. *J Embryol Exp Morphol* **48,** 269-86.

Soeno, Y., Shimada, Y., and Obinata, T. (1999). BDM (2,3-butanedione monoxime), an inhibitor of myosin-actin interaction, suppresses myofibrillogenesis in skeletal muscle cells in culture. *Cell Tissue Res* **295,** 307-16.

Soong, H. K., Dass, B., and Lee, B. (1990). Effects of cytochalasin D on actin and vinculin in cultured corneal epithelial cells. *J Ocul Pharmacol* **6,** 113-21.

Spooner, B. S. (1973). Microfilaments, cell shape changes, and morphogenesis of salivary epithelium. *Amer. Zool.* **13,** 1007-22.

Srinivas, S., Goldberg, M. R., Watanabe, T., D'Agati, V., al-Awqati, Q., and Costantini, F. (1999). Expression of green fluorescent protein in the ureteric bud of transgenic mice: a new tool for the analysis of ureteric bud morphogenesis. *Dev Genet* **24,** 241-51.

Steinberg, G., and McIntosh, J. R. (1998). Effects of the myosin inhibitor 2,3-butanedione monoxime on the physiology of fission yeast. *Eur J Cell Biol* **77,** 284-93.

Stephens, F. D., Smith, E. D., and Hutson, J. M. (1996). "Congenital Anomalies of the Urinary and Genital Tracts." Isis Medical Media Inc., Oxford.

Sternlicht, M. D., and Werb, Z. (2001). How matrix metalloproteinases regulate cell behavior. *Annu Rev Cell Dev Biol* **17,** 463-516.

Stevenson, B. R., and Begg, D. A. (1994). Concentration-dependent effects of cytochalasin D on tight junctions and actin filaments in MDCK epithelial cells. *J Cell Sci* **107,** 367-75.

Stuart, R. O., Bush, K. T., and Nigam, S. K. (2001). Changes in global gene expression patterns during development and maturation of the rat kidney. *Proc Natl Acad Sci U S A* **98,** 5649-54.

Tang, M. J., Cai, Y., Tsai, S. J., Wang, Y. K., and Dressler, G. R. (2002). Ureteric bud outgrowth in response to RET activation is mediated by phosphatidylinositol 3-kinase. *Dev Biol* **243,** 128-36.

Tang, M. J., Worley, D., Sanicola, M., and Dressler, G. R. (1998). The RET-glial cell-derived neurotrophic factor (GDNF) pathway stimulates migration and chemoattraction of epithelial cells. *J Cell Biol* **142,** 1337-45.

Taraviras, S., Marcos-Gutierrez, C. V., Durbec, P., Jani, H., Grigoriou, M., Sukumaran, M., Wang, L. C., Hynes, M., Raisman, G., and Pachnis, V. (1999). Signalling by the RET receptor tyrosine kinase and its role in the development of the mammalian enteric nervous system. *Development* **126,** 2785-97.

Tarone, G., Hirsch, E., Brancaccio, M., De Acetis, M., Barberis, L., Balzac, F., Retta, S. F., Botta, C., Altruda, F., Silengo, L., and Retta, F. (2000). Integrin function and regulation in development. *Int J Dev Biol* **44,** 725-31.

Ten Have-Opbroek, A. A. (1981). The development of the lung in mammals: an analysis of concepts and findings. *Am J Anat* **162,** 201-19.

Thesleff, I., and Jernvall, J. (1997). The enamel knot: a putative signaling center regulating tooth development. *Cold Spring Harb Symp Quant Biol* **62,** 257-67.

Tokuda, Y., Satoh, Y., Fujiyama, C., Toda, S., Sugihara, H., and Masaki, Z. (2003). Prostate cancer cell growth is modulated by adipocyte-cancer cell interaction. *BJU Int* **91,** 716-20.

Torres, M., Gomez-Pardo, E., Dressler, G. R., and Gruss, P. (1995). Pax-2 controls multiple steps of urogenital development. *Development* **121,** 4057-65.

Towers, P. R., Woolf, A. S., and Hardman, P. (1998). Glial cell line-derived neurotrophic factor stimulates ureteric bud outgrowth and enhances survival of ureteric bud cells in vitro. *Exp Nephrol* **6,** 337-51.

Uehara, Y., Minowa, O., Mori, C., Shiota, K., Kuno, J., Noda, T., and Kitamura, N. (1995). Placental defect and embryonic lethality in mice lacking hepatocyte growth factor/scatter factor. *Nature* **373,** 702-5.

Vainio, S., Lehtonen, E., Jalkanen, M., Bernfield, M., and Saxen, L. (1989). Epithelial-mesenchymal interactions regulate the stage-specific expression of a cell surface proteoglycan, syndecan, in the developing kidney. *Dev Biol* **134,** 382-91.

Vainio, S., and Lin, Y. (2002). Coordinating early kidney development: lessons from gene targeting. *Nat Rev Genet* **3,** 533-43.

Vainio, S. J., Itaranta, P. V., Perasaari, J. P., and Uusitalo, M. S. (1999). Wnts as kidney tubule inducing factors. *Int J Dev Biol* **43,** 419-23.

Vainio, S. J., and Uusitalo, M. S. (2000). A road to kidney tubules via the Wnt pathway. *Pediatr Nephrol* **15,** 151-6.

van Adelsberg, J., Sehgal, S., Kukes, A., Brady, C., Barasch, J., Yang, J., and Huan, Y. (2001). Activation of hepatocyte growth factor (HGF) by endogenous HGF activator is required for metanephric kidney morphogenesis in vitro. *J Biol Chem* **276,** 15099-106.

Van Aelst, L., and D'Souza-Schorey, C. (1997). Rho GTPases and signaling networks. *Genes Dev* **11,** 2295-322.

VanBuren, P., Begin, K., and Warshaw, D. M. (1998). Fluorescent phalloidin enables visualization of actin without effects on myosin's actin filament sliding velocity and hydrolytic properties in vitro. *J Mol Cell Cardiol* **30,** 2777-83.

Vanderwinden, J. M., Mailleux, P., Schiffmann, S. N., and Vanderhaeghen, J. J. (1992). Cellular distribution of the new growth factor pleiotrophin (HB-GAM) mRNA in developing and adult rat tissues. *Anat Embryol (Berl)* **186,** 387-406.

Vasioukhin, V., Bauer, C., Yin, M., and Fuchs, E. (2000). Directed actin polymerization is the driving force for epithelial cell-cell adhesion. *Cell* **100,** 209-19.

Vasioukhin, V., and Fuchs, E. (2001). Actin dynamics and cell-cell adhesion in epithelia. *Curr Opin Cell Biol* **13,** 76-84.

Vega, Q. C., Worby, C. A., Lechner, M. S., Dixon, J. E., and Dressler, G. R. (1996). Glial cell line-derived neurotrophic factor activates the receptor tyrosine kinase RET and promotes kidney morphogenesis. *Proc Natl Acad Sci U S A* **93,** 10657-61.

Vize, P. D., Seufert, D. W., Carroll, T. J., and Wallingford, J. B. (1997). Model systems for the study of kidney development: use of the pronephros in the analysis of organ induction and patterning. *Dev Biol* **188,** 189-204.

Wallner, E. I., Yang, Q., Peterson, D. R., Wada, J., and Kanwar, Y. S. (1998). Relevance of extracellular matrix, its receptors, and cell adhesion molecules in mammalian nephrogenesis. *Am J Physiol* **275,** F467-77.

Weaver, M., Dunn, N. R., and Hogan, B. L. (2000). Bmp4 and Fgf10 play opposing roles during lung bud morphogenesis. *Development* **127,** 2695-704.

Werb, Z. (1997). ECM and cell surface proteolysis: regulating cellular ecology. *Cell* **91,** 439-42.

Winyard, P. J., Risdon, R. A., Sams, V. R., Dressler, G. R., and Woolf, A. S. (1996). The PAX2 tanscription factor is expressed in cystic and hyperproliferative dysplastic epithelia in human kidney malformations. *J Clin Invest* **98,** 451-9.

Woolf, A. S., Kolatsi-Joannou, M., Hardman, P., Andermarcher, E., Moorby, C., Fine, L. G., Jat, P. S., Noble, M. D., and Gherardi, E. (1995). Roles of hepatocyte growth factor/scatter factor and the met receptor in the early development of the metanephros. *J Cell Biol* **128,** 171-84.

Woolf, A. S., Winyard, P. J. D., Hermanns, M. M., and Welham, S. J. M. (2003). Maldevelopment of the human kidney and lower urinary tract: an overview. *In* "The Kidney: From normal development to congenital disease", pp. 377-394. Academic Press, London.

Worby, C. A., Vega, Q. C., Zhao, Y., Chao, H. H., Seasholtz, A. F., and Dixon, J. E. (1996). Glial cell line-derived neurotrophic factor signals through the RET receptor and activates mitogen-activated protein kinase. *J Biol Chem* **271,** 23619-22.

Worley, D. S., Pisano, J. M., Choi, E. D., Walus, L., Hession, C. A., Cate, R. L., Sanicola, M., and Birren, S. J. (2000). Developmental regulation of GDNF response and receptor expression in the enteric nervous system. *Development* **127,** 4383-93.

Wulf, E., Deboben, A., Bautz, F. A., Faulstich, H., and Wieland, T. (1979). Fluorescent phallotoxin, a tool for the visualization of cellular actin. *Proc Natl Acad Sci U S A* **76,** 4498-502.

Xu, P. X., Adams, J., Peters, H., Brown, M. C., Heaney, S., and Maas, R. (1999). Eya1-deficient mice lack ears and kidneys and show abnormal apoptosis of organ primordia. *Nat Genet* **23,** 113-7.

Zent, R., Bush, K. T., Pohl, M. L., Quaranta, V., Koshikawa, N., Wang, Z., Kreidberg, J. A., Sakurai, H., Stuart, R. O., and Nigam, S. K. (2001). Involvement of laminin binding integrins and laminin-5 in branching morphogenesis of the ureteric bud during kidney development. *Dev Biol* **238,** 289-302.